Elucidating the mechanism of cardiac ischemia and reperfusion by proteomics approach

Xin, Li

2011

Xin, L. (2011). Elucidating the mechanism of cardiac ischemia and reperfusion by proteomics approach. Doctoral thesis, Nanyang Technological University, Singapore.

https://hdl.handle.net/10356/48669

https://doi.org/10.32657/10356/48669

ELUCIDATING THE MECHANISM OF CARDIAC ISCHEMIA AND REPERFUSION BY PROTEOMICS APPROACH

LI XIN

SCHOOL OF BIOLOGICAL SCIENCES

NANYANG TECHNOLOGICAL UNIVERSITY

2011

Elucidating the Mechanism of Cardiac Ischemia and Reperfusion by Proteomics Approach

LI XIN

School of Biological Sciences

A thesis submitted to the Nanyang Technological University in fulfillment of the requirement for the degree of Doctor of Philosophy

2011

Acknowledgements

First of all, I would like to thank Nanyang Technological University and School of Biological Sciences for offering me the opportunity to study as a Ph.D candidate and also the scholarship to support my life in Singapore.

I want to show my sincere appreciation for those who have inspired and helped me in my four year study.

Among them, I am most grateful for my supervisor Prof. Sze Siu Kwan, who has introduced me into the field of mass spectrometry and proteomics research. He always inspires me with brilliant ideas and provides precious guidance on my study. Many of the ideas in this thesis should be attributable to him. I have earned valuable experiences from Prof. Sze on mass spectrometry and data analysis.

I would like to thank Prof Lim Sai Kiang, who has provided wise suggestions and helped with my manuscript revising; and Prof Dominique de Kleijn who had offered me the precious animal tissues for my study. I also want to thank the members of my thesis advisory committee, Prof Kambadur Ravi and Prof Su I-Hsin for their advices on my study and experiment planning.

Furthermore, I profoundly appreciate the kind help, passionate discussion and great brainstorming from my current and former colleagues, Dr. Anita Ravindran, Arnab Datta, Bamaprasad Dutta, Dr. Gan Chee Sian, Guo Tiannan, Hao Piliang, Meng Wei, Dr. Park Jung Eun, Qian Jing Ru, Ren Yan, Dr. Sunil Shankar Adav, Yuan Ran Dong, Prof. Zhang Huo Ming, Zhu Yi. Especially, I would like to thank Prof Zhang Huo Ming for his great

help and advice on my research and job hunting; Tiannan and Zhu Yi for all those interesting discussions on proteomics and chemistry; Meng Wei for her helps on my lab duty and of course for the greatest parties thrown by her; and Arnab for his nice suggestions and kind comfort.

I also want to show my gratitude to my best friends, Dr. Barry Wang, who knows me from undergraduate period, for his critical information sharing; Zhang Chen and Holly Ge Xiao Jia for their friendship and the good times during these four years.

Last but not least, I am so willing to show my greatest thankfulness to my parents and sister who have supported me and offered me understanding, encouragement for all the up and down years, and my wife Elynn Phang Hui Qun, who has greatly helped and inspired me in my research and showered me with her gentleness and invaluable love.

Wish you all live long and prosper!

Table of Contents

Summary

Despite decades of intensive research, there is still no effective treatment for cardiac ischemia/reperfusion (I/R) injury, an important corollary in the treatment of ischemic disease. I/R injury is initiated when the altered biochemistry of cells after ischemia is no longer compatible with oxygenated microenvironment (or reperfusion). To better understand the molecular basis of this alteration and subsequent incompatibility, we assessed the temporal and quantitative alterations in the cardiac proteome of a mouse cardiac I/R model by iTRAQ approach at 30 mins of ischemia, and at 60 or 120 mins of reperfusion after 30 mins of ischemia using sham operated mouse heart as the baseline control. Modulation on fatty acid oxidation, glycolysis, TCA cycle and electron transport chain suggested pivotal metabolic switch from oxidative phosphorylation to anaerobic glycolysis during ischemia. The delay of reversion of the proteome alteration upon reperfusion indicated a refractory period in which the ischemic cells cannot adjust to the presence of oxygen. Proteins found to be quantitatively altered during ischemia are therefore candidate targets for mitigating this refractory period and enhancing cellular recovery from an ischemic to a normoxic microenvironment. Among the regulated proteins, functions of Park7 and Ppia were further studied in an *in vitro* model by the cell biological method and immunoprecipitation-MS approach.

Under ischemia and reperfusion stresses, the cardiac cells may secrete proteins to modulate its microenvironment and into the circulation system to alert the host body. To understand the process, we performed a secretome analysis by both iTRAQ-based

and label free-based quantitative proteomics approaches using LC-MS/MS on a rat heart myoblast cell line subjected to 16 hr hypoxia and 24 hr reoxygenation. Large quantities of secreted proteins were identified, which provides novel knowledge on the secretion of cardiomyocytes. Secreted proteins related to important biological functions such as SERPINH1, PPIA, ATRN, EMC1, POSTN, THBS1 and TIMP1 were found to be altered by hypoxia and reoxygenation stresses. Further analysis on the modulated subproteome suggests that angiogenesis, inflammation, ECM remodeling including collagen deposition and cross-linking are regulated during hypoxia; while in the subsequent reperfusion or re-oxygenation, proteins involved in anti-inflammation, ECM modulation are up-regulated and anti-apoptosis proteins decline. The profile and modulation of the secretome identified herein could potentially advance our understanding of the cardiac biology, and facilitate the follow-up investigations on the extracellular molecular events during hypoxia and reoxygenation as well as the ischemia/reperfusion injury.

Chapter 1. Introduction

Cardiac ischemia reperfusion injury

Ischemic heart disease (IHD) remains the leading cause of human mortality with about 7.6 million deaths worldwide, despite tremendous advances in the knowledge of the pathophysiology of IHD. Various treatments to acute cardiac event including Percutaneous Coronary Intervention (PCI), Coronary Artery Bypass Grafting (CABG) and medical management all have some efficacy, but ischemia/reperfusion (I/R) injury is a major contributory factor to cardiac dysfunction and infarct size after the treatment. The I/R injury determines patient prognosis after acute myocardial infarction in IHD. Tremendous molecular events are activated during ischemia and reperfusion; such events can be beneficial or detrimental to the cardiac functions. In present study proteomics approaches were employed to determine these molecular events and try to elucidate the underlying mechanism.

Mass spectrometry-based proteomics and bioinformatics methods

Proteomics is a high-throughput technology to study the complexity of proteins and their biological roles, including biophysical properties, structure, and function[1]. Rather than assessing single molecules one at a time, a proteomic analysis provides a broad-based portrait of the proteome profile. Proteins are the final effectors of the biological system and play a central role in a systemic view of biological processes. It is assumed that the diversity of proteins, comprising their isoforms, Single-nucleotide polymorphisms(SNPs), and posttranslational modifications (PTMs), underlies

biology[1]. Hence the proteomics study that attempts to provide a systemic view of biological organization on protein level is essential to understand the complicated underlying mechanisms.

Protein separation

Proteins expressed intracellularly or extracellularly both have a large dynamic range of abundance. The detection of low-abundance proteins are usually masked by high-abundance proteins such as albumin, collagen etc. To identify proteins from a complicated biological sample, we first need to overcome the barrier of interference from high-abundance proteins. By separating the proteome, the sample complexity is reduced and the fraction that is subjected to mass spectrometry analysis contains fewer proteins, which lowers the possibility of interference from high-abundant proteins. Hence, the protein separation methods are essential to assure a successful proteomics research, which can usually be categorized into two groups: gel-based and gel-free separations. For gel-based separation one dimensional or two dimensional SDS-PAGE gel (2DE) is used to separate the intact proteins according their molecular weight / pI values. Recently, gel-eluted liquid fraction entrapment electrophoresis (GELFrEE) was developed for protein separation and intact protein analysis instead of peptide analysis which is usually done in gel-based methods due to the trapping of protein into the gel[2-3]. Tube gel is adopted in the method instead of slab gel to increase the loading capacity. The proteins are eventually eluted from the gel column and collected in the solution phase. Thus the separation and obtaining of intact proteins are achieved. For gel-free separation, proteome sample is digested to peptides and then fractionated by high pressure liquid chromatography (HPLC). Different HPLC columns can be used

for peptide separation such as C18, strong cation exchange (SCX), strong anion exchange (SAX), weak anion exchange (WAX) etc. Those very acidic or basic proteins, extremely big or small proteins and membrane proteins are difficult to be separated by 2DE. Moreover, 2DE is notoriously difficult to automate, which limits throughput and results in greater experimental variation with tedious manual manipulation. To the opposite, LC separation overcomes these weak points and provides convenience and robust reproducibility. However, 2DE visualizes the proteome allowing the determination of the quantity and potential PTM or isoform status of proteins. In a cardiac ischemia-reperfusion research, phosphorylation status of mitochondrial aldehyde dehydrogenase 2 was found to be changed under cardioprotection treatment by 2DE coupled with MS identification[4]. This research shows the potential of 2DE MS proteomics in identifying novel therapeutic target.

Protein identification

For shotgun proteomics, the tryptic digested peptides from different proteins are mixed and analyzed by the mass spectrometry to generate MS1 mass spectrum composed of the mass over charge (m/z) peaks of the peptides and selected peaks are subjected to fragmentation to generate the MS^2 spectrum. The MS^2 spectrum reveals the sequence information of the selected ions (peaks) from the MS1 spectrum. The MS^2 spectrum is interpreted by computer algorithm and assigned to particular amino acid sequence in the post-run stage. To avoid the masking effect from high-abundant peptides, automated data dependent acquisition (DDA) is applied to avoid repeating selection of the peak with the same m/z from the MS1 spectrum; hence the peptide that has lower abundance can be selected for fragmentation to generate MS^2 spectrum.

The fragmentation of the selected peptide follows certain rules; hence the MS^2 spectrum containing m/z values of the fragments from the peptide can be used to obtain the sequence information. However due to imperfect experimental condition, the MS^2 spectrum can be explained by several different sequences. Each calculated value which falls within a given mass tolerance of an experimental value counts as a match. By calculating the significance of a match away from the random matches by the Mascot scoring algorithm, the result ranks each match and shows the homology and identity score as well as the score of the peptide sequence. The identity score shows the significance threshold for the peptide identification to differ from random match. Under some situation the peptide score may not exceed the identity score, but it still can be recognized as an outlier away from the random match. Therefore a second and lower threshold named homology score is given to compare with the peptide score. In the present study, all peptides from Mascot search result pass the homology score; and if the homology is not given the peptides are reported only if they pass the identity threshold.

Once the identification of peptides is fixed, the proteins represented by these peptides can be clarified. However a peptide can be derived from different protein isoforms, and a group of peptides may be derived from a group of proteins, which makes the protein inference more complicated. The ProteinPilot software uses a protein grouping strategy to solve this problem. Generally, the protein grouping strategy determines the existence priority of the protein based on the spectral proof, which means the protein that explains more spectra has a higher probability of existence and addresses the following issues:

1. The equivalent winner proteins and subset proteins

2. Competitor proteins

3. Multiple related protein forms

If a group of peptides can all be explained by one or more proteins, these proteins that share the same set of peptides are equivalent winners; and if a subset of peptides can also be explained by some other proteins, these proteins are subset proteins. The existence of the equivalent winner proteins cannot be excluded by each other. Because the winner proteins use up all the identified peptides, the subset proteins should be included into the same group with the winners and not be reported as extra proteins. If the winner proteins generate just one or a few peptides more than the subset proteins, in an extreme case if the extract peptide(s) which contribute(s) to the winner protein(s) is identified incorrectly, the subset of proteins are as good an explanation for the data as the reported winners. Because these subset proteins are as close to being as correct as the equivalent winners shown, they are considered to be competitor proteins. They are close enough to being correct that they should be kept in view. However, one should keep in mind that the protein proof is based on spectra but not on peptides. If a spectrum can be explained by two distinct peptides, and the peptides are the ones that differ one protein to another, there will be certain probability that one protein is enough to explain all the peptide including the spectrum with two peptide explanations. If there is a protein that can explain several additional spectra as well as some of the peptides belonging to the winner protein (primary form that explains most of the spectra), which makes a solid case for its presence, this protein is a related

secondary form. However, many peptides can be explained by the primary protein form and its competitors, therefore, the protein score that indicates the identification of the protein should be calculated only based on the peptides that have not been used by the primary form.

For Mascot strategy, the peptide assignment (explained by certain protein) is bases on similar rules. One peptide has two parameters which are ‘pep_rank’ and ‘pep_isbold’. ‘pep_rank’ value 1 means the peptide is the first-ranked explanation for the spectra. ‘pep_isbold’ value 1 means the peptide is first time used in the according protein and 2 means second time. However, protein score is based on all peptides that can be assigned no matter the peptide has been used or not. Hence for Mascot result, protein groups are generated by in-house script based on the peptide sharing information. Each group contains the proteins that share the same peptide(s) and for each protein the peptides that can be assigned to (total peptides) and only be assigned to (specific peptides) are displayed, *i.e.*:

Group	Uniprot AC	Name	Peptide Num
37	P05708	Hexokinase-1	(8)12*
37	P27881	Hexokinase-2	(3)7*

* 8 specific peptides can only be assigned to and in total 12 peptides can be assigned to Hexokinase-1. 3 specific peptides can only be assigned to and in total 7 peptides can be assigned to Hexokinase-2.

Quantitative profiling

Several techniques have been developed to profile the proteome alteration under different conditions. These techniques can be roughly divided into two groups: isotope labeling and label-free methods. Isotope labeling method includes metabolic labeling: stable isotope labeling with amino acids in cell culture (SILAC), and chemical labeling: isotope-coded affinity tag (ICAT), isobaric tag for relative and absolute quantitation (iTRAQ), tandem mass tags (TMT) and 2D fluorescence difference gel electrophoresis (2D-DIGE) by using multiplex fluorescent labeling dye (CyDye). The labeling method performs on either the peptide level or the protein level.

The 2D-DIGE method allows detection and quantification of differences in protein abundance between different biological samples within one single gel by labeling fluorophores in complex protein mixtures prior to IEF and SDS-PAGE. The CyDyes react over an NHS-ester group with ε-amino residues of lysine (CyDye DIGE Fluor minimal dyes) or over a maleimide group with all available cysteine residues in the protein sample (CyDye DIGE Fluor saturation dyes), which enables co-electrophoresis of up to three different samples (CyDye DIGE Fluor minimal dyes) or 2 different samples (CyDye DIGE Fluor saturation dyes) in one approach with a dynamic range up to five orders of magnitude. No charge alteration is applied on the labeled protein. For CyDye DIGE Fluor minimal dyes about 3% of the available proteins are labeled and then only on a single lysine per protein whereas the rest remains, hence labeling optimization is usually not necessary. For CyDye DIGE Fluor saturation dyes, they provide a high labeling concentration and enable analysis on low sample amount (5 μg protein/image). This method eliminates experimental gel-to-gel

variation and improves accuracy of protein quantification comparing to the classic 2-D electrophoresis.

iTRAQ is a available commercially as 4-plex or 8-plex peptide labeling reagent kit. For 4-plex iTRAQ, the labeling reagent forms covalent bond with the primary amine(s) and adds 145 Dalton to the peptide (hence it is called isobaric). Each labeling tag is composed of one reporter group, which is 114 or 115 or 116 or 117 Dalton, and one balance group which compensates the difference between reporter groups (Figure 1).

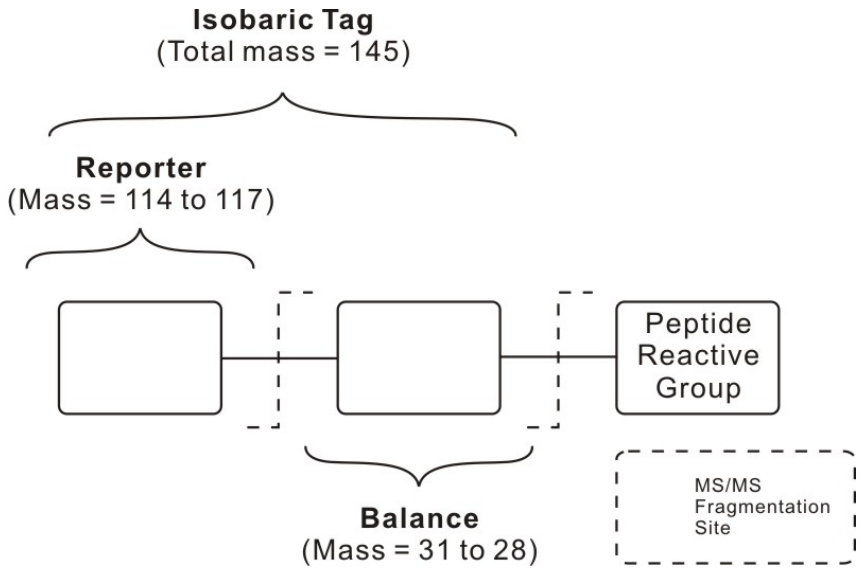

Figure 1 Schematic representation of the iTRAQ reagents

The peptides labeled with the four tags are combined and analyzed by MS together. During fragmentation in MS^2 step the bond between the reporter and balance groups is broken and the former is released. Peaks corresponding to the four reporter groups can be observed in the MS^2 spectrum. By comparing the peak area of the reporter groups the relative abundance of the same peptide from different conditions is obtained (Figure 2).

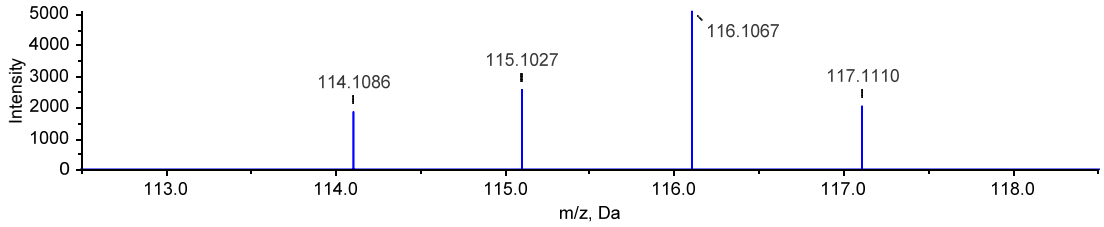

Figure 2 Representative MS^2 spectrum for iTRAQ reporter

Normalization is done at the med post-run stage during which the peak areas of specific labeling tag of total peptides are summed. Sums of the peak areas of four iTRAQ tag are compared to generate the bias factor.

Label-free method is less expensive and requires no chemical modification on the experimental stage, in which samples from each condition are analyzed separately. The abundance alteration is measured by comparing peak area or spectrum numbers from the same protein in each condition depending on the label free method.

For peak area comparison, the extracted ion chromatogram (XIC) of a specific peptide is used to represent the abundance of this peptide. Briefly, the peak that represents the peptide in each MS1 spectrum is located according to the peptide mass within a certain range (*e.g.*10 ppm). The peak area of the chromatogram is then calculated by using the peak intensity at certain sampling time point and the duration between these time points. The XIC of each peptide from a specific protein is then summed to generate the peak area of the protein. Normalization is done by dividing the peak area of a specific protein the by total peak area for all identified proteins.

For the spectrum counting method the normalized spectral abundance factor (NSAF) is calculated for comparison, the formula is as below:

$$(NSAF)_k = \left(\frac{Spc}{L}\right)_k / \sum_{i=1} \left(\frac{Spc}{L}\right)_i$$

Spc is the sum of spectrum numbers of each unique peptide from protein k. L is the length of protein k. The NSAF of protein k is a normalized factor by dividing the sum of Spc of each protein.

However, the spectrum counting ignores the peak intensity and the peak area calculation may include wrong peaks that share the same mass with the target peptide. Hence a new method name SI_N is developed which uses both fragment ion intensity (MS^2 level) and spectrum counting to calculate the protein abundance[5]. The formula of SI_N is as below:

$$SI = \sum_{k=1}^{pn} (\sum_{j=1}^{sc} i_j)_k$$

sc is the spectral count for the peptide *k*, *i* is the fragment ion intensity of peptide *k*, *j* is the *j*th spectral count of *sc* total spectral counts for peptide *k* and *pn* is the number of peptides identified for that protein.

$$SI_{GI} = SI / \sum_{j=1}^{n} SI_j$$

SI_{GI} is the normalized factor that the SI of divided protein is divided by the sum of SI of all the identified proteins.

$$SI_N = SI_{GI}/L$$

To further divide the SI_{GI} by L which is the length of the according protein, the SI_N represents the abundance level of each protein. Hence SI_N can be used for measuring the abundance alteration for specific protein across conditions and also for estimating the abundance difference between different proteins within the same experiment. Because both spectrum count and fragment ion intensity are taken into account, The SI_N method is superior to the spectrum counting method.

Data analysis and bioinformatics techniques

Overrepresentation Quantitative proteomics approach usually generates a list containing proteins of which the abundances are significantly altered in studied biological conditions. Data analysis on the protein list is important for the high throughput research to understand the biological meaning of the modulation on the subproteome. The biological process, cellular location and molecular function annotation of each regulated protein are essential to interpreting the biological meaning of all regulated proteins, *e.g.* if most regulated proteins are annotated as mitochondrial proteins in a proteomics study, this may indicate that mitochondria is influenced in the scenario. However in an extreme case, even all regulated proteins being annotated as mitochondrial proteins does not mean the mitochondrial proteome is significantly modulated if only mitochondrial proteins are subjected to the proteomics study; in a less extreme case the functional annotations of the regulated subproteome may only represent similar functional annotation terms that assigned to the total proteome under study, in which the biological meaning of the annotation for the former is generated by chance. Hence to distinguish the significant biological

meaning provided by the functional annotation from those produced by chance, we need to calculate the probability whether the functional annotation to the modulated proteins occurs by chance. Total proteome (as background) contains M protein annotated to some term *t* (*e.g.* mitochondrial) and N genes not annotated to the term. The modulated protein set contains k genes, r of which are annotated to the term *t*. The hypergeometric distribution then gives the probability of sampling exactly r genes annotated term *t:*

$$h_{k,N,M}(r) = \frac{\binom{M}{r}\binom{N}{k-r}}{\binom{N+M}{k}}$$

To calculate the chance of seeing r or more annotations in the study set:

$$\sum_{i=r}^{k} h_{k,N,M}(i)$$

The method is the same as the one-tail Fisher Exact Test which calculates the probability of over-representation of the term *t.* Over-representation of a certain functional term annotated to the modulated proteins indicates that the frequency of the annotation to the proteins is statistically higher than the frequency of annotation to the total proteome (the background), hence the functional term can be deemed as significantly modulated. Measuring the over-represented biological terms offers a systemic view of the influenced functions of the proteome. Several annotation databases can be used for biological term over-representation measurement, such as UniProt Knowledgebase, Kyoto Encyclopedia of Genes and Genomes (KEGG), SwissProt PIR keyword, InterPro for protein sequence analysis & classification etc.

Text mining For protein functional annotation, great effort has been endeavored to generate database such as UniProt Knowledgebase, Human Protein Reference Database (HPRD), InAct molecular interaction database, KEGG etc. For secreted protein research by proteomics approach, secreted proteins contained in conditioned medium are collected and digested to peptides and detected by MS. However, not all proteins present in conditioned medium can be considered *per se* as actively secreted proteins. Some proteins may be contaminants resulting from cell death or the culture media. Hence the secreted protein should be discriminated from the intracellular contaminants. Besides the database mentioned above, bioinformatics tools have been developed to predict the proteins that are secreted based on their primary sequence. SignalP is used to predict the existence of signal peptide that guides the protein to be secreted out by classical pathways. TransMembrane prediction using Hidden Markov Models (TMHMM) predicts the existence of transmembrane helices based on the protein sequence. Its rationale bases on the possibility that proteins located on the plasma membrane are shed and released to the extracellular space. SecretomeP predicts mammalian secretory proteins participating in non-classical pathways. In addition, given the recent observations on exosomal proteomics, a database named Exocarta is established to record the proteins secreted through these endocytic-like vesicles.

The primary, text-based biomedical literature that contains a much greater wealth of biological knowledge about proteins can also be used for distinguishing the secreted protein in the dataset by applying a text mining approach. Text mining refers to the process of deriving high-quality information from text by using informatics techniques.

In a previous research conducted by Hui Sun *et al*, a text mining technique was developed for over-representation analysis of microarray data by exploiting the information contained in the abstracts of the biomedical literature[6], which can also be applied on proteomics dataset. Inspired by this study, a similar strategy is adopted in secreted protein discrimination in the present study: The abstracts of biomedical literatures that relate to a specific identified protein are scanned by keywords including 'secreted', 'secretome' and 'secreted'. The hit abstracts are manually checked to confirm that the identified protein was considered as, used as or identified as a secreted protein in the literature. The center of this text mining technique is the *gene2pubmed* database provided by NCBI and the Esearch Entrez Utility service[7]. The *gene2pubmed* contains GeneID and the PubMed ID of the publication which relates to GeneID. However, usually SwissProt or International Protein Index (IPI) fasta database is used for proteomics data search, the protein identifier in the search result is UniProt or IPI accession number. Therefore IPI cross reference database (ipi.RAT.v3.78 in present study) is required to convert the UniProt or IPI accession number to GeneID. By using GeneIDs of the identified proteins in proteomics dataset to search in the *gene2pubmed,* the associated literatures with PubMed ID are obtained and the according abstracts are then retrieved by Esearch Entrez Utility web service. Upon retrieval, the abstracts were tokenised on white space to produce single-word terms. Any redundancies were removed to produce text corpus composed of unique set of tokens for each gene. Then, a stemming operation was applied to convert plural to singular forms, verb tenses to their root etc. by using Porter stemming algorithm in Ruby language. This text corpus can be searched by any stemmed input keyword, e.g.

secretion, secreted, secretome. Hits of search indicate mentioning of the keywords in the abstract of the literature related to the specific identified protein. The full text of the hit abstract is then outputted into a list for manual check. This method re-discovers the already known secreted proteins from previous biomedical literature. For those secreted proteins only recognized by the prediction algorithm, the text mining method provides supportive information.

Protein interaction network Protein-protein interactions are important for nearly all biological processes. Aberrant protein-protein interactions can lead to cancer and other human diease[8-10]. Molecular biologists have traditionally studied the interactions and relative influence of focused molecules one at a time; tremendous experimental proofs of the protein-protein interaction have been accumulated. However it is believed that a system has functions that none of the entities of the system has, which means the total is more than the sum of its parts. The protein interaction network provides precious information in the understanding of cellular function and biological processes. Advances in proteomics make it possible to study the behavior and attributes of proteins that make up the entire proteome. Several databases of protein interaction recorded the experimental proof of protein interaction generated by traditional molecular experiment and proteomics approaches are available, which include Molecular Interaction database (MINT), Human Protein Reference Database (HPRD), IntAct etc. These databases can be used for protein interaction network generation. In the present study, the human protein interactions in HPRD and IntAct databases are extracted and used for network generation because the human protein-protein interaction information is more complete than those of rat or mouse. An interaction

network is composed of two elements: nodes, which are the interconnected objects, and edges, which are the links that connect some pairs of nodes. Similar to other networks such as the internet and social network, protein interaction network has several topological features, such as clustering coefficient and degree distribution. Clustering coefficient C is a parameter that quantifies the tendency of each node in the network to form clusters. Specifically, if node *a* is directly connected to nodes *b* and *c*, then *Ca* is the probability that *b* and *c* are also directly connected to each other[11]. The average clustering coefficient C characterizes the overall tendency of nodes to form clusters of nodes. A biological network has a much higher average clustering coefficient than a random network, *e.g.* 0.225 in the epithelial junction complex A system comparing to 0.039 in a random network with the same 132 nodes (proteins) and 384 edges (interactions)[11]; and 0.24 in focal adhesions[12], 0.28 in the neural network of the nematode[13]. In the system with 11073 nodes and 56878 edges of the present study, the clustering coefficient is 0.03776 comparing to 0.002469 in a random network with the same proteins and randomly assigned interactions. The clusters of the highly connected proteins indicate similar functions or that the proteins form functional complexes. In a quantitative proteomics research with interaction network analysis focusing on cisplatin resistance in Hela cells, the significantly increased or decreased proteins were found to form clusters with interactions within the network. Several important biological processes were represented by these clusters[14].

The adjacent interactions to other protein that a protein has is called degree, degree distribution of the network components is used to quantify the diversity of the whole

network. The degree distributions of numerous networks, such as the Internet, human collaboration networks and metabolic networks, follow power law:

$$P(k) = Ak^{-\gamma}$$

A is a constant and the degree exponent γ is usually in the range $2 < \gamma < 3$ [15]. The degree distribution of the epithelial junction complex A system has a γ=0.15 ($P(k)_{JC}=0.18e^{-0.15k}$ $R^2=0.86$). As the probability of finding nodes with very high *k* is practically prohibited in exponential networks, proper hub proteins are absent from the JC network[11]. The degree distribution of the human protein interaction network adopted in present study is $P(k)=0.7959k^{-1.724}$, $R^2=0.896$. The degree distributions of the human protein interaction network and a random network with the same number of nodes and edges are shown in figure 3,

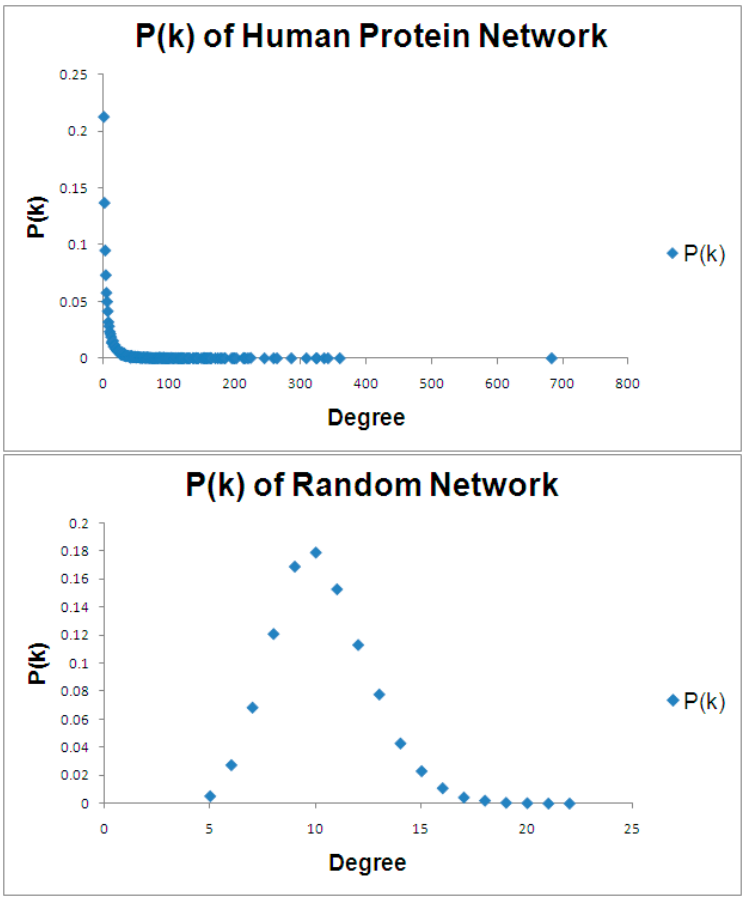

Figure 3 Degree distribution of human protein interaction network or random network with the same number nodes and randomly assigned interactions

The bell-shaped degree distribution of random network peaks at the average degree 10 and decreases fast for both smaller and larger degrees, indicating that these graphs are statistically homogeneous. By contrast, the degree distribution of the human protein interaction network follows power law, which indicates a high diversity of node degrees and no typical node in the network could be used to characterize the rest of the nodes. As can be seen in the graph, low degree nodes have the highest frequencies and very highly connected nodes have much lower frequencies. The inhomogeneity renders the protein interaction network robust against random mutations. Random mutations in the genome of *S. cerevisiae*, simulated by the removal of randomly

selected yeast proteins, do not affect the overall topology of the network[16]. This is in agreement with results from systematic mutagenesis experiments that identified a remarkable capacity of yeast to tolerate the deletion of a substantial number of proteins from its proteome[17-18]. The highly connected nodes are also called 'hubs' which have been shown to be topologically and biologically important. 0.7% of the yeast proteins with more than 15 links have known phenotypic profiles, but single deletion of 62% or so of these proves lethal (Figure 4)[16]. Hence the hub proteins are deemed as important proteins which are worth to investigate.

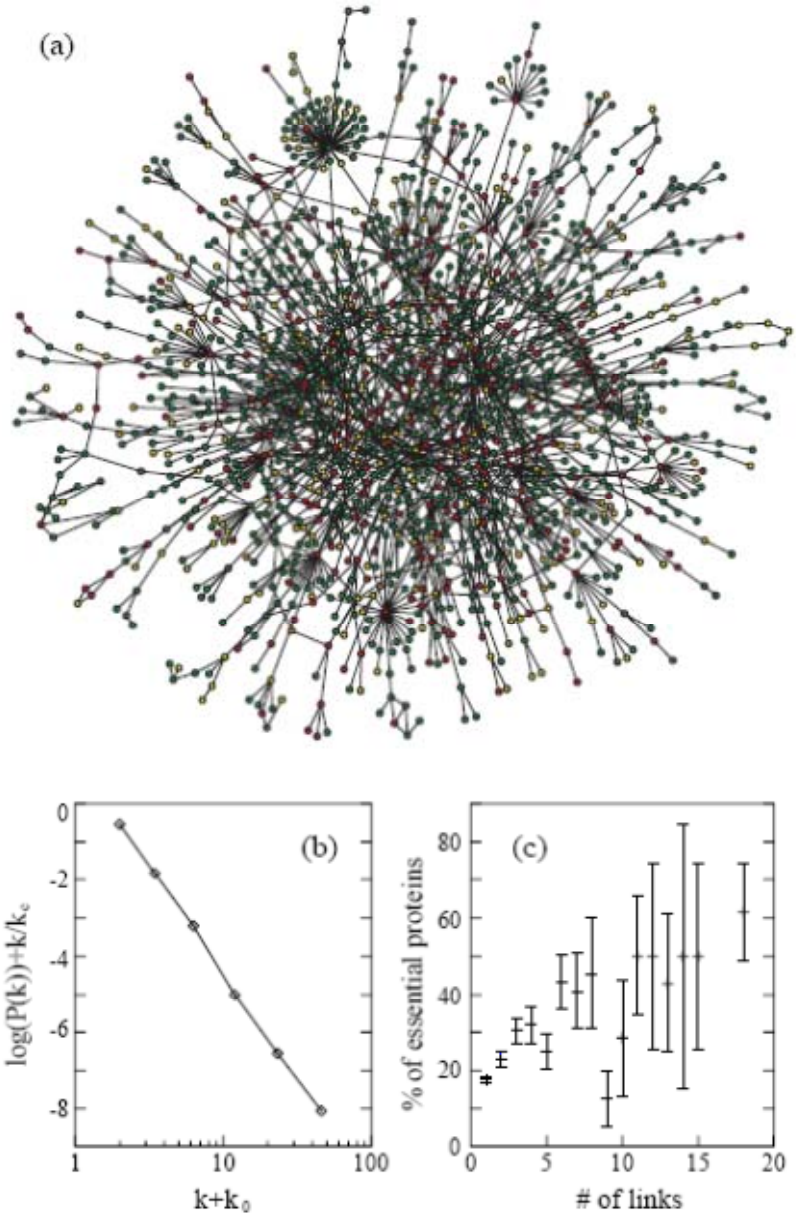

Figure 4 The protein-protein interaction network of S. cerevisiae. (Lethality and centrality in protein networks, Nature, 2001)

The protein-protein interaction network provides a global view on the cellular functions influenced by the interactome. In a systemic investigation of heparin sulfate interactome, the protein-protein interaction network of the interactome was generated

and the topological properties of the network, the identification of functional and structural features that are associated with the heparin/HS binding activity were studied[19]. The study compared three interaction networks: the human extracellular heparin sulfate interactome, the extracellular protein interactome and the extracellular none-heparin sulfate interactome. The comparison found that the heparin sulfate interactome has a relatively higher clustering coefficient, and of course a relatively shorter characteristic path length, which indicates the interactome of heparin sulfate has a higher tendency to form clusters and stronger tendency to form highly interconnected modules than other extracellular proteins (Figure 5).

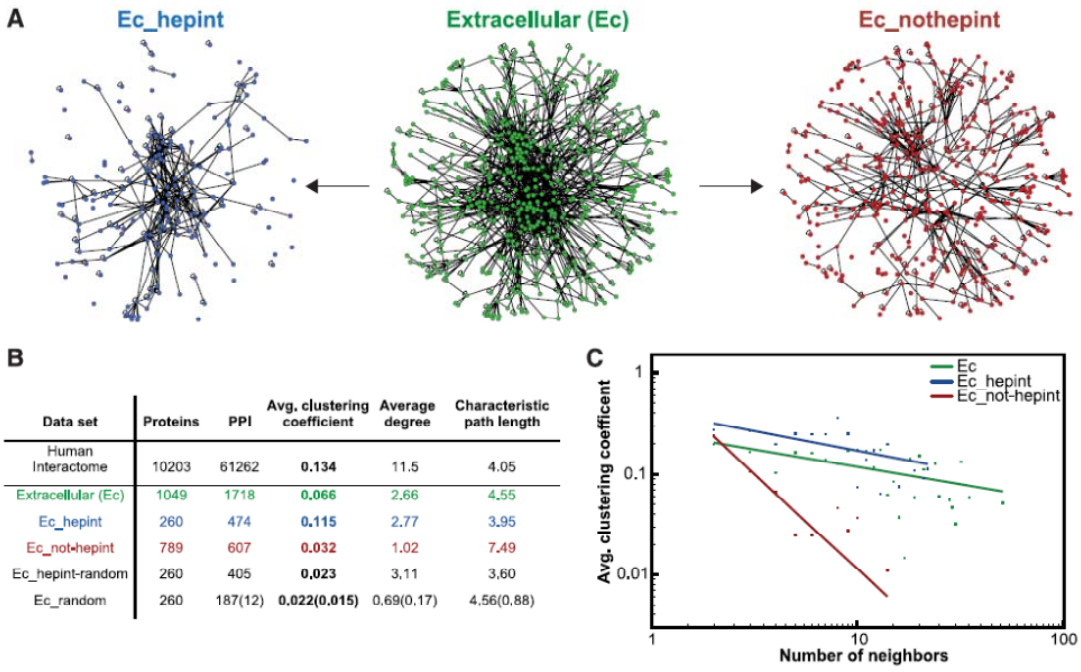

Data set	Proteins	PPI	Avg. clustering coefficient	Average degree	Characteristic path length
Human Interactome	10203	61262	**0.134**	11.5	4.05
Extracellular (Ec)	1049	1718	**0.066**	2.66	4.55
Ec_hepint	260	474	**0.115**	2.77	3.95
Ec_not-hepint	789	607	**0.032**	1.02	7.49
Ec_hepint-random	260	405	**0.023**	3.11	3.60
Ec_random	260	187(12)	**0.022(0.015)**	0.69(0.17)	4.56(0.88)

Figure 5 The comparison of the human extracellular heparin sulfate interactome, the extracellular interactome and the extracellular none-heparin sulfate interactome. (A Systems Biology Approach for the Investigation of the Heparin/Heparan Sulfate Interactome, The Journal Of Biological Chemistry, 2011)

As indicated by the clustering coefficient and the average characteristic path length of heparin sulfate interactome network, several highly clustered modules were found within the network, including VEGFB and transforming growth factor-β2 (TGFβ2) and their transmembrane receptors, structural components of the ECM such as fibrillins (Figure 6). These modules support the view of heparan sulfate proteoglycans as key mediators of the protein complexes at the cell surface and in the extracellular space.

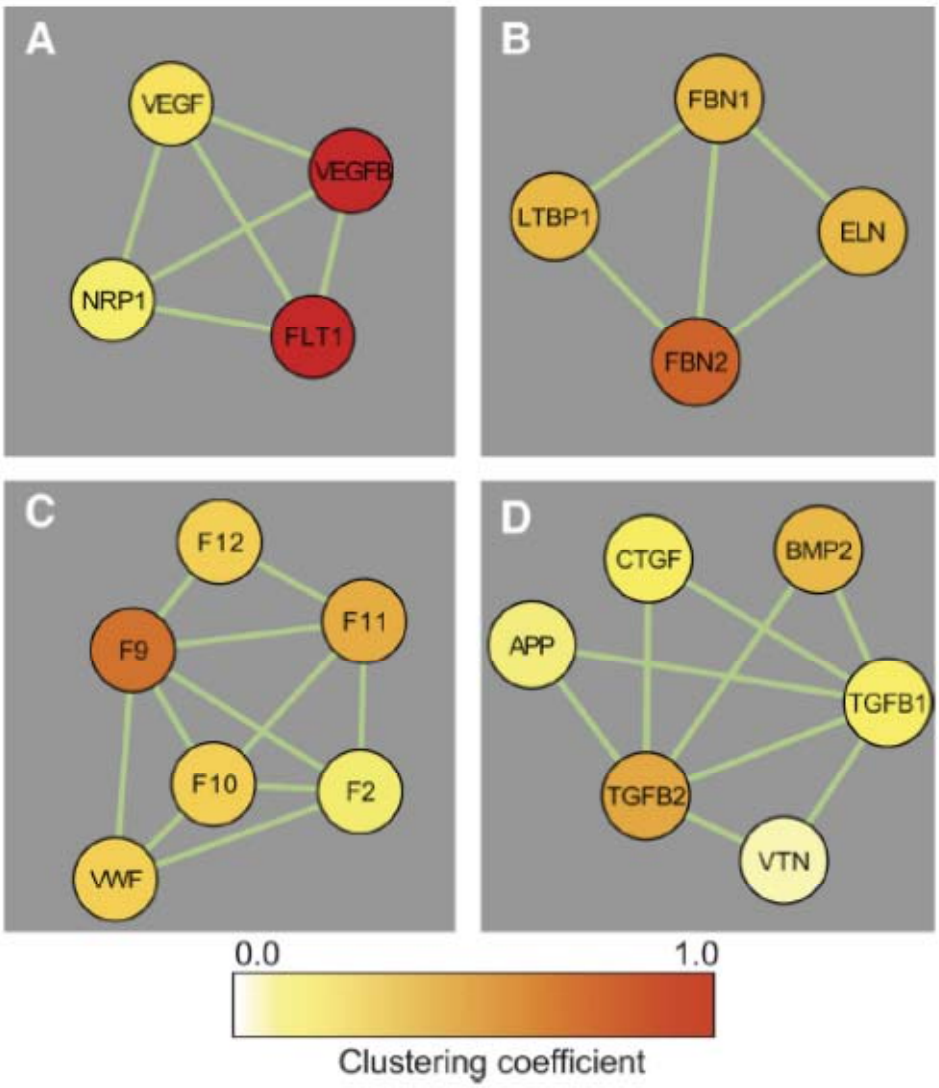

Figure 6 The highly clustered modules located within the heparin sulfate interactome network . (A Systems Biology Approach for the Investigation of the Heparin/Heparan Sulfate Interactome, The Journal Of Biological Chemistry, 2011)

The gene ontology analysis on the heparin sulfate interactome network provides a universal view of biological processes that are associated with the network (Figure 7). Crucial processes including “response to wounding”, “taxis”, “chemotaxis”, “inflammatory response” etc. were significantly over-represented by the proteins of

the interactome, which facilitate the understanding of the functional role of the interaction between heparin sulfate and its interactome as well as the interactome network.

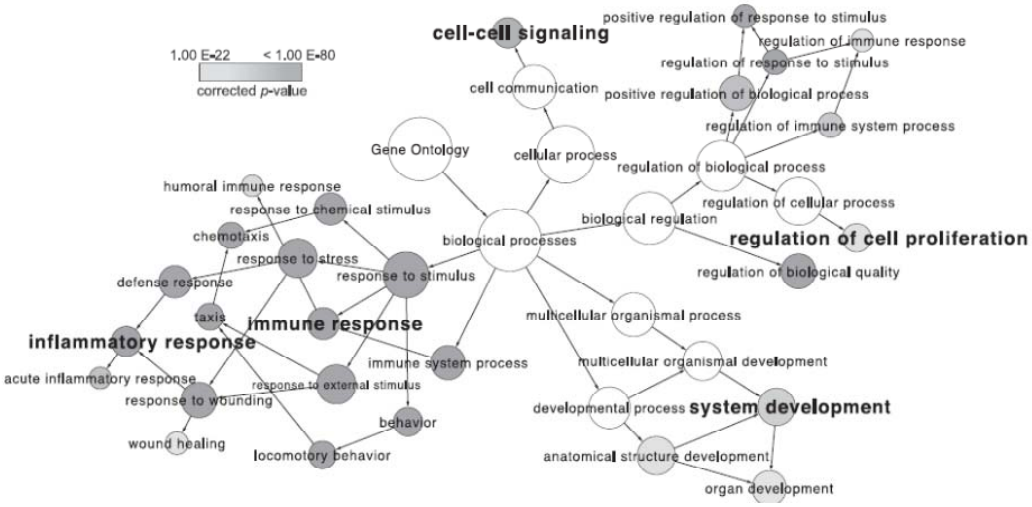

Figure 7 Hierarchies and relationships of the over-represented biological processes for the heparin sulfate network. (A Systems Biology Approach for the Investigation of the Heparin/Heparan Sulfate Interactome, The Journal Of Biological Chemistry, 2011)

In the present thesis, the iTRAQ quantitative proteomics approach was employed to study the cardiac ischemia/reperfusion pathological condition in mice model. The functions of modulated proteins including PARK7and PPIA were further studied in the *in vitro* model using H9C2 cells. Immunoprecipitation coupled with the label-free technique was applied on PPIA interactome study. The secretome of H9C2 cells under hypoxia and reoxygenation were studied by both the iTRAQ and label-free proteomics methods. Bioinformatics techniques were used for further analysis of the regulated secreted proteins under the oxidative stress.

Chapter 2. Metabolic Adaptation to a Disruption in Oxygen Supply During Myocardial Ischemia and Reperfusion is Underpinned by Temporal and Quantitative Changes in the Cardiac Proteome

Xin Li[1], Fatih Arslan[2], Ren Yan[1], Sunil S Adav[1], Kian Keong Poh[3], Vitaly Sorokin[3], Chuen Neng Lee[3,4], Dominique de Kleijn[2], Sai Kiang Lim[5]*, Siu Kwan Sze[1]*

[1]School of Biological Sciences, Nanyang Technological University, 60 Nanyang Drive, Singapore 637551.

[2] Experimental Cardiology Laboratory, Cardiology, University Medical Center Utrecht, the Netherlands & Interuniversity Cardiovascular Institute of the Netherlands, Utrecht, the Netherlands.

[3] National University Heart Centre, Department of Cardiac, Thoracic & Vascular Surgery, Singapore 119228.

[4]Department of Surgery, Yong Loo Lin School of Medicine, Singapore 119228.

[5]Institute of Medical Biology, 8A Biomedical Grove, #05-505 Immunos, Singapore 138648

Corresponding author

Siu Kwan SZE
School of Biological Sciences,
Nanyang Technological University,
60 Nanyang Drive, Singapore 63755
Tel: (+65)6514-1006, Fax: (+65)6791-3856
Email: sksze@ntu.edu.sg

Sai Kiang LIM
Institute of Medical Biology,
8A Biomedical Grove, #05-505 Immunos, Singapore 138648
Email: saikiang.lim@imb.a-star.edu.sg

Abstract

Despite decades of intensive research, there is still no effective treatment for ischemia/reperfusion (I/R) injury, an important corollary in the treatment of ischemic disease. I/R injury is initiated when the altered biochemistry of cells after ischemia is no longer compatible with an oxygenated microenvironment (or reperfusion). To better understand the molecular basis of this alteration and subsequent incompatibility, we assessed the temporal and quantitative alterations in the cardiac proteome of a mouse cardiac I/R model by iTRAQ approach at 30 mins of ischemia, and at 60 or 120 mins of reperfusion after 30 mins of ischemia using sham operated mouse heart as the baseline control. Of the 509 quantified proteins identified, 109 proteins exhibited significant changes (P-value<0.05) over time and were mostly clustered in four functional groups: Fatty acid oxidation, Glycolysis, TCA cycle and ETC (electron transport chain). Incidentally, these groups are intimately involved in the pivotal metabolic switch from oxidative phosphorylation fueled by fatty acid oxidation to anaerobic glycolysis in cardiac tissues during ischemia. Our data demonstrated that this switch involved temporal and quantitative alterations of the cardiac proteome and that upon reperfusion, reversion of these alterations to a pre-ischemia level required at least 120 mins, suggesting a refractory period in which the ischemic cells cannot adjust to the presence of oxygen. Proteins found to be quantitatively altered during ischemia are therefore candidate targets for mitigating this refractory period and enhancing cellular recovery from an ischemic to a normoxic microenvironment.

Among these proteins, Park7 and Ppia were selected and their functions under hypoxia were investigated *in vitro.*

Keywords

Ischemia, hypoxia, reperfusion, PARK7, PPIA, ROS imbalance, ER stress

Introduction

Cardiovascular disease presents the biggest health challenge in both developed and developing countries. In fact, the primary cause of death in the world is acute myocardial infarction (AMI)[20-22] where blood supply to the heart muscle cell is usually reduced by an occlusion in the coronary artery leading to myocardial infarction. Reperfusion therapy through the removal of the occlusion by thrombolytic therapy, bypass surgery or percutaneous coronary intervention (PCI) is currently the mainstay of treatment for AMI and is responsible for the significant reduction in AMI mortality [23]. The efficacy of reperfusion therapy has increased patient survival including those with severe AMI. However many (65%) of these survivors progress to fatal heart failure within 5 years[24]. The progression of AMI survivor to heart failure patient is a complex multifactorial process that is largely dependent on the size of infarcted myocardium. It has been shown that reperfusion of the severely ischemic tissue itself causes lethal injury, also known as the ischemia/reperfusion (I/R) injury and contribute to the final infarct size in AMI patients undergoing reperfusion therapy[25]. Therefore, alleviating I/R injury could reduce this final infarct size thereby

enhancing the efficacy of reperfusion therapy. However, I/R injury has proven to be intractable to pharmaceutical interventions [26].

Traditional biological studies on ischemia and reperfusion injury

Critical information on the ischemia and reperfusion injury was revealed by intensive studies carried out by traditional biological methods.

Mitochondria and the K^+ channels

The mitochondrion is not just a "powerhouse" of the cell, but also a decision-maker regarding cell survival by use of its built-in machineries of cell death and survival[27-40]. Tremendous molecular events are triggered during ischemia and reperfusion. Many of them originate from or directe to the mitochondria, which makes mitochondria an important target for the disease research.

During ischemia, consumption of ATP by myosin ATPase for contraction ceases soon after the onset of stress, however ATP is consumed by mitochondrial ATPase to maintain mitochondrial membrane potential, causing ATP depletion in ischemic myocardium[41-42]. Intracellular Na^+ concentration increases due to three mechanisms: Na^+ influx via acidosis-driven Na^+-H^+ exchange, un-inactivated Na^+ channels and reduced Na^+ efflux via Na^+-K^+ ATPase[43-47]. Cytosolic Ca^{2+} also accumulates via several ways: the reverse mode operation of Na^+-Ca^{2+} exchange, reduction of Ca^{2+} uptake into the sarcoplasmic reticulum and reduced Ca^{2+} efflux via sarcolemmal Ca^{2+}-ATPase. Limited increase of cytosolic Ca^{2+} to a modest level by ischemia may be due to two mechanisms, which are the inhibition of Na^+-Ca^{2+} exchange by acidosis[47] and Ca^{2+} uptake by the mitochondria[42, 48].

During the reperfusion stage, washout of H^+ accumulated in the extracellular space by reperfusion withdraws inhibition of Na^+-Ca^{2+} exchange in the reverse mode during the ischemia period, resulting in massive Ca^{2+} overload in the cell[43, 46-47]. The overloaded Ca^{2+} activates a Ca^{2+} activated protease calpain, which compromises the Na^+-K^+ pump function. The compromise of the Na^+-K^+ pump delays normalization of Na^+ and thus $Ca2^+$ homeostasis[44]. Respiration of impaired mitochondria produces excessive ROS[42, 49-50], and restoration of mitochondrial membrane potential may facilitate Ca^{2+} influx into the mitochondrial matrix, resulting in mitochondrial Ca^{2+} overload.

Oxygen and water supplied by reperfusion to the ischemic cardiomyocytes which have intracellular hyper-osmolarity, Ca^{2+} overload and fragility of the sarcolemma lead to considerable cell edema and hyper-contraction upon reperfusion, resulting in rupture of the sarcolemma[51].

Mitochondrial permeability transition pore (mPTP), which is a non-specific channel in the mitochondrial inner membrane, allows molecules smaller than 1.5 kDa to pass through[52-54]. mPTP shuts down under physiological conditions but opens in response to various noxious stimuli, including ischemia/reperfusion. Irreversible opening of mPTP eliminates the potential of mitochondrial membrane and thus the capacity of ATP production. Under the stress of ischemia and reperfusion, there are several factors contributing to mPTP opening including elevation of inorganic phosphate(Pi) level, Ca^{2+} overloading to the mitochondria, binding of cyclophilin-D(Cyp-D) and adenine nucleotide translocase(ANT), and the ROS generation.

In the inner membrane of mitochondria, four types of K^+ channels have been located: the ATP-sensitive K^+ channel (mK_{ATP} channel), the Ca^{2+}-activated K^+ channel (mK_{Ca} channel), the voltage-gated KV1.3 K^+ channel and the twin-pore domain TASK-3 K^+ channel. The structure and function of these mitochondrial K^+ channels were yet to be clarified, however their essential roles in cardioprotection against ischemia/reperfusion were observed by previous studies.

Ischemic preconditioning (IPC) was first described by Murry et al[55]. It consists of brief periods (a few minutes) of ischemia, separated from one another by brief periods (a few minutes) of reperfusion prior to a sustained period of ischemia followed by reperfusion. Preconditioning reduces the severity of the I/R injury. Preconditioning also limits I/R arrhythmias and may reduce contractile dysfunction. During IPC, mK_{ATP} channel is activated by PKG downstream of signaling cascades from stimulated G-protein coupled receptor[56-58]. Presumably the activated mK_{ATP} channel induces ROS production at complex I in mitochondria. The ROS signal increases the affinity of the adenosine A2b receptor to adenosine via protein kinase c (PKC)[56, 59-60]. The interaction of adenosine and the A2b receptor upon reperfusion is responsible for the higher level of activation of pro-survival kinases, including extracellular-signal-regulated kinases (ERK), phosphatidylinositol 3-kinases (PI3K) and glycogen synthase kinase-3β (GSK-3β). GSK-3β was found to be phosphorylated by multiple pro-survival signaling pathways; the phosphorylation at Ser9 inactivates GSK-3β. The threshold for mPTP opening was shown to be elevated by inactivation of GSK-3β[61]. mK_{ATP} was found to be regulated by PKG-regulated PKC-ε (PKC-ε1), and the activation of the ion channel induces ROS production, which leads to inhibition of

mPTP opening by PKC-ε2[57-58, 62]. mK_{Ca} channel in the cardiomyocyte induces changes similar to changes induced by opening of the mK_{ATP} channel. Transient activation of the mK_{Ca} channel by NS1619 has been shown to increase ROS production, resulting in transmission of cytoprotective signaling[63-64]; it was also found that protein kinase A(PKA) is an important regulatory mechanism of the mK_{Ca} channel[65].

Role of TLR2 in ischemia and reperfusion

Toll like receptors (TLRs) recognize the pathogen associated molecular patterns (PAMPs) and trigger the downstream pro-inflammatory responses[66]. Besides the PAMPs, it is postulated that molecules released during cell stress such as ischemia may serve as endogenous ligands for TLRs. These endogenous ligands have been termed danger-associated molecular patterns (DAMPs) and can be recognized by TLR2, TLR4 and TLR9. TLR2 and TLR4 are extracellular TLRs and have a wide range of putative endogenous ligands including heat shock proteins, high mobility group box 1 (HMGB1) and breakdown products of fibronectin, heparan sulfate, and hyaluronic acid.

Increasing evidence links TLRs, particularly TLR2 and TLR4, to the deleterious inflammatory effects observed in I/R injury. Reperfusion-induced inflammation is characterized by complement deposition, adhesion molecules up-regulation, inflammatory cell infiltration, and cytokine release[67-70]. Monocytes and lymphocytes are the major immune cells involved in this course and facilitate tissue impairment through secretion of pro-inflammatory cytokines, reactive oxygen species, and

chemokines. Both TLR2(−/−) and TLR4(−/−) render protection against I/R injury resulting in decreased infarct size and improved cardiac function[71-72]. In another study using the Langendorff reperfusion mode, without the detrimental effects of blood components after reperfusion, it was shown that infarct size did not differ between TLR2(−/−) and wild type (WT) hearts, but contractile performance was significantly impaired in WT hearts [73]. Impaired relaxation responses, *aka* no reflow phenomenon, after cardiac I/R injury were seen in isolated coronary arteries of WT mice and TLR2(−/−) mice with WT bone marrow [74]. WT mice with TLR2(−/−) bone marrow showed similar cardiac infarction size to that in complete knockouts mice. However, TLR2(−/−) mice with WT bone marrow were not protected against the cardiac I/R injury [40]. The data indicates the exclusive role of circulating TLR2 to mediate the TLR2-dependent cardiac I/R injury.

Metabolic adaption under ischemia

I/R injury is essentially precipitated by the disruption and then subsequent restoration of oxygen supply to cardiomyocytes. A disruption in oxygen supply is particularly detrimental to the heart which has to maintain a high rate of metabolic activity to sustain ionic homeostasis and an unremitting contractile activity. Although the heart is relatively dexterous in its use of carbon substrates which include glucose, lactate, ketone bodies and amino acids, fatty acids is the preferred carbon source of ATP under normal circumstances and β-oxidation of fatty acids is responsible for >95% of ATP in the heart [75] . When oxygen supply is limiting, ATP synthesis by aerobic metabolism mediated by electron chain transport (ETC)-mediated mitochondrial oxidative phosphorylation is inhibited. To generate ATP, ischemic cardiomyocytes

have to switch to the much less efficient anaerobic glycolytic ATP synthesis that is inadequate to support normal cardiac function. Consequently, ischemic cardiomyocytes have to adapt and curtail some cellular activities to conserve ATP. The extent of this adaptation depends on the degree and duration of ischemia. As ischemia persists with increasing reliance on anaerobic glycolytic ATP synthesis, an ATP deficit grows with an increasing accumulation of metabolic products such as ADP, inorganic phosphates, reduced coenzymes e.g. NADH and FADH and lactic acid. Consequently, ATP-dependent cellular activities such as protein synthesis and turnover, gene transcription, ion pumps or transporters etc are further curtailed, intracellular pH acidifies, ion homeostasis is lost and intracellular osmotic pressure increases[41, 47, 76-77] .

Proteomics-based cardiovascular researches

As the proteomics technique is getting matured, it has been integrated and incorporated into cardiovascular research. Proteomics methodological researches, proteome profiling, quantitation of the modulation on protein abundance as well as post-translational modification (PTM) were carried out to achieve a better understanding of the cardiovascular system and the underlying disease mechanism.

By using protein samples extracted from mouse heart by neutral and acidic buffers, four different fractionation methods, including the high-pH reversed-phase chromatography (pH-RP), SCX, C_8 protein reversed-phase (C_8-RP) and high-recovery protein reversed-phase (hr-RP) column, were compared to evaluate the ability on protein identification[78]. With the pH-RP and hr-RP, 1338 and 1303 proteins were identified from 100 μg and 40 μg of sample, respectively. It was also shown that

acidic buffer containing 15 mM trifluoroacetic acid (TFA) and 1mM TCEP extracted more proteins than the neutral buffer. In the result of pH-RP method, acidic buffer extracted 933 proteins and neutral buffer extracted 405 proteins.

The function and regulation of cardiac 20S proteasome complex were elucidated by a proteomics investigation[79]. The binding partners of cardiac 20S proteasome were identified by native gel electrophoresis coupled with mass spectrometry. Protein phosphatase 2A (PP2A) and protein kinase A (PKA) were found to be the binding partners. The regulation mechanism of the 20S proteasome and its binding partners was further investigated. The phosphorylation of the proteasome was shown to enhance the peptidase activity of individual subunits in a substrate-specific fashion. It was found that α and β subunits of the 20S proteasome are the targets of PKA and PP2A and the phosphorylation may serve as a key mechanism for regulation.

Besides the proteome profile, PTM profile is also a valuable target for proteomics studies. A comprehensive characterization of the murine cardiac mitochondrial phosphoproteome was carried out to provide systemic information about mitochondrial signaling networks, metabolic pathways, and intrinsic mechanisms of functional regulation in the heart[80]. A platform using both collision-induced dissociation (CID) and electron transfer dissociation (ETD) successfully identified 236 phosphorylation sites, of which 210 were novel. These 236 sites were mapped to 181 phosphoproteins and 203 phosphopeptides. That study also found that 45 phosphorylation sites were only captured by CID and 185 sites were only identified by ETD, which underscores the advantage of a combined CID and ETD strategy.

Previous proteomics studies on cardiac ischemia and reperfusion

Although limited numbers of proteomics researches focus on ischemia/ reperfusion injury, valuable targets and mechanism have been identified by systematically studying the pathological condition.

iTRAQ quantitative profiling was performed on cardiac sarcomeric proteins from ischemic and non-ischemic heart tissues to reveal the protein abundance alteration [81]. Left coronary artery ligation was performed to achieve ischemia in rat heart. Sarcomeric proteins from ischemic area and non-ischemic area tissues were extracted by differential centrifugation. The iTRAQ labeled samples were fractionated by nano LC and analyzed by an LTQ running in the pulsed Q dissociation (PQD) mode. About 220 proteins were identified with a 5% false discovery rate (FDR) and 22 proteins were found significantly changed. These data demonstrated that proteins involved in regulating metabolism, chaperone transport, intracellular Ca^{2+}, thin filament length, and cytoskeleton structure changed significantly in abundance with myocardial infarction.

In the study comparing the murine heart mitochondrial proteome alteration between ischemia/reperfusion and cardioprotective treatment including preconditioning (PC) and GSK-3 inhibitor AR-A014418 (GSK Inhib VIII) treatment under the same stress in a Langendorff-perfused model, cytochrome-c oxidase subunits Va and VIb, ATP synthase-coupling factor 6, and cytochrome b-c1 complex subunit 6 were found to increase in abundance while the abundance of cytochrome c was decreased under both protective treatments by 2DE coupled MS[82]. This study suggested cardioprotection through PC and GSK-3 inhibition increased the phosphorylation levels of the complex

IV subunits as well as cytochrome c. Further investigation also showed that PC and GSK-3 inhibition leads to change in mitochondrial supercomplex assembly, and this modulation may contribute to the cardioprotection of PC and GSK-3 inhibition.

The cardioprotection of natural compound Salvianolic acid B (SB) against hypoxia/reperfusion on rat heart myoblast cells H9C2 was investigated by 2DE MS[83]. 14 proteins were found to be regulated either between the control group and the SB treated group or between ischemia/reperfusion and ischemia/reperfusion plus SB treatment. Since epidermal growth factor receptor (EGFR) was predicted as the most possible binding target of SB, the protein-protein interaction network between EGFR and the regulated proteins was generated by adopting protein interaction databases HPRD, MINT, IntAct, Database of Interacting Proteins (DIP), biogrid and MIPS. Only the shortest pathways were used in the network. It is found that the 9 out of 14 regulated proteins could be included into the network with direct connection or only one intermediate partner to EGFR, which shows the signal cascade triggered by binding of SB to EGFR and reveals the underlying mechanism of the cardioprotective effect of SB.

During heart failure which is induced by ischemia in some cases, ROS is produced by imperfect coupling of mitochondrial respiration. The secreteome from cardiac myocyte and fibroblast under oxidative stress were analyzed by one dimensional LC coupled with MS[84]. It is found that H_2O_2 caused an elevated cystatin C protein and 126-amino acid pro hormone (ProANP) in the conditioned medium from cardiomyocytes. The study of modulation on cystatin C was then extended to *in vivo* models of heart failure. Both chronic administrations of doxorubicin and myocardial

ischemia by left anterior descending coronary artery occlusion lead to an increase in the level of cystatin C protein in the plasma. In myocardial tissues from the ischemic area, an increase of cystatin C correlates with the inhibition of cathepsin B activity and accumulation of fibronectin and collagen I/III. Overexpressing the cystatin C gene or exposing fibroblasts to cystatin C protein leads to the inhibition of cathepsin B and fibronectin and collagen I/III accumulation. This finding indicates that cystatin C can be a molecular target for blocking the detrimental effect of ECM remodeling.

Oxygen is reduced by two pathways in cardiomyocytes: the prevailing pathway is via the mitochondrial electron transport system, which reduces 95% of oxygen to H_2O; the remaining 5% of oxygen is processed by intracellular enzymes to produce ROS. The antioxidant defense system may be undermined and ROS-induced damage to the tissue can occur under certain pathological conditions such as I/R. Proteomics approach have been employed to study the ROS stress on cardiac myocyte and the effects of antioxidants on ROS-induced oxidative stress associated with I/R.

Hydrogen peroxide treatment of H9C2 rat cardiomyocytes is used as a model of oxidative stress in heart ischemia–reperfusion injury. Coupling anti-phosphotyrosine affinity purification with LC-MS/MS, A total of 23 proteins were identified with high confidence in the H_2O_2 treated group, including platelet-derived growth factor receptor-β and γ-adducin; and 3 proteins were immunoprecipitated and identified from the untreated cells [85]. A significant fraction of the identified proteins including catenin-α1, catenin-β1, cortactin-Src substrate, focal adhesion kinase-2 (FAK2), breast cancer anti-estrogen resistance protein-1, platelet-derived growth factor receptor-β (PDGFRβ), and focal adhesion kinase-1 associate with the Src kinase. This

indicates the important role of Src kinase in mediating H_2O_2-induced tyrosine phosphorylation events, which is validated by the reduced H_2O_2-induced tyrosine phosphorylation with Src kinase inhibitor PP1 treatment. The function of Src kinase in H_2O_2-induced loss of cell adhesion and viability was further studied. Partially rescuing H_2O_2-induced protein expression changes that may be involved in H9C2 cell survival and/or adhesion by blocking Src kinase activity was shown by global protein profiling with 2DE MS.

The antioxidative role of Glutathione peroxidase 1 (GPx1) was studied by 2DE MALDI-TOF approach in a GPx1 knockout mice model[86]. The proteome alteration between wild type mice and GPx1 knockout mice under hypoxia-reperfusion condition was analyzed. 36 proteins showed differentiated abundance between the wild type and knockout mice. By gene ontology analysis, "carbohydrate transport and metabolism proteins," "cytoskeletal proteins," "proteins involved in signal transduction," "proteins involved in energy production and conversion," and "intracellular trafficking and secretion proteins" were found to associate with these altered proteins. 16 down-regulated proteins were localized in mitochondria and involved in several crucial metabolic pathways including tricarboxylic acid cycle, glucose metabolism, and oxidative phosphorylation. As a protein that increases the resistance of cells to oxidative injury induced by H_2O_2 exposure[87] and minimizes the infarct size, improves the contractile function, and attenuates cardiac IR injury[88], HSP27 was also found down regulated in the absence of GPx1, which shows the reduced ability of mitochondria to cope with reoxygenation-induced ROS generation in GPx1 knockout mice.

To better understand I/R injury and to identify novel candidate targets for therapeutic intervention, we took advantage of the recent advances in proteomics and bioinformatics to monitor relative quantitative changes in the cardiac proteome over time during ischemia and reperfusion to identify the critical changes in biochemical activity in the cardiomyocytes. By applying an iTRAQ approach, novel proteins that exhibited dynamic quantitative changes in the heart tissues of a mouse model of myocardial I/R injury were identified. These regulated proteins were functionally classified and mechanisms that could initiate the detrimental cascade of reperfusion injury were discussed; functions of two regulated proteins, *i.e.* PARK7 and PPIA were further studied in rat heart myoblast cell line H9C2. We showed that over-expression of PARK7 significantly improves cell survival under hypoxia stress. Interactome analysis reveals that many proteins are associated with PPIA after 16hr hypoxia treatment, which may contribute to protein folding assistance under limited oxygen supply condition.

Materials and methods

Experimental design

All animal experimentations were performed in the Experimental Cardiology Laboratory, University Medical Center Utrecht, Netherlands in accordance with the national guidelines on animal care and with prior approval by the Animal Experimentation Committee of Utrecht University.

In vivo myocardial ischemia-reperfusion injury

Male mice C57Bl6/J (10-12 wks, 25-30 g) received standard diet and water *ad libitum*. Mice were anesthetized with a mixture of Fentanyl (Jansen-Cilag) 0.05 mg/kg, Dormicum (Roche) 5 mg/kg, and medetomidine 0.5 mg/kg through an intraperitoneal injection. Atropine 0.05 mg/kg SC was administered after coronary ligation. The body temperature was maintained at 37±1°C during surgery using automatic heating blanket. Mice were incubated and ventilated (Harvard Apparatus Inc.) with 100% oxygen. The left coronary artery (LCA) was ligated for 30 mins followed by reperfusion using an 8-0 vicryl suture with a section of polyethylene-10 tubing placed over the LCA. Total occlusion and subsequent ischemia was confirmed by bleaching of the myocardium and ventricular tachyarrhythmia. Reperfusion was initiated by releasing the ligature and removing the polyethylene-10 tubing. In sham operated animals, the same operation procedure was performed except that the suture was placed beneath the LCA without ligation. Reperfusion of the endangered myocardium was characterized by typical hyperemia in the first few mins. We have shown that the above mentioned protocol is highly reproducible and results in ~40% ischemic myocardium (area at risk; AAR) of the total left ventricle[40, 89-91]. The infarct size (IS; necrotic core) within the AAR (IS/AAR) is dependent on the reperfusion time. We and others have shown that 30 mins ischemia followed by 120 mins reperfusion results in ~20% IS/AAR, whereas 24-hours reperfusion results in ~38% IS/AAR[40, 89-92]. For monitoring the proteome alteration during ischemia and the onset of reperfusion, 30 mins ischemia, 60 mins and 120 mins reperfusion time points were chosen. During these time points, selective protein degradation occurs induced by oxidative stress from ROS burst in the

early phase of reperfusion[77]. Before harvesting, the hearts were flushed with 1M HEPES buffer (Invitrogen). The right ventricles were removed and the left ventricles *in toto* were snap frozen in liquid nitrogen and subsequently stored in -80°C until use. 3 animals were used for each condition.

In vitro hypoxia model

Rat heart myoblast H9C2 was purchased from American Type Culture Collection (ATCC, Manassas, VA, USA). Cells were cultured in Dulbecco's Modified Eagle Medium (DMEM) containing 10% fetal bovine serum. At 80% confluence, cells were washed with PBS and then incubated in serum free DMEM. The cells were then subjected to hypoxia by incubating the cells in GasPak EZ Anaerobe Pouch System (BD, MD, USA) for 16 hours. Both cells in serum free medium as control and cells in GasPak system were cultured in a humidified incubator containing 95% air/5% CO_2. All media and supplements were bought from Gibco, Invitrogen (Invitrogen, Carlsbad, CA, USA).

Protein extraction

The biological replicates of either operated or sham-operated heart at each time point were pooled, cut into small pieces and then homogenized in liquid nitrogen using a mortar with pestle. The tissue powders were collected and lyzed with a buffer containing 50mM triethylammonium bicarbonate (TEAB) (pH8.5), 1% SDS, Complete protease inhibitor cocktail tablet and PhosSTOP phosphatase inhibitor cocktail tablets (Roche Molecular Biochemicals, Mannheim, Germany). The samples were then sonicated by VCX500 sonicator (Sonics and Material, Connecticut, USA) with 25% amplitude and 8s pulse in 3 cycles. After centrifugation at 20,000 x g for

15mins at 4°C, proteins in the supernatant were quantified using the BCA Protein Assay kit.

iTRAQ labeling and LC-MS/MS analysis

The protein samples were reduced by TCEP, alkylated with MMTS and digested with trypsin as previously reported[93-94]. The tryptic peptides from mice subjected to sham operation, 30 mins cardiac ischemia, 60 mins or 120 mins reperfusion following ischemia were labeled with 114, 115, 116 and 117 4-plex iTRAQ tag respectively. The iTRAQ labeling of peptide samples were performed using the iTRAQ reagent multiplex kit (Applied Biosystems, Foster City, CA, USA) according to the manufacturer's protocol. The peptides were labeled with respective isobaric tags, incubated for 2 h, then combined into a single sample and vacuum centrifuged to dryness. The vacuum dried samples were reconstituted in Buffer A (10 mM KH_2PO_4, 25% acetonitrile, pH 2.85) and iTRAQ labeled peptides were fractionated using PolySULFOETHYL A^{TM} SCX column (200 x 4.6 mm, 5 μm particle size, 200 Å pore size) by an HPLC system (Shimadzu, Japan) at a flow rate of 1.0 ml min^{-1}. The 50 mins HPLC gradient consisted of 100% buffer A (10 mM KH_2PO_4, 25% acetonitrile, pH 2.85) for 5 mins; 0-20% buffer B (10 mM KH_2PO_4, 25% ACN, 500 mM KCl, pH 3.0) for 15 mins; 20-40% buffer B for 10 mins; 40-100% buffer B for 5 mins followed by 100% buffer A for 10 mins. During sample fractionation, chromatograms were recorded at 214 nm. In total, 50 fractions were collected, concentrated to dryness using a vacuum centrifuge, and then combined to 19 fractions according to the 214nm reading in the LC spectrum and reconstituted in 0.1% trifluroacetic acid and desalted with Sep-Pak Vac C18 cartridges (Waters, Milford, MA, USA). After desalting,

samples were again concentrated to dryness by vacuum centrifugation and reconstituted in 100 µL of 0.1% formic acid for LC-MS/MS analysis.

The mass spectrometric analysis of the iTRAQ labeled sample was performed in triplicate using a Q-Star Elite mass spectrometer (Applied Biosystems; MDS-Sciex, USA), coupled with an online micro flow HPLC system (Shimadzu, JAPAN). The peptides were separated using a nanobored C18 column with a picofrit nanospray tip (75 µm ID x 15 cm, 5 µm particles) (New Objectives, Wuburn, MA, USA). The flow rate was maintained at 20 µL min^{-1} and the separation was performed with a splitter to get an effective flow rate of 0.2 µL min^{-1}. The MS data were acquired in the positive ion mode with a selected mass range of 300-2000 m/z. Peptides in +2 to +4 charge states were selected for MS/MS. The three most abundantly charged peptides above a 10 count threshold were selected for MS/MS and dynamically excluded for 30 sec with ±30 mDa mass tolerance. Smart information-dependent acquisition (IDA) was activated with automatic collision energy and automatic MS/MS accumulation. The fragment intensity multiplier was set to 20 and the maximum accumulation time was 2 sec. The peak areas of the iTRAQ reporter ions reflect the relative abundance of the proteins in the samples.

For in-gel digestion each dried fraction was reconstituted in 100 µl of 0.1% formic acid and analyzed using an LTQ-FT Ultra mass spectrometer (Thermo Electron) coupled with a Prominence^{TM} HPLC unit (Shimadzu, JAPAN). For each analysis, the sample was injected from an autosampler (Shimadzu, JAPAN) and concentrated in a Zorbax peptide trap (Agilent, Palo Alto, CA, USA). The peptide separation was performed in a capillary column (200 µm inner diameter × 10 cm) packed with C_{18}

AQ (5 μm particles, 300 Å pore size; Michrom Bioresources, Auburn, CA, USA). Mobile phase A (0.1% formic acid in H_2O) and mobile phase B (0.1% formic acid in acetonitrile) were used to establish the 90 mins gradient comprising 3 mins of 0–5% B and then 52 mins of 5–25% B followed by 19 mins of 25–80% B, maintenance at 80% B for 8 mins, and finally re-equilibration at 5% B for 8 mins. The HPLC system was operated at a constant flow rate of 30 μL min^{-1}, and a splitter was used to create a flow rate of ~500 nL min^{-1} at the electrospray emitter (Michrom Bioresources). Samples were injected into an LTQ-FT through an ADVANCE™ CaptiveSpray™ source (Michrom Bioresources) with an electrospray potential of 1.5 kV. The gas flow was set at 2, ion transfer tube temperature was 180 °C, and collision gas pressure was 0.85 millitorr. The LTQ-FT was set to perform data acquisition in the positive ion mode as described previously[95]. Briefly, a full MS scan (350–2000 *m*/*z* range) was acquired in the FT-ICR cell at a resolution of 100,000 and a maximum ion accumulation time of 1000 ms. The automatic gain control target for FT was set at 1*e*+06, and precursor ion charge state screening was activated. The linear ion trap was used to collect peptides and to measure peptide fragments generated by CID. The default automatic gain control setting was used (full MS target at 3.0*e*+04, MS^n at 1*e*+04) in the linear ion trap. The 10 most abundant ions above a 500-count threshold were selected for fragmentation in CID (MS^2), which was performed concurrently with a maximum ion accumulation time of 200 ms. For CID, the activation Q was set at 0.25, isolation width (*m*/*z*) was 2.0, activation time was 30 ms, and normalized collision energy was 35%.

Mass spectrometric data analysis

The iTRAQ data acquisition was performed with the Analyst QS 2.0 software (Applied Biosystems/MDS SCIEX). Protein identification and quantification were performed using the ProteinPilot Software 2.0.1, Revision Number: 67476 (Applied Biosystems, Foster City, CA, USA). The Paragon algorithm in the ProteinPilot software was used for the peptide identification which was further processed by the Pro Group algorithm where isoform-specific quantification was adopted to trace the differences between expressions of various isoforms. User defined parameters were as follows: (i) Sample Type, iTRAQ 4-plex (Peptide Labeled); (ii) Cysteine alkylation, MMTS; (iii) Digestion, Trypsin; (iv) Instrument, QSTAR Elite ESI; (v) Special factors, None; (vi) Species, None; (vii) Specify Processing, Quantitate; (viii) ID Focus, biological modifications, amino acid substitutions; (ix) Database, concatenated mouse database (target: IPI mouse, version 3.55, 55956 sequences; 25155114 residues) and the corresponding reverse sequence (decoy: for false discovery rate (FDR) estimation); (x) Search effort, thorough. For iTRAQ quantitation, the peptide for quantification was automatically selected by the Pro Group algorithm to calculate the reporter peak area, error factor (EF) and P-value. The resulting data was auto bias-corrected to get rid of any variations imparted due to the unequal mixing when combining different labeled samples. During bias correction, the software identifies the median average protein ratio and corrects it to unity, and then applies this factor to all quantitation results. Bias correction is performed only when there are at least 20 proteins having an average ratio. If there are fewer than 20 proteins with ratios, the sample size is too small for the median to be meaningful and no bias correction is applied.

Label-free experiment - The extract_msn (version 4.0) program found in Bioworks Browser 3.3 (Thermo Electron, Bremen, Germany) was used to extract tandem MS spectra in the dta format from the raw data of LTQ-FT ultra. These dta files were then converted into MASCOT generic file format using an in-house program. Intensity values and fragment ion *m*/*z* ratios were not manipulated. This data was used to obtain protein identities by searching against the IPI rat protein database (version 3.40; 40381 sequences) by means of an in-house MASCOT server (version 2.2.03) (Matrix Science, Boston, MA, USA), 40381 decoy sequences (reverse IPI rat sequences) were also included in the database to estimate the FDR. The search was limited to a maximum of 2 missed trypsin cleavages; #^{13}C of 2; mass tolerances of 10 ppm for peptide precursors; and 0.8 Da mass tolerance for fragment ions. Fixed modification was carbamidomethylation Cys residue(s), whereas variable modification was oxidation at Met residue(s). The search results were exported as Microsoft CSV files. FDR was controlled at below 1%. Spectrum count of each identified protein wasextracted from CSV files by an in-house script. The spectrum count of the identified proteins was compared between control and Ppia+ condition. For the IP experiment under hypoxia and normoxia, spectrum count of binding partners was normalized by spectrum number of Ppia.

Interaction network – Uniprot annotated human proteins from Human Protein Reference Database (HPRD)[96] and IntAct[97] database were extracted with the interaction information. 31037 and 41302 pairs of interaction respectively were obtained. In total 56878 pairs of interactions were extracted after combination and an in-house database was generated based on this. Interactome information acquired in

the present IP study was added to the in-house human interaction database. Shortest pathway within the Ppia interactome was calculated by an in-house script and visualized by Cytoscape[98].

Results and discussion

Proteomic data analysis

An LC-MS/MS shotgun approach with iTRAQ-based quantification was used to analyze the whole proteome of the C57Bl6J mouse heart tissue subjected to ischemia-reperfusion. Proteome variation between sham (labeled with 114 tag), 30 mins ischemia (115 tag), 60 mins/120 mins reperfusion after 30 mins ischemia (116 tag, 117 tag respectively) was acquired.

Raw data was searched by ProteinPilot 2. The protein inference problem was handled by the Pro Group algorithm of ProteinPilot 2 and the representative protein was shown for its protein group. The complete dataset output (protein summary report) from Protein Pilot is summarized in the supplemental data 1. The Unused ProtScore was used to measure the reliability of the protein identification. A ProtScore of 2.0 and 1.3 is equivalent to 99% and 95% confidence in protein identification respectively. The summary also included sequence coverage of the protein with all identified peptides (%Cov), with peptides > 50% confidence (%Cov(50)) and with peptides > 95% confidence (%Cov(95)). In addition, the peptide number used for identifying each protein was listed in supplemental table 2. Peptide number used for each protein quantitation was listed in supplemental table 3.

In total, 513 proteins were identified with <1% FDR, the corresponding lowest ProtScore is 2.64. 509 proteins were quantified by at least 2 peptides with < 1% false discovery rate (FDR= (2×decoy hit/total hit)×100%). The P-value of each iTRAQ ratio is displayed in the supplemental data1. The P-value is a measurement of the certainty of a change in the protein expression level. Thus, if the P-value is <0.05, the confidence of a change in protein expression level is at least 95%, independent of the magnitude of the iTRAQ ratio.

To gain biological insight into regulated proteins, the iTRAQ quantified proteins were functionally classified using UniProt Knowledgebase (UniProtKB) with GO annotation. The 121 proteins with significant changes (P-value<0.05) were categorized into 8 functional groups (Table.1). These include fatty acid metabolism, glycolysis, tricarboxylic acid (TCA) cycle, electron transport chain (ETC), redox homeostasis, apoptosis, glutathione S-transferase and heat shock proteins (Figure 1).

Abundance alteration of electron transport chain, fatty acid oxidation, glycolysis and TCA cycle under ischemia/reperfusion

43 significantly altered proteins were clustered in functional groups involved in ATP synthesis. This is particularly noteworthy as the most prominent effect of ischemia on cardiomyocytes is the inhibition of ATP production by ETC-mediated oxidative phosphorylation driven by protons generated by β-oxidation of fatty acids, causing the cells to switch over to anaerobic glycolysis for ATP production. As reviewed by Lopaschuk et al [99], the latter process is a much less efficient process producing 2 ATPs per glucose molecule against the 31 ATPs per glucose molecule produced during aerobic glycolysis and 105 ATPs by oxidation of one palmitate molecule[99].

However, the former does not consume oxygen while the latter consume 12 and 46 atoms of oxygen, respectively. As a result, this switch from aerobic to anaerobic metabolism during ischemia causes a precipitous decrease in ATP and this is particularly critical for the heart which needs a high rate of ATP production to sustain an unrelenting contractile function. The heart hydrolyses ~30μmole ATP per gram wet weight in a minute at rest with a complete turnover of myocardial ATP pool every ten seconds[100].

Improved cardiac performance did not result from, nor require, increased glycolysis secondary to the activation of pyruvate dehydrogenase complex (PDH). Rather, restoring carbon flux through PDH alone was sufficient to improve mechanical work by postischemic hearts[101] which synthesize most of their ATP through those proteins clustered in fatty acid oxidation and the ETC generally increased during ischemia and 30 mins after reperfusion before they began declining towards the pre-ischemia baseline. On the other hand, the proteins clustered in glycolysis and TCA were reduced during ischemia and 30 minutes after reperfusion before they returned to the pre-ischemia baseline. Some proteins associated with fatty acid oxidation, glycolysis and TCA cycle declined, while others like hexokinase-1 (HEX1), and succinate dehydrogense α/β subunits were up-regulated. Such changes on the abundance are not likely to be only caused by protein synthesis inhibition under tissue ischemia[102]. It may also reflect the net effect of protein depletion due to increased usage of enhancing ATP production and selective inhibition of proteasomal activity which only degrades specific protein under ischemia and reperfusion[77]. Proteins associated with the ETC, namely complex I, II, III, IV and ATP synthase were increased during ischemia and

60 min reperfusion before returning to normal levels after 120 min reperfusion (Figure 1D). The increase in ETC enzymes which contrasted sharply with other enzymes in energy metabolism such as fatty acid production, glycolysis, and the TCA cycle, indicating proteins associated with ETC become inactive and may have a lower turnover rate when there is little or no oxygen to drive ETC activity. As mentioned before, the increased protein levels may be also due to the selective inhibition of proteasomal activity during ischemia[77].

The electron donor NADH generated from the fatty acid oxidation and glycolysis under ischemia, lowered oxygen level and the higher amount of ETC enzymes may lead to electron leak through ubisemiquinone at Q_0 site of complex III and result in ROS production[103-105]. Consistent with this, it was observed that blockage of electron transport enhances the retention of cytochrome c by cardiac mitochondria after reperfusion, decreases the release of ROS from mitochondria and reduces myocardial injury[106-107].

Redox homeostasis and GST proteins declined during ischemia/reperfusion

The redox homeostasis protein including peroxiredoxin-1 (PRDX1), peroxiredoxin-5 (PRDX5), thioredoxin-dependent peroxide reductase (PRDX3), thioredoxin (TXN1), protein disulfide-isomerase A3 (PDIA3), superoxide dismutase [CU-ZN] (SOD1), superoxide dismutase [Mn] (SOD2) and protein DJ-1 (PARK7) were reduced due possibly to depletion from increased cellular usage during ischemia and/or 60 mins reperfusion, which shows the deficiency of cellular antioxidative stress function (Figure 1 E). The decrease of SOD level or activity during cardiac ischemia reperfusion has been reported earlier[108-109]. After 120 mins reperfusion, the levels of

PRDX1, PRDX3 and SOD2 were significantly restored as well as the peroxiredoxin-2 (PRDX2) and SOD1 that had no change during the first two time point, indicating a protective but delayed response. The glutathione S-transferases including glutathione S-transferase P 1 (GSTP1), glutathione S-transferase kappa 1 (GSTK1), glutathione S-transferase mu 1 (GSTM1), glutathione S-transferase mu 2 (GSTM2) and glutathione S-transferase A4 (GSTA4) were decreased following ischemia and reperfusion (Figure 1 F).

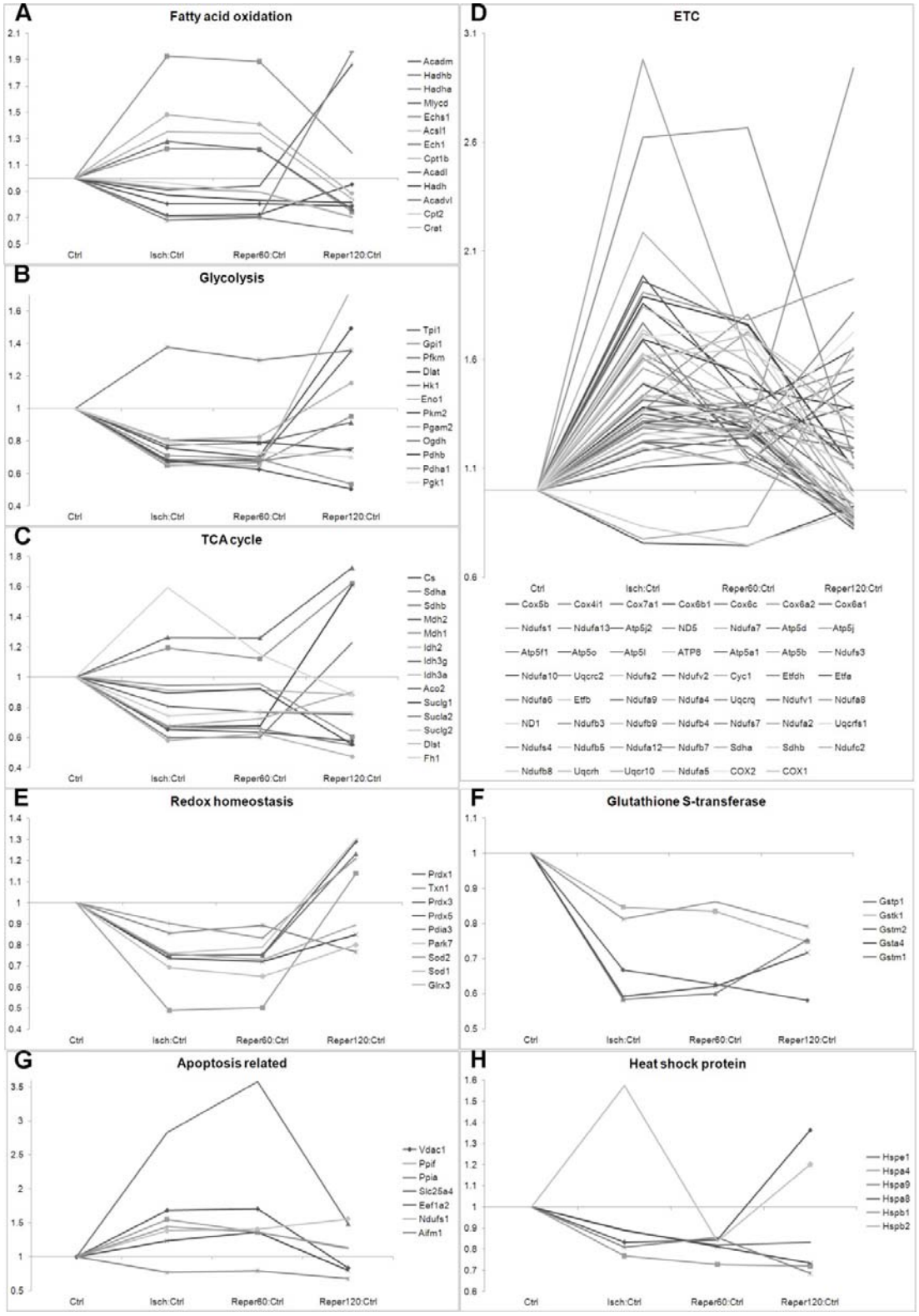

Figure 1. Functional classification on regulated proteins with iTRAQ ratio

FUNCTIONAL GROUP	IPI	GENE SYMBOL	ISCH:CTRL	P-VALUE	REPER60:CTRL	P-VALUE	REPER120:CTRL	P-VALUE
FATTY ACID OXIDATION	IPI:IPI00134961.1	ACADM	0.72	6.14E-17	0.72	3.59E-17	0.95	2.24E-02
	IPI:IPI00115607.3	HADHB	1.22	2.57E-03	1.22	1.14E-03	0.75	6.88E-17
	IPI:IPI00223092.5	HADHA	1.28	3.44E-17	1.22	5.98E-15	0.76	5.39E-33
	IPI:IPI00114866.1	MLYCD	0.87	2.63E-01	0.83	7.65E-02	0.82	9.89E-03
	IPI:IPI00454049.4	ECHS1	0.68	2.93E-10	0.70	5.61E-08	0.59	8.81E-20
	IPI:IPI00112549.1	ACSL1	1.48	2.36E-10	1.41	1.44E-10	0.88	1.86E-04
	IPI:IPI00130804.1	ECH1	0.91	1.36E-01	0.94	2.91E-01	1.86	4.84E-03
	IPI:IPI00136563.	CPT1B	1.35	1.54E-	1.34	2.85E-	0.84	1.41E-

	4			03		03		05
	IPI:IPI00119114.2	ACADL	0.71	1.37E-24	0.71	2.60E-27	1.96	3.77E-07
	IPI:IPI00121105.2	HADH	0.81	3.19E-03	0.81	1.59E-03	0.79	2.01E-06
	IPI:IPI00119203.4	ACADVL	1.93	4.11E-03	1.89	4.01E-03	1.19	9.27E-01
	IPI:IPI00881401.1	CPT2	0.96	6.76E-01	0.90	2.96E-01	0.71	2.20E-04
	IPI:IPI00113347.3	CRAT	0.93	5.10E-02	0.89	8.52E-03	0.70	1.42E-05
GLYCOLYSIS	IPI:IPI00467833.5	TPI1	0.76	1.07E-10	0.70	1.31E-20	1.50	3.74E-02
	IPI:IPI00228633.7	GPI1	0.65	5.48E-12	0.67	6.53E-10	0.95	7.10E-02
	IPI:IPI00331541.5	PFKM	0.77	1.64E-07	0.79	9.35E-07	0.91	8.90E-03
	IPI:IPI00153660.	DLAT	0.81	4.33E-	0.80	2.11E-	0.74	4.54E-

	4			03		03		06
	IPI:IPI00283611.1	HK1	1.38	1.34E-02	1.30	7.58E-03	1.36	1.39E-03
	IPI:IPI00462072.3	ENO1	0.81	7.41E-04	0.82	4.59E-03	1.16	5.95E-03
	IPI:IPI00845840.1	PKM2	0.67	1.80E-22	0.69	1.79E-23	1.35	9.25E-02
	IPI:IPI00230706.5	PGAM2	0.65	6.16E-04	0.65	2.37E-04	1.73	2.09E-01
	IPI:IPI00626237.2	OGDH	0.69	7.81E-24	0.67	1.01E-27	0.75	1.17E-37
	IPI:IPI00132042.1	PDHB	0.68	4.76E-16	0.62	5.74E-19	0.50	5.39E-28
	IPI:IPI00337893.2	PDHA1	0.71	5.69E-05	0.69	4.51E-06	0.53	1.38E-11
	IPI:IPI00555069.3	PGK1	0.80	1.19E-05	0.73	1.77E-08	0.70	1.71E-12
TCA CYCLE	IPI:IPI00113141.	CS	0.66	2.72E-	0.63	6.12E-	0.58	2.85E-

	1			04		05		11
	IPI:IPI00230351.1	SDHA	1.19	2.35E-05	1.12	4.53E-04	1.62	6.52E-41
	IPI:IPI00338536.1	SDHB	1.26	6.19E-05	1.26	1.81E-06	1.72	2.82E-31
	IPI:IPI00323592.2	MDH2	0.67	9.59E-41	0.68	3.60E-38	1.61	2.00E-05
	IPI:IPI00336324.11	MDH1	0.60	2.38E-33	0.60	2.70E-34	1.23	1.09E-01
	IPI:IPI00318614.9	IDH2	0.58	2.10E-36	0.63	1.09E-37	0.47	0.00E+00
	IPI:IPI00109169.1	IDH3G	0.81	3.61E-04	0.77	2.04E-05	0.75	5.88E-14
	IPI:IPI00459725.2	IDH3A	0.91	2.24E-01	0.91	2.53E-01	0.88	5.18E-04
	IPI:IPI00116074.1	ACO2	0.67	5.75E-40	0.66	0.00E+00	0.55	0.00E+00
	IPI:IPI00406442.	SUCLG1	0.90	8.06E-	0.92	2.17E-	0.55	1.28E-

	2			02		01		19
	IPI:IPI00261627.1	SUCLA2	0.95	2.88E-01	0.96	3.91E-01	0.61	2.17E-15
	IPI:IPI00459487.3	SUCLG2	1.60	6.01E-01	1.15	3.44E-01	0.89	2.68E-02
	IPI:IPI00134809.2	DLST	0.68	2.11E-05	0.73	1.41E-04	0.90	3.62E-02
	IPI:IPI00129928.2	FH1	0.74	2.39E-11	0.77	8.32E-08	0.77	3.42E-13
ETC	IPI:IPI00785410.1	COX5B	1.86	7.49E-14	1.47	3.95E-16	1.38	1.44E-13
	IPI:IPI00117978.1	COX4I1	1.38	5.77E-12	1.25	1.05E-09	0.86	2.97E-07
	IPI:IPI00113196.1	COX7A1	1.22	1.32E-01	1.20	1.56E-01	0.82	2.32E-05
	IPI:IPI00225390.5	COX6B1	1.69	2.43E-05	1.53	7.92E-06	1.11	1.04E-02
	IPI:IPI00131771.	COX6C	1.96	4.70E-	1.76	5.79E-	1.10	8.81E-

	3			08		09		02
	IPI:IPI00320238.3	COX6A2	1.43	5.14E-02	1.81	4.51E-03	0.97	5.90E-01
	IPI:IPI00121443.1	COX6A1	1.31	4.32E-02	1.40	8.94E-03	1.24	6.07E-01
	IPI:IPI00308882.4	NDUFS1	1.38	4.43E-21	1.40	4.01E-30	1.56	1.05E-03
	IPI:IPI00230715.5	NDUFA13	1.42	1.37E-03	1.35	2.15E-03	1.00	9.58E-01
	IPI:IPI00271986.6	ATP5J2	1.89	1.49E-09	1.76	3.50E-08	1.10	7.76E-02
	IPI:IPI00553262.1	ND5	1.32	1.19E-03	1.31	1.78E-03	1.52	2.99E-01
	IPI:IPI00130322.5	NDUFA7	1.56	2.03E-04	1.38	9.02E-03	1.20	8.14E-01
	IPI:IPI00453777.2	ATP5D	1.99	2.81E-01	1.38	6.54E-01	1.65	4.85E-11
	IPI:IPI00125460.	ATP5J	1.23	2.84E-	1.26	2.93E-	2.94	1.06E-

	1			02		03		10
	IPI:IPI00341282.2	ATP5F1	1.49	6.95E-11	1.31	2.71E-08	0.87	9.41E-08
	IPI:IPI00118986.1	ATP5O	1.38	7.69E-08	1.29	3.12E-07	0.84	1.29E-07
	IPI:IPI00876323.1	ATP5L	1.77	3.83E-01	1.15	7.16E-02	0.90	1.21E-02
	IPI:IPI00116896.1	ATP8	2.19	2.07E-06	1.69	7.33E-05	1.00	9.86E-01
	IPI:IPI00130280.1	ATP5A1	1.18	8.02E-10	1.24	3.84E-13	1.39	0.00E+00
	IPI:IPI00468481.2	ATP5B	1.37	2.48E-02	1.73	6.13E-01	1.29	0.00E+00
	IPI:IPI00121309.2	NDUFS3	1.31	1.27E-05	1.28	3.61E-05	1.19	7.88E-06
	IPI:IPI00116748.1	NDUFA10	1.49	4.92E-06	1.28	2.81E-06	0.84	4.47E-05
	IPI:IPI00119138.	UQCRC2	1.22	2.37E-	1.11	7.22E-	0.88	7.36E-

	1			06		03		08
	IPI:IPI00128023.3	NDUFS2	1.35	1.04E-12	1.34	2.19E-14	1.27	2.07E-18
	IPI:IPI00169925.2	NDUFV2	1.11	3.56E-02	1.13	1.11E-02	1.50	1.28E-12
	IPI:IPI00132728.2	CYC1	1.33	6.10E-11	1.25	7.89E-10	0.84	3.16E-10
	IPI:IPI00121322.2	ETFDH	1.41	4.88E-10	1.38	1.47E-09	1.17	4.52E-08
	IPI:IPI00116753.4	ETFA	0.76	1.35E-21	0.75	4.09E-19	0.93	2.35E-06
	IPI:IPI00133399.1	NDUFA6	1.63	9.29E-08	1.38	3.16E-05	0.85	9.09E-05
	IPI:IPI00121440.4	ETFB	0.83	7.06E-03	0.75	2.86E-08	0.90	1.64E-04
	IPI:IPI00120212.1	NDUFA9	1.35	4.05E-10	1.27	1.12E-10	0.90	2.13E-04
	IPI:IPI00125929.	NDUFA4	1.72	5.87E-	1.53	6.05E-	0.89	1.62E-

	2			05		04		02
	IPI:IPI00224210.5	UQCRQ	2.62	3.51E-05	2.67	6.75E-05	1.15	2.46E-02
	IPI:IPI00130460.1	NDUFV1	1.69	6.02E-02	1.17	3.85E-04	0.94	2.60E-02
	IPI:IPI00120984.5	NDUFA8	1.91	1.47E-09	1.78	1.38E-07	1.97	3.87E-02
	IPI:IPI00341550.1	ND1	1.63	6.17E-01	1.13	4.05E-01	0.86	4.15E-02
	IPI:IPI00133403.1	NDUFB3	1.61	1.14E-01	1.29	4.11E-02	0.88	9.31E-02
	IPI:IPI00132623.3	NDUFB9	1.43	2.22E-02	1.48	2.40E-03	1.12	1.25E-01
	IPI:IPI00132390.5	NDUFB4	2.98	1.23E-02	1.61	7.54E-03	0.91	1.37E-01
	IPI:IPI00120232.1	NDUFS7	1.29	4.47E-02	1.24	5.18E-03	1.82	1.65E-01
	IPI:IPI00315302.	NDUFA2	1.29	4.38E-	1.28	1.31E-	0.94	3.29E-

	5			03		02		01
	IPI:IPI00133240.1	UQCRFS1	1.26	3.91E-03	1.19	2.63E-03	0.98	5.15E-01
	IPI:IPI00229008.2	NDUFS4	0.78	4.19E-02	0.84	2.82E-02	1.66	5.51E-01
	IPI:IPI00132531.1	NDUFB5	1.62	2.88E-02	1.65	1.86E-02	1.32	7.15E-01
	IPI:IPI00344004.3	NDUFA12	1.84	7.16E-04	1.59	9.84E-07	0.97	7.60E-01
	IPI:IPI00133215.3	NDUFB7	1.26	5.78E-02	1.33	8.02E-03	1.12	8.76E-01
	IPI:IPI00230351.1	SDHA	1.19	2.35E-05	1.12	4.53E-04	1.62	6.52E-41
	IPI:IPI00338536.1	SDHB	1.26	6.19E-05	1.26	1.81E-06	1.72	2.82E-31
	IPI:IPI00132050.1	NDUFC2	1.44	3.54E-06	1.33	3.91E-04	0.87	3.00E-03
	IPI:IPI00387430.	NDUFB8	1.50	9.46E-	1.35	7.77E-	1.11	8.59E-

	1			03		03		01
	IPI:IPI00129516.1	UQCRH	1.59	3.53E-01	1.72	3.01E-01	1.39	2.50E-03
	IPI:IPI00153381.1	UQCR10	1.13	5.84E-02	1.20	8.16E-03	0.89	9.21E-03
	IPI:IPI00331332.6	NDUFA5	1.74	2.56E-04	1.42	3.37E-05	1.34	4.68E-04
	IPI:IPI00131176.1	COX2	1.70	1.57E-12	1.74	4.48E-13	0.98	4.13E-01
	IPI:IPI00355248.5	COX1	1.36	8.97E-03	1.35	2.89E-02	0.90	4.04E-01
REDOX HOMEOSTASIS	IPI:IPI00121788.1	PRDX1	0.75	1.44E-03	0.75	2.06E-03	1.29	5.35E-04
	IPI:IPI00226993.5	TXN1	0.49	7.60E-03	0.50	1.39E-02	1.14	1.44E-02
	IPI:IPI00116192.1	PRDX3	0.75	4.58E-11	0.75	3.36E-09	1.23	7.12E-10
	IPI:IPI00129517.	PRDX5	0.74	4.03E-	0.72	1.26E-	0.85	8.36E-

	1			08		08		06
	IPI:IPI00230108.6	PDIA3	0.86	3.40E-02	0.89	4.47E-02	0.77	1.55E-03
	IPI:IPI00117264.1	PARK7	0.69	2.26E-02	0.65	8.33E-03	0.80	3.34E-03
	IPI:IPI00109109.1	SOD2	0.90	3.70E-02	0.83	8.04E-05	1.21	1.23E-07
	IPI:IPI00130589.8	SOD1	0.76	4.62E-02	0.79	1.37E-01	1.30	1.08E-03
	IPI:IPI00315550.3	GLRX3	0.76	2.35E-02	0.73	2.32E-03	0.90	2.70E-01
HEAT SHOCK PROTEIN	IPI:IPI00263863.8	HSPE1	0.83	2.70E-02	0.84	2.60E-02	1.36	4.47E-08
	IPI:IPI00331556.5	HSPA4	0.77	1.13E-02	0.73	6.74E-03	0.72	2.03E-03
	IPI:IPI00880839.1	HSPA9	0.89	1.51E-02	0.82	2.50E-06	0.83	3.72E-11
	IPI:IPI00323357.	HSPA8	0.89	5.84E-	0.81	3.13E-	0.73	3.28E-

	3			02		05		11
	IPI:IPI00128522.1	HSPB1	0.81	3.14E-02	0.85	8.73E-02	0.69	8.77E-06
	IPI:IPI00121420.1	HSPB2	1.58	2.22E-01	0.84	3.61E-01	1.20	2.74E-02
GLUTATHIONE S-TRANSFERASE	IPI:IPI00555023.2	GSTP1	0.67	4.24E-10	0.63	7.65E-13	0.58	1.84E-16
	IPI:IPI00121051.3	GSTK1	0.85	4.23E-03	0.83	1.33E-03	0.75	3.40E-09
	IPI:IPI00228820.5	GSTM2	0.58	1.95E-04	0.60	3.19E-04	0.75	8.32E-05
	IPI:IPI00323911.3	GSTA4	0.59	3.50E-03	0.62	1.64E-02	0.72	1.79E-03
	IPI:IPI00649135.2	GSTM1	0.81	1.98E-02	0.86	9.47E-02	0.79	2.32E-04
APOPTOSIS RELATED	IPI:IPI00122549.1	VDAC1	1.68	2.60E-11	1.70	1.85E-12	0.83	2.43E-09

	IPI:IPI00116228.1	PPIF	1.55	1.60E-02	1.36	6.60E-02	1.12	4.88E-01
	IPI:IPI00554989.3	PPIA	2.83	2.22E-01	0.84	3.61E-01	1.20	2.74E-02
	IPI:IPI00115564.5	SLC25A4	1.23	3.64E-02	1.36	1.27E-05	0.80	1.13E-14
	IPI:IPI00119667.1	EEF1A2	0.77	5.10E-09	0.79	2.81E-07	0.67	7.54E-24
	IPI:IPI00308882.4	NDUFS1	1.38	4.43E-21	1.40	4.01E-30	1.56	1.05E-03
	IPI:IPI00129577.1	AIFM1	1.44	8.49E-03	1.36	4.31E-03	1.13	2.43E-01

Table 1. Functional classification of regulated proteins. Isch: ischemia Ctrl: control (sham) Reper60: reperfusion 60 mins Reper120: reperfusion 120 mins

ROS imbalance and down regulation of PARK7

ROS products generally have a very short half-life and react rapidly with DNAs, proteins, and lipids to cause oxidative damages. ROS levels and oxidative stress are known to be considerably increased during cardiac ischemia and reperfusion[110-111]. In addition to the observed increase in ETC proteins, we also found that the apoptotic protein VDAC1 and SLC25A4 increased during ischemia and 60 mins reperfusion, which are the components of mitochondrial permeability transition pore (MPTP). Their increase may contribute to a higher possibility of mitochondrial permeability transition induction. A previous study has observed ROS burst along with the mitochondrial permeability transition induction triggered by ROS, *i.e.* ROS induced ROS release, a positive feedback loop. Such ROS burst was inhibited by mitochondrial permeability transition inhibitor, which shows the relation between MPTP and ROS induction[112]. Hence the increase of VDAC1 and SLC25A4 in the present data implies ROS induction during ischemia and reperfusion. Moreover, a collective decrease of redox homeostasis proteins and the GST proteins were seen in the present experiment. The failure of antioxidant system plus the ROS induction would result a relatively high oxidative stress comparing to the normal situation.

It is shown by the iTRAQ data that PARK7 protein was decreased in this I/R mouse model. Recently, PARK7 has been reported to play a key role in stroke induced damage to the brain, which also acts as an ischemia model[113], As reported previously, PARK7 is involved in oxidative stress sensing[114-115], cell survival[116] and Parkinson disease[117]; and is a binding partner of antioxidant transcriptional master regulator nuclear erythroid 2-related factor 2 (NRF2)[118]. NRF2 associates with kelch-like ECH-

associated protein 1 (KEAP1) under unstimulated conditions; the latter targets NRF2 for ubiquitination by a Cullin-3-dependent mechanism[119-122], leading to proteosome-dependent degradation[123]. PARK7 stabilizes NRF2 by thwarting its association with KEAP1[118]. The stabilized NRF2 translocates to nucleus and binds to antioxidant response element (ARE) that induces the expression of endogenous antioxidant and detoxification enzymes[124]. However, it is reported that PARK7 loses its stability under oxidation and is specifically cleaved under oxidative stress by unclear mechanism[125-126]. We found down regulation of PARK7 following ischemia and 60 mins reperfusion; while it began to restore after 120 mins reperfusion. The modulation on PARK7 was validated using western blot (Figure 2 B). Comparing to the RT-PCR result (Figure 2 A), the western blot suggests that differential expression was mainly at the protein level. This suggests that PARK7 protein was degraded under ischemia and oxidative stress despite the level of mRNA was not seriously compromised. Associated with our previous analysis, the ROS imbalance caused by up-regulated ETC and depleted antioxidant enzymes may be the major reason for PARK7 degradation. Due to declination of PARK7, we expect a decrease in NRF2 and that was confirmed by Western blot (Figure 2 C). The decreased level of NRF2 may lead to difficulty in maintaining the basal level of ARE genes expression. Several ARE gene products including PRDX1, GSTM1, GSTM2, AKR1B3, SOD1 and SOD2 identified in our study belong to redox homeostasis and GST proteins and were regulated with similar trend like NRF2 (Figure 2 D). The decreased activities of GST and SOD during short duration of ischemia were reported by preceding studies[127-129]. Interestingly, NRF2 regulated genes have fast response on the transcriptional level (some of them can be

modulated in 60 mins)[130], which should compensate the decreased proteins. However, in our case NRF2 remained depleted during the early reperfusion stage suggesting that the replenishment of the decreased antioxidant enzymes cannot be fulfilled. Hence, once the redox homeostasis and GST proteins decrease, the depleted PARK7 will probably diminish the re-establishment of the antioxidant enzyme system needed for the scavenging of ROS. This makes the down-regulation of these proteins' both the cause and result of ROS imbalance, i.e. a positive feedback pathway that worsened the oxidative damage on the cellular system. Based on the obtained results, we propose the mechanism as outlined in (Figure 2 E). A previous study has shown that during renal I/R NRF2 protected by antioxidant leads to the induction of the genes under its regulation and also improvement on I/R induced injury, which supports our speculation[131].

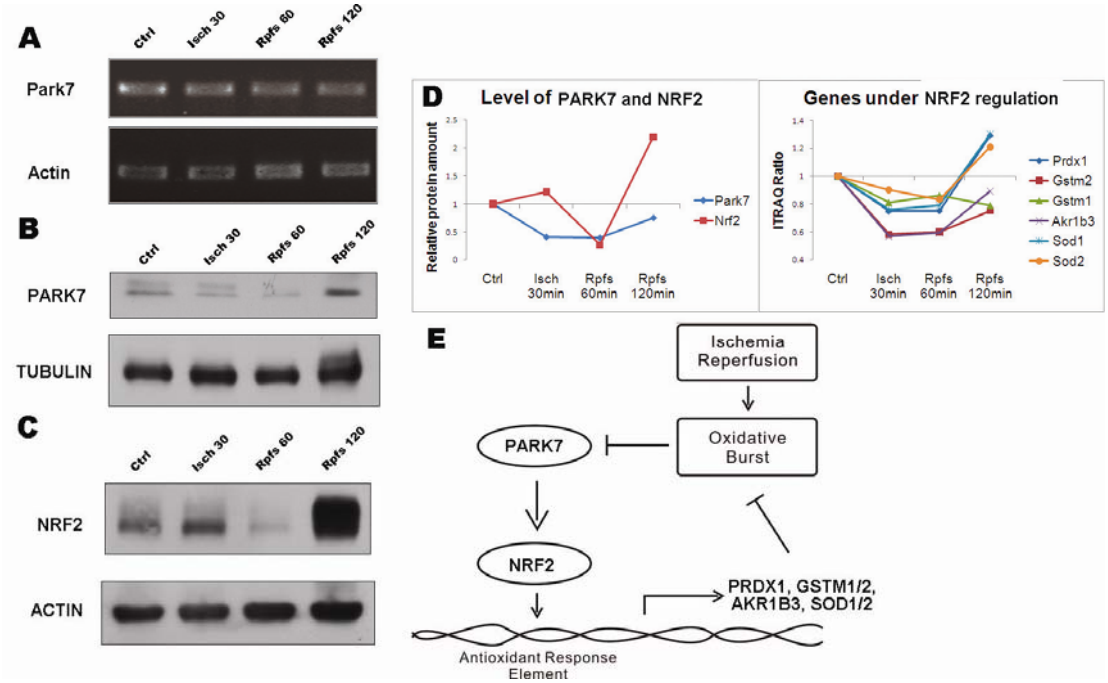

Figure 2. Alteration of PARK7 and NRF2 protein abundance during ischemia and reperfusion

A. mRNA level of Park7 measured by reverse -transcriptional PCR B. Western blot on PARK7 protein abundance C. Western blot on NRF2 abundance D. Calculated PARK7 and NRF2 variation based on Western blot result as well as the iTRAQ ratio of gene products regulated by NRF2 E. Proposed mechanism of PARK7 and NRF2 on balancing the ROS stress.

To further study the role of PARK7 under ischemia/hypoxia, full length rat *Park7* gene was cloned into p3×FLAG-CMV-10 vector and transfected into rat heart myoblast H9C2. After 16 hr hypoxia, FLAG-tagged PARK7 expressed H9C2 showed higher NRF2 abundance comparing to wild type which was transfected with empty vector and also subjected to hypoxia (Figure 3 A, B). mRNA levels of *Sod1* and *Sod2* which are regulated by NRF2 were measured by reverse-transcriptional PCR. The mRNA levels of these two anti-oxidative stress genes were shown to be increased in FLAG-*Park7* transfected cells comparing to wild type under hypoxia (Figure 3 C). Annexin V and PI staining apoptosis assay conducted by FACS was performed to evaluate the cell survival rate (Cell survival rate: cell numbers of which were not stained by Annexin V and PI divided by total cell number within the FACS cutoff) after 16 hour hypoxia on both wild type and FLAG-tagged PARK7 expressed H9C2. About 5% significant increase (P=0.009) of cell survival on the cells with FLAG-PARK7 was observed (Figure 3 D). These results agree with the function of PARK7 in the proposed mechanism, in which PARK7 prevents NRF2 from degradation hence higher PARK7 protein level leads to more NRF2. Consequently, higher mRNA level of *Sod1* and *Sod2* is observed, which may help the cells to survive better after hypoxia. Conversely, lower PARK7 under ischemia and reperfusion causes less *Sod1* and *Sod2* transcription, which dampened the anti-oxidative stress function of the cardiomyocyte. Our observation that PARK7 decreased during cardiac ischemia and reperfusion in mouse cardiomyocyte and the functional validation of PARK7 that positively

influences the NRF2 protein quantity, *Sod1*, *Sod2* transcriptions as well as the cell survival after hypoxia in cardio myoblast shows the importance of its role in the scenario.

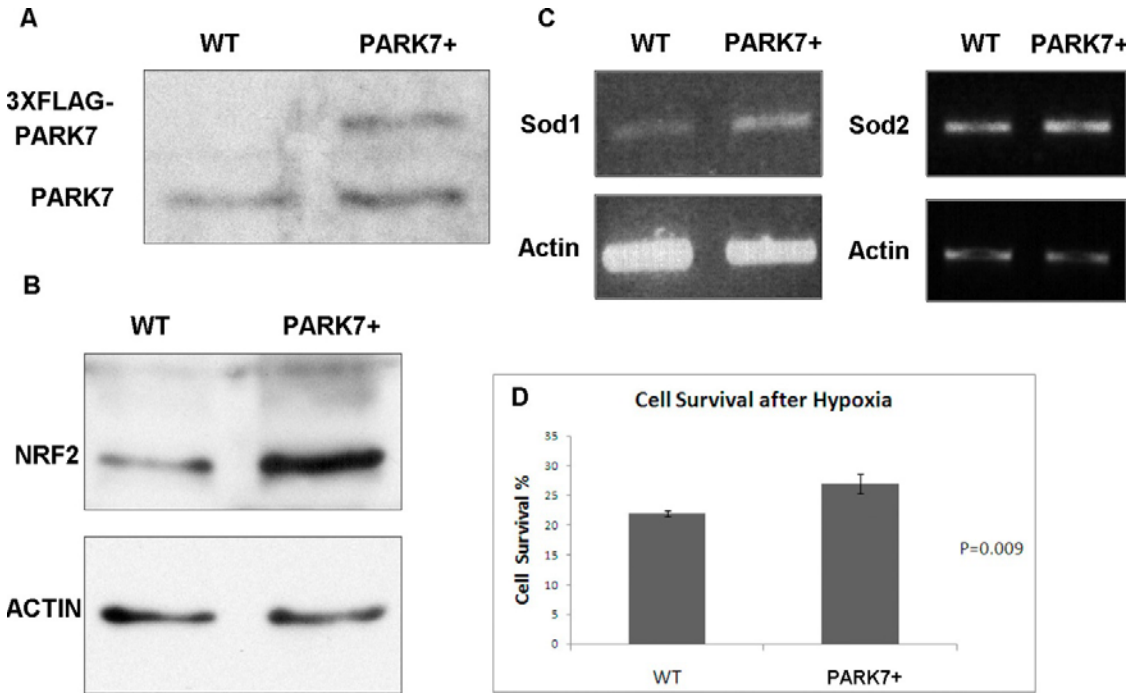

Figure 3. The effect of PARK7 overexpression on NRF2, ARE genes Sod1/2 and cell survival under ischemia

A. 3XFLAG-tagged Park7 was transfected into H9C2 cells. The western blot was stained with anti-PARK7 antibody B. Both of the FLAG-PARK7 expressed and empty vector transfected H9C2 were subjected to hypoxia. NRF2 was detected to be increased in 3XFLAG-tagged PARK7 expressed H9C2 by western blot. C. The 3XFLAG-tagged PARK7 expressed and empty vector transfected H9C2 were subjected to hypoxia. mRNA level of Sod1, Sod2 and Actin was detected by reverse-transcriptional PCR. D. H9C2 cells were transfected with 3XFLAG-tagged PARK7 or empty vector and then subjected to normoxia or hypoxia. After 16 hr incubation, cells were stained with FITC-Annexin V and PI, non-apoptosis population under hypoxia were detected by flow cytometry and compared with the one under normoxia (Cell survival percentage). The increase cell survival rate on 3XFLAG-tagged PARK7 expressed cells was significant (P>0.009). WT: wild type that transfected with empty vector, PARK7+: 3xFLAG-PARK7 expressed

PPIA and protein folding assistance

Peptidyl-prolyl cis-trans isomerase (PPIA) was found to be increased during ischemia and reperfusion stage and validated by Western blot (Figure 4). PPIA is an 18 kDa protein of multiple functions. A previous study indicated its role as secreted redox-sensitive mediator and vascular smooth muscle cell growth factor which stimulates cell growth and inhibits apoptosis[132]. Under hypoxia/reoxygenation, secreted PPIA plays a role in protecting cardiac myocytes against oxidative stress-induced apoptosis in an autocrine fashion[133]. PPIA is also a molecular chaperone that acts as an acceleration factor in protein folding and assembly[134]. Expression of PPIA was found to increase in rat cardiac myocytes under hypoxia and reoxygenation[133]. Moreover, overexpression of PPIA in cancer cells renders resistance to hypoxia- and cisplatin-induced cell death[135].

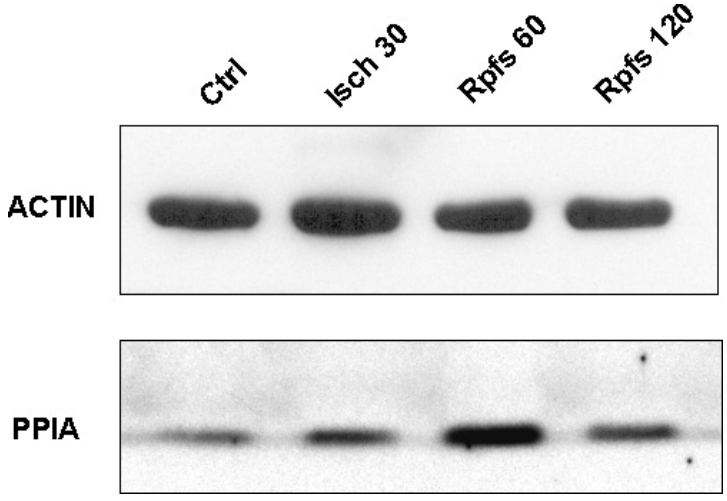

Figure 4. Abundance alteration of PPIA in mouse heart tissue under ischemia and reperfusion

The Ppia abundances in sham, ischemia, reperfusion 60 mins and 120 mins mouse heart tissue were detected by Western blot

To study the function of PPIA in heart cells, FLAG-tagged full length rat Ppia was transfected into H9C2 and its interaction partners were obtained by immunoprecipitation (IP) using anti-FLAG agarose beads (Figure 5 A). The eluent fraction was separated by SDS-PAGE and visualized by silver stain (Figure 5 C). In-gel digestion and mass spectrometry identification was performed to acquire the protein information on whole gel lanes of control and FLAG-PPIA+. Among the 136 proteins identified by both sets of experiments (supplemental Table 4), 11 proteins existed in both experiments and in the FLAG-PPIA lane only; 5 proteins have a maximum of 6 peptides identified in the control lane but hundreds in the pull-down lane. Comparing to other identified proteins these 5 proteins have significantly higher pull-down lane peptide to control lane peptide ratio, ranging from 50.25:1 to 284.5:1. The peptide number was marked as 0.1 if no peptides were identified in either lane to facilitate the ratio calculation. Ratio of each protein represents the peptide number from the IP lane divided by peptide number from the control lane. To visualize the specific binding partners which have strong binding (high ratio) similarly as previously described[136], the average log ratio of each protein from 2 IP experiments is plotted versus peptide number of each protein normalized by protein length, which is proportional to the protein abundance (Figure 5 B). Proteins with 4 peptides or above identified in both experiments were selected. In the scatter plot, outliers can be easily spotted. A cutoff to the outliers was set since some outliers have positive average log ratio even one of the ratio is negative, which should be excluded from the binding partner list. Combining together, 15 proteins were identified as binding partners of

PPIA, which are T-complex protein 1 subunit α, β, γ, δ, ε, ζ, η, θ, NIBAN, isoform 2 of nestin, heat shock protein 105 kDa, ubiquitin specific protease 47, AHNAK and PRDX2 (Table 2).

Table 2

Description	1st Ctrl	1st IP	2nd Ctrl	2nd IP
CHAPERONIN SUBUNIT 6A.	NA	(105)309	NA	(257)570
CHAPERONIN SUBUNIT 7.	NA	(167)167	NA	(381)381
CHAPERONIN SUBUNIT 8.	(1)1	(269)269	(4)4	(471)471
59 KDA PROTEIN (T-COMPLEX PROTEIN 1 SUBUNIT Zeta).	NA	(2)191	NA	(2)267
T-COMPLEX PROTEIN 1 SUBUNIT EPSILON.	NA	(178)178	NA	(368)380
T-COMPLEX PROTEIN 1 SUBUNIT ALPHA.	NA	(203)203	(2)2	(569)571
T-COMPLEX PROTEIN 1 SUBUNIT GAMMA.	(2)2	(280)281	NA	(639)645
T-COMPLEX PROTEIN 1 SUBUNIT BETA.	(3)3	(387)388	(6)6	(690)696
T-COMPLEX PROTEIN 1 SUBUNIT DELTA.	(4)4	(201)201	(2)2	(436)448
NIBAN.	NA	(8)16	NA	(9)17
65 KDA PROTEIN.	NA	(4)12	NA	(11)19
ISOFORM 2 OF NESTIN.	NA	(4)4	NA	(4)4
HEAT SHOCK PROTEIN 105 KDA.	NA	(5)5	NA	(9)12
UBIQUITIN SPECIFIC PROTEASE 47.	NA	(6)6	NA	(12)12
AHNAK	NA	(7)7	NA	(7)7
PRDX2	NA	(4)4	NA	(6)6

Table 2. Peptide number of binding partners of PPIA

The peptide number of the binding partners was shown as: (specific peptide that only belongs to the protein) total peptide number that can be assigned to the protein

Further, immunoprecipitation-MS for transfected cells under normoxia and hypoxia was carried out (Figure 5 D). Change on interactome of PPIA was quantified by using spectrum counting normalized by spectrum numbers of PPIA in each condition, *i.e.* the spectrum number for each binding partner was divided by the number of spectrum assigned to PPIA in normoxia or hypoxia. Such ratio reflects the binding efficiency of the interaction. Cells were more stressful because serum free condition was required for this experiment; hence only strong signals were obtained and some binding partners were not identified. By comparing the interaction efficiency between binding partners and Ppia in normoxia and hypoxia the variation on Interactome was obtained. It is found that more chaperonin containing TCP1 complex (T-complex protein 1 subunit α, β, γ, δ, ε, ζ, η, θ) and ubiquitin specific protease 47 (USP47) bind to PPIA after 16hr hypoxia comparing to normoxia in 2 set of experiments (Figure 5 E).

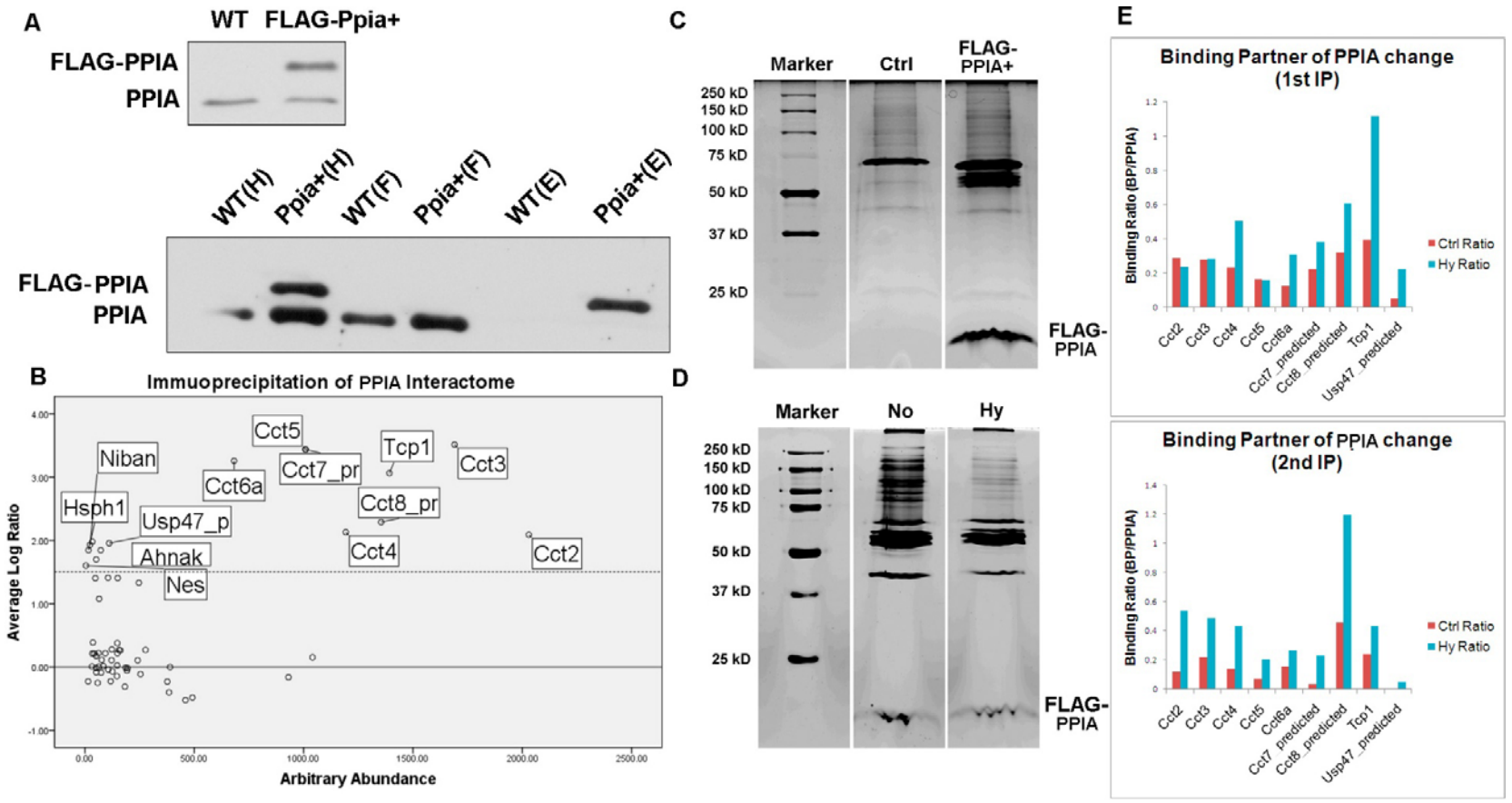
A
WT FLAG-Ppia+
FLAG-PPIA
PPIA
WT(H)
Ppia+(H)
WT(F)
Ppia+(F)
WT(E)
Ppia+(E)
FLAG-PPIA
PPIA
B
Immuoprecipitation of PPIA Interactome
Average Log Ratio
Arbitrary Abundance
Niban
Cct5
Cct6a
Cct7_pr
Tcp1
Cct3
Hsph1
Usp47_p
Cct8_pr
Ahnak
Cct4
Cct2
Nes
C
Marker
Ctrl
FLAG-PPIA+
250 kD
150 kD
100 kD
75 kD
50 kD
37 kD
25 kD
FLAG-PPIA
D
Marker
No
Hy
250 kD
150 kD
100 kD
75 kD
50 kD
37 kD
25 kD
FLAG-PPIA
E
Binding Partner of PPIA change (1st IP)
Binding Ratio (BP/PPIA)
Ctrl Ratio
Hy Ratio
Cct2
Cct3
Cct4
Cct5
Cct6a
Cct7_predicted
Cct8_predicted
Tcp1
Usp47_predicted
Binding Partner of PPIA change (2nd IP)
Binding Ratio (BP/PPIA)
Ctrl Ratio
Hy Ratio
Cct2
Cct3
Cct4
Cct5
Cct6a
Cct7_predicted
Cct8_predicted
Tcp1
Usp47_predicted

Figure 5. . Interactome of PPIA under normoxia and hypoxia condition determined by IP-MS

A. FLAG-tagged Ppia was transfected into H9C2 cells. The western blot was stained with anti-PPIA antibody. FLAG-PPIA was immunoprecipitated by using anti-FLAG antibody bond agarose beads. B. The peptide number was marked as 0.1 if no peptides identified in either lane to facilitate the ratio calculation. The ratio of each protein represents the peptide number from IP lane divided by peptide number from control lane. The average log ratio of each protein from 2 IP experiments is plotted versus peptide number of each protein normalized by protein length times 1000, which is proportional to the protein abundance. Proteins with 4 or above peptides identified in both experiments were selected. A cutoff was set to distinguish the proteins with positive average log ratio even one ratio is negative. C. Silver stain of Ppia interactome. Lysate of H9C2 transfected with FLAG-PPIA (FLAG-PPIA+) or empty vector (Ctrl) was subjected to anti-FLAG agarose beads IP. The eluent was separated on SDS-PAGE gel and visualized by silver stain. D. Hypoxia IP. IP of PPIA and its interactome was performed on the lysate of H9C2 cells transfected with FLAG-PPIA and subjected to hypoxia or normoxia. The IP eluent was separated on SDS-PAGE gel and visualized by silver stain. E. The PPIA interactome alteration between hypoxia and normoxia. The interactome alteration was detected by IP-MS. From the result, peptide number of specific binding partner in each condition normalized by identified PPIA peptide number in the corresponding condition was plot. H: whole cell lysate F: flow through (cell lysate after incubated with anti-FLAG agarose beads) E: Eluent eluted from anti-FLAG beads using FLAG peptide. WT: wild type that transfected with empty vector, PPIA+: FLAG-PPIA expressed

Chaperonin containing TCP1 complex consists of two identical stacked rings, each containing eight different proteins (T-complex protein 1 subunit α, β, γ, δ, ε, ζ, η, θ). It is involved in the folding of cytoskeleton proteins, actin and tubulin, and other intracellular proteins, *e.g.* cyclin E1, histone deacetylase, and protein phosphatase PP2A regulatory subunit B[137]. The function of Chaperonin containing TCP1 complex strongly correlates with PPIA which is also a folding assisting protein. The interaction and the functional similarity supports each other which shows that the chaperoning process of these two may happen together or sequentially.

USP47 is a deubiquitinating enzymes belonging to the ubiquitin-specific proteases (USPs) subclass[138]. Some USP members play crucial roles in a variety of biological processes like regulation of DNA damage checkpoint response[139], epigenetic

regulation[140] and protein stablization[141]. A previous study showed that USP47 is an interactor of β-Trcp which is an F-box protein acting as a subunit of ubiquitin ligase (E3). It is found that genetic and siRNA-mediated depletion of USP47 causes decrease of cell survival and augments anti-proliferation effect of anticancer drugs[142].

Chaperones, foldases and oxygen are required in the sophisticated protein folding assisting machinery in yeast. As a major electron acceptor oxygen provides the driving force for protein folding in the endoplasmic reticulum (ER). It is shown in the previous study this pathway is similarly dependent on oxygen in mammalian cells, however the existence of a similar mechanism is yet to be clarified[143]. Oxygen supply declines under hypoxia may lead to failure on protein folding in ER and also there are also other findings showing that accumulation of misfolded proteins in ER is a natural consequence under hypoxia[144-145], which is ER stress. The capacity of protein folding is increased by unfolded protein response (UPR) to cope with the stress because the built up misfolded polypeptides is potentially toxic. Though no evidence of Ppia involvement in the UPR pathway emerged, the increased binding efficiency of chaperonin containing TCP1 complex and USP47 to Ppia under hypoxia observed in the present study implies that Ppia may be in favor of protein folding assistance and stabilization to counteract the unfolded protein stress.

Interestingly, silencing of NIBAN, which is one of the Ppia interactome components identified in our IP-MS experiment, was found to up-regulate the phosphorylation of eIF2α[146], and the inhibition of global mRNA translation evoked by phosphorylation of eIF2α is part of the UPR under hypoxia[147]. Hence NIBAN is considered involved in the ER stress response. Though the binding efficiency change between hypoxia and

normoxia is not observed in our experiment, the interaction between NIBAN and PPIA shows that its function may not be limited to indirect modulation of the protein translation, but it could also assist in the protein maturation.

To further understand the data, physical interaction network with shortest path was calculated by the in-house script and visualized by the Cytoscape software[98] with the combined interactome information obtained in our experiment and HPRD[96], IntAct[97] protein interaction database (Figure. 6). The human protein counterparts were used because its interaction network is more complete than the murine's. We found that functionally important proteins such as Guanine nucleotide exchange factor VAV2 (VAV2_HUMAN), transcription factor p65 (TF65_HUMAN) and mediator of RNA polymerase II transcription subunits (MED9_HUMAN and MED29_HUMAN) were located within the network, which implies that besides protein folding assistance, angiogenesis, NF-kappa-B function and RNA polymerase II-dependent genes transcriptional regulation may also relate to the interactome of PPIA.

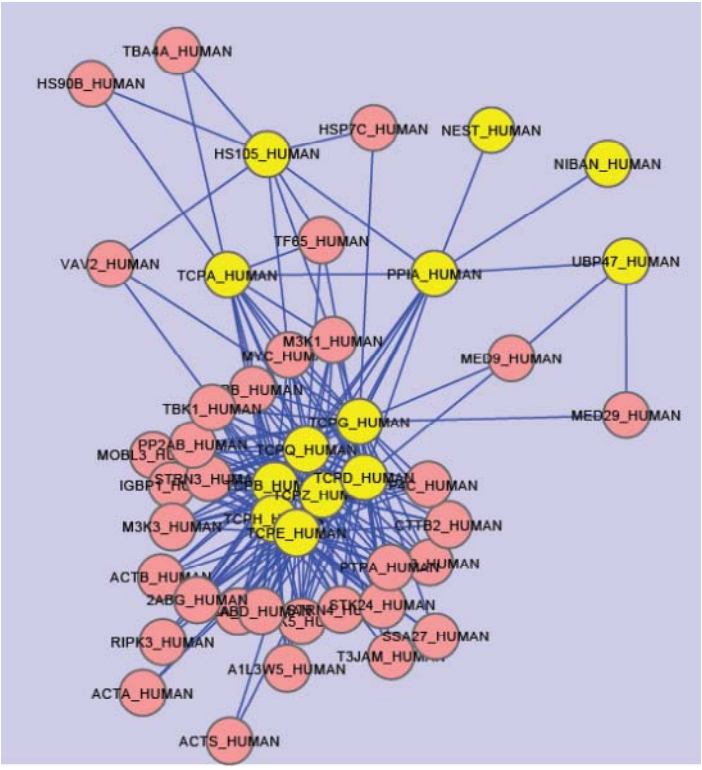

Figure 6. Interaction network of PPIA and its indentified interactome

The interactome and PPIA is connected by shortest path Yellow circles represent PPIA and the binding partner identified in present study, pink circles represent the intermediate proteins in the network.

Conclusion

Proteome alteration during cardiac ischemia and reperfusion in mice model were measured by the iTRAQ quantitative approach in the present study. Several functional groups of proteins were found to be regulated which indicates the perturbation caused by the oxygen and energy depletion circumstance. Analysis shows ETC protein up-regulation and anti-oxidative proteins decrease and possible involvement of ROS imbalance may be involved. Protein abundance of oxidative stress sensing protein

PARK7 decreased during the ischemia and reperfusion stages. The antioxidant transcriptional master regulator NRF2, which is protected by PARK7 from degradation, was also decreased along with its downstream gene products shown in the iTRAQ data. To validate the proposed mechanism that PARK7 plays an important role in the antioxidative stress pathway, FLAG-tagged PARK7 was expressed in rat heart myoblast cell line. Increase on the protein level of NRF2 as well as on the *Sod1* and *Sod2* mRNAs were observed in the expressed cell line under hypoxia. Cell survival on the expressed cells was statistically significantly improved under hypoxia stress. This *in vitro* experiment shows that the protein level of PARK7 affects the NRF2 protein level and the transcriptional level of its downstream anti-oxidative stress proteins, and implies the importance of PARK7 under ischemia and reperfusion. However, the mechanism resulting in degradation of PARK7 during ischemia and reperfusion is yet to be clarified.

Under hypoxia, protein folding in ER is interrupted and the unfolded polypeptides and improperly folded proteins cause ER stress and UPR. Protein maturation is important especially when the cells are stressed. The folding assisting protein PPIA was found to be up-regulated during cardiac ischemia and reperfusion. The interactome of PPIA was studied by IP-MS in FLAG-tagged Ppia expressed H9C2 cells. Some of the interaction partners are related to protein folding and stabilization, which is coincident with the function of cytoplasmic PPIA. Interactome variation between normoxia and hypoxia was also acquired by the label-free IP-MS approach. It is shown that Chaperonin containing TCP1 complex and USP47 have higher binding efficiency to PPIA under hypoxia. This indicates that PPIA may help to increase the protein folding

capacity when unfolded protein stress was induced by hypoxia. Further, proteins involved in important biological processes were found to locate within the interaction network of PPIA by using bioinformatics technique. The functional study of the PPIA interactome indicates that up-regulation of PPIA during ischemia and reperfusion helps to cope with the accumulated unfolded polypeptide stress.

By applying the iTRAQ quantitative proteomics technique protein abundance regulation in an *in vivo* cardiac ischemia reperfusion model was observed. The function of two significantly changed proteins selected from iTRAQ result was studied *in vitro.* These data reveal novel information about the molecular events on oxidative stress and unfolded protein stress and provide a better understanding of the I/R injury.

Chapter 3: Profiling Rat Heart Myoblast Secretome under Hypoxia and Reoxygenation Stress by Label Free and iTRAQ-based Quantitative Proteomics Approach

Xin Li, Ren Yan, Siu Kwan Sze*

School of Biological Sciences, Nanyang Technological University, 60 Nanyang Drive, Singapore 637551

Corresponding author

Dr. Siu Kwan SZE

School of Biological Sciences,
Nanyang Technological University,
60 Nanyang Drive, Singapore 63755
Tel: (+65)6514-1006, Fax: (+65)6791-3856
Email: sksze@ntu.edu.sg

To be submitted to Journal of Proteome Research

Abstract

Cell secretion to the microenvironment plays an important role in the cell survival, wound healing and maintaining the tissue function. Secreted proteins participate in and also regulate the cardiac infarction healing process; therefore quantitative profiling of the cardiac myocyte secretome under pathophysiological stress will provide valuable insight for potential prevention and treatment of heart diseases. In this study, the alteration of the secretome of rat heart myoblast H9C2 cells under 16 hr hypoxia and 24 hr reoxygenation were analyzed by both iTRAQ-based and label-free quantitative proteomics approaches using LC-MS/MS. 2007 proteins were identified in the label-free based experiment and 860 proteins were identified in the iTRAQ experiment. Among the 2165 total proteins identified by label-free and iTRAQ, 1363 proteins were recognized as secreted proteins. The profile and modulation of the secretome identified herein could potentially advance our understanding of the cardiac biology, and facilitate the follow-up investigation on the extracellular molecular events during hypoxia and reoxygenation as well as the ischemia/reperfusion injury. Proteins related to important biological functions such as SERPINH1, PPIA, ATTRACTIN, EMC1, POSTN, THBS1 and TIMP1 were found to be regulated by hypoxia and reoxygenation stresses. Further analysis on the modulated subproteome suggests that secreted proteins involved in angiogenesis, inflammation, ECM remodeling including collagen deposition and cross-linking are regulated during hypoxia; while in subsequent reperfusion or re-oxygenation, proteins involved in anti-inflammation, ECM modulation are up-regulated and anti-apoptosis proteins decline.

In addition, regulations on secreted proteins such as STIP1, ROBO2 and FAT1 by hypoxia/reoxygenation stress were detected in the secretome for the first time.

Keywords

Hypoxia, reoxygenation, secretome, label free, iTRAQ, heart, text mining, H9C2

Introduction

Obstruction of blood flow to the myocardium muscle induces heart attack or myocardial infarction (MI), which is the main cause of coronary heart disease. Restoration of blood flow through the occluded coronary artery is currently the most effective therapy to limit the infarct size and preserve cardiac function after acute myocardial infarction[148]. However, reperfusion following ischemia causes additional cell death and increase in infarct size has been demonstrated by a previous study which is the phenomenon called myocardial ischemia/reperfusion (I/R) injury[149].

The cardiac extracellular matrix (ECM) related reparative response of the I/R injury can be divided into three overlap stages, which are the inflammatory stage, the proliferative stage and the final maturation stage.

At the inflammatory stage, cardiomyocyte death triggers instant activation of the complement system, generates free radicals such as ROS and activates TLR2/4 mediated pathways, which stimulate the production of cytokines, chemokines and adhesion molecules[150]. Cytokines such as tumour necrosis factor alpha (TNFα), IL-1b, and IL-6 can mediate repair and remodeling through activating matrix metalloproteinases (MMPs) and collagen formation, and regulate integrins and angiogenesis and progenitor cell mobilization (Figure 1). Cytokines also induce a

protease-rich environment leading to ECM degradation. The degraded ECM facilitates extravasation of plasma proteins to form a provisional matrix containing fibronectin and fibrin. Such provisional matrix provides a scaffold for inflammatory cells to migrate and proliferate[151-152]. Inflammatory cells migrate into the infarct tissue and remove necrotic myocytes[153]. The ECM proteins including fibrillar collagen and glycosaminoglycans are degraded by MMPs which generates low molecular weight fragments with pro-inflammatory properties[154-155]. Thus, the alteration of the matrix components also regulates the inflammatory pathways.

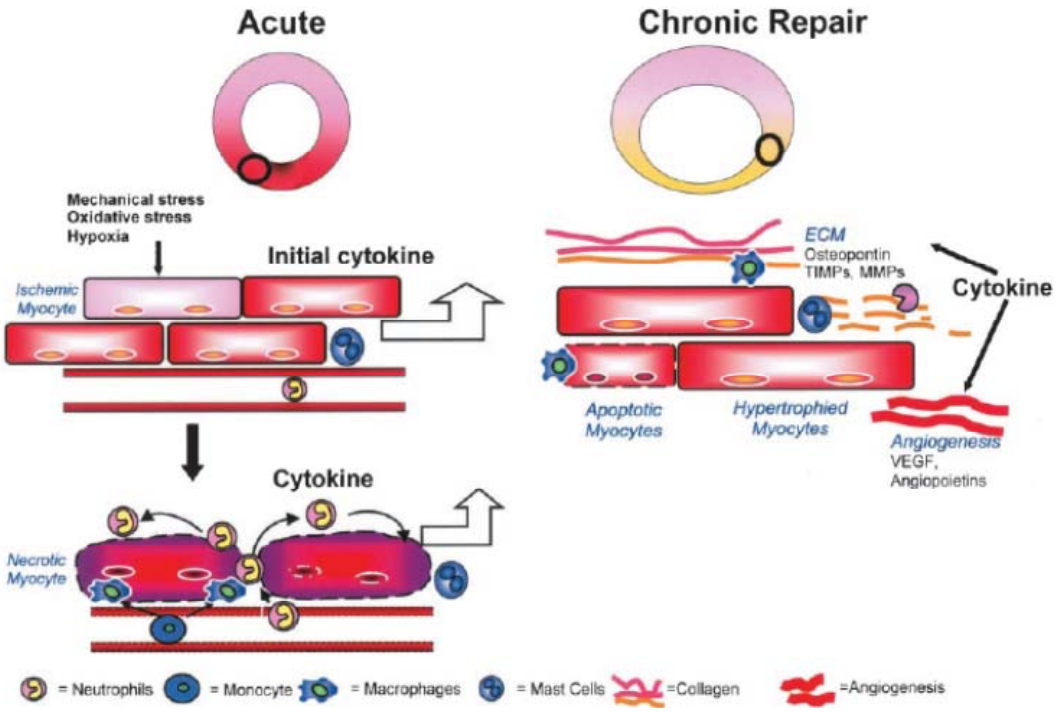

Figure1 Cytokines mediated remodeling in the post-infraction stage. Myocardial stress, i.e. mechanical stretch, oxidative stress, and hypoxia in the setting of ischemia, will rapidly induce cytokines such as tumor necrosis factor (TNF) or interleukin-6, which can improve survival or speed up myocyte necrosis and apoptosis and reduce contractility. This is followed by cytokine increase through transmigration of macrophages and neutrophils. During the chronic postinfarction, the activation of MMPs and TIMPs contributes to the accumulation of collagen

and wound healing. Angiogenic and progenitor cell mobilization factors further contribute to the healing of the wound. (Inflammatory Cytokines and Postmyocardial Infarction Remodeling, Circulation Research 2004)

At the following proliferative stage, the initial plasma derived provisional matrix is lysed and replaced by fibroblast derived provisional matrix containing cellular Fibronectin [156]. The Fibronectin regulates the deposition of collagen-1[157]. Matricellular proteins are a family of extracellular matrix proteins that contribute to the modulation of cell function and activity but not its constitution. Induction of matricellular proteins such as thrombospondin (Thsp1/2), tenascin-C/X, osteonectin/SPARC (secreted protein, acidic and rich in cysteine), osteopontin (OPN) and periostin (Postn), which are not expressed in normal heart, is an important feature of the proliferative stage.

As a critical TGF-β activator with effective angiostatic properties Thsp1 is strikingly up-regulated in experimental models of infarction[158]. Enhanced and prolonged expression of chemokines was exhibited in the infarcted heart and expansion of the inflammatory infiltration into the non-infarcted area was shown in the THSP1-/- mice, which increased adverse remodeling of the ventricle[158]. However, inflammation inhibition mechanisms of thsp1 remains unknown. Tenascin-C is also strikingly but transiently up-regulated during the proliferative phase of healing by fibroblasts[159-160]. However, the role of tenascin-C in infarct healing and post-infarction remodeling is still unclear. OPN is induced early following myocardial infarction and is prevailingly localized in macrophages in both murine and canine infarcts. OPN is significantly up-regulated during monocyte differentiating to macrophage[161]. The mechanisms of OPN-mediated effects on attenuating adverse matrix remodeling[162] and cardiac

protection[163] remain poorly understood. SPARC is induced in healing infarcts. The study on SPARC null mice suggested that SPARC-mediated actions are important for matrix organization[164]. Postn is significantly related to fibrosis and ECM metabolism in a range of disease conditions, including cardiovascular disease and cancer[165] and also has genomic associations with ventricular hypertrophy[166] and heart failure[167]. Abundant expression of Postn was found in the border zone in both mouse and human myocardial infarction and significantly modulated the phenotype and function of fibroblast in the infarcted myocardium[168]. POSTN null mice had impaired healing and higher risk of cardiac rupture[168-169].

At the final stage, deposition of collagen increases and cross-linking enzymes like lysyl-oxidase induce cross-linking of matrix in the infarcted myocardium[170] to form a scar to mechanically support the injured myocardium. Such mechanical support is important to maintain the cardiac function. Decrease in tensile strength in healing of myocardial infarct may lead to enhanced left ventricular remodeling and considerable ventricular dysfunction [171]. ECM response to the mechanical burden caused by I/R damage induces collagen synthesis which leads to stiffer ventricular wall and increases left ventricular diastolic pressure.

Because there is no postnatal cardiac myoblast within the heart equivalent to the one in skeletal muscle, the self-recovery process after I/R injury only compensates the myocardium lost with collagen-based scar. Moreover, additional damage is caused at the reperfusion stage. To overcome this problem, cell transplantation including bone marrow mononuclear cells (MNCs)[172-173], mesenchymal stem cells (MSCs)[174] and skeletal myoblasts (SkMb)[175] has been investigated to improve the infarction healing.

The paracrine factors released by transplanted exogenous stem cells were found to influence neovascularization, myocardial protection, cardiac remodeling, and contractility[176]. A proteomics study on the secretion proteome of human MSCs revealed 201 unique proteins involved in important signaling pathways in cardiovascular biology, bone development, and hematopoiesis, which indicates its potential in modulating the tissue repair or replacement[177].

As indicated by these researches, the microenvironment of cardiac infarction area undergoes dynamic changes and the infarct healing process can be regulated by the secreted proteins within the niche. Hence the profile of the secretion from cardiac myocytes will be of great interest to better understand the mechanism of I/R injury and stem cells transplantation therapy.

Recent advances in proteomics and bioinformatics have not only enabled us to profile the proteome of biological samples qualitatively but also quantitatively across multiple biological samples in different stages, which has been increasingly used in cardiovascular research to provide a broad-based portrait of the proteome profile and alteration[1, 178]. Embryonic rat heart myoblast H9C2 has been widely used as an alternative to primary cardiomyocytes. Characterization demonstrated that H9C2 cells show morphological characteristics similar to those of immature embryonic cardiomyocytes, but have preserved several features found in adult cardiac cells[179-180]. In this study secreted proteins from conditioned medium of H9C2 subjected to 16 hr normoxia, 16 hr hypoxia, and 16 hr hypoxia followed by 24 hr reoxygenation were analyzed. 2007 proteins from conditioned medium were quantitatively profiled by a label-free method and 860 proteins from the same conditions were quantified by the

isobaric tag for relative and absolute quantitation (iTRAQ) experiment. In total, 2165 proteins were identified. Mining the data found that 1363 proteins were recognized in various databases as secreted proteins. The proteins in the secretome modulated by hypoxia and reoxygenation were selected for further detailed analysis if they have similar expression trend in both label-free and iTRAQ datasets. Further analysis suggested that the biological processes of angiogenesis, inflammation response, ECM remodeling including collagen deposition and cross-linking were up-regulated during hypoxia; while the processes of anti-inflammation, ECM modulation and apoptosis were modulated in the reoxygenation step. Proteins related to important biological functions such as SerpinH1, Ppia, Attractin, EMC1, Postn, Thbs1 and Timp1 were found to be regulated by hypoxia and reoxygenation stresses. Taken together, by applying mass spectrometry-based quantitative proteomics approach, secreteome containing a large amount of novel secreted proteins from rat heart myoblast cells was identified; modulation on the secretome under hypoxia and reoxygenation was detected, which sheds light on the underlying mechanism and provides useful information for the follow-up investigation in the future.

Material and methods

Cell culture and conditioned medium

Rat heart myoblast H9C2 was purchased from American Type Culture Collection (ATCC, Manassas, VA, USA). Cells were cultured in Dulbecco's Modified Eagle Medium (DMEM) containing 10% fetal bovine serum. After reaching 60% confluence, cells were adapted to serum deprivation by washing with PBS and then incubating in serum free DMEM for 6 hr. After 6 hr, the medium was aspirated and replaced by

fresh or hypoxic serum free DMEM generated by pumping in hypoxia gas (<0.1% O_2, 5% CO_2) to exclude the dissolved oxygen. Conditioned media (CMs) were collected from H9C2 cells culture after 16 hr normoxia (21% O_2, 5% CO_2) or hypoxia (<0.1% O_2, 5% CO_2). For reoxygenation stressed conditioned medium, fresh DMEM was added in after having collected the hypoxia conditioned medium and incubated with the cells for additional 2 hr or 24 hr. The CMs were collected and centrifuged at 500×g for 5 mins and then filtered by 0.2 μM filter. The filtered medium was concentrated by 10 kD Amicon Ultra-15 centrifugal filter units (Millipore, Carrigtwohill, Ireland). The concentrated CMs were then lyophilized to obtain the secreted proteins.

In-gel digestion for secretome

The freeze dried secreted protein sample was reconstituted in SDS running buffer and separated on SDS-PAGE gel followed by silver staining. The gel lane of each condition (normoxia, hypoxia and reoxygenation) was sliced separately into 6 pieces. The gel pieces were destained; trapped proteins were reduced by dithiothreitol (DTT) and alkylated by Iodoacetamide (IAA). Tryptic digestion was performed by using porcine trypsin (Sequencing Grade Modified, Promega, WI, USA) overnight. The tryptic peptides were extracted by 5% formic acid in 50% acetonitrile (ACN) and vacuum dried by speedvac.

LC-MS/MS analysis

Label free Each dried fraction was reconstituted in 100 μl of 0.1% formic acid and analyzed using an LTQ-FT Ultra mass spectrometer (Thermo Electron) coupled with a Prominence^{TM} HPLC unit (Shimadzu, JAPAN). For each analysis, samples was

injected from an autosampler (Shimadzu, JAPAN) and concentrated in a Zorbax peptide trap (Agilent, Palo Alto, CA, USA). The peptide separation was performed in a capillary column (200 μm inner diameter × 10 cm) packed with C_{18} AQ (5 μm particles, 300 Å pore size; Michrom Bioresources, Auburn, CA, USA). Mobile phase A (0.1% formic acid in H_2O) and mobile phase B (0.1% formic acid in acetonitrile) were used to establish the 90 mins gradient comprising 3 mins of 0–5% B and then 52 mins of 5–25% B followed by 19 mins of 25–80% B, maintenance at 80% B for 8 mins, and final re-equilibration at 5% B for 8 mins. The HPLC system was operated at a constant flow rate of 30 μL $mins^{-1}$, and a splitter was used to create a flow rate of ~500 nL $mins^{-1}$ at the electrospray emitter (Michrom Bioresources). Samples were injected into an LTQ-FT through an ADVANCE™ CaptiveSpray™ source (Michrom Bioresources) with an electrospray potential of 1.5 kV. The gas flow was set at 2, ion transfer tube temperature was 180 °C, and collision gas pressure was 0.85 millitorr. The LTQ-FT was set to perform data acquisition in the positive ion mode as described previously[95]. Briefly, a full MS scan (350–1600 *m*/*z* range) was acquired in the FT-ICR cell at a resolution of 100,000 and a maximum ion accumulation time of 1000 ms. The automatic gain control target for FT was set at 1*e*+06, and precursor ion charge state screening was activated. The linear ion trap was used to collect peptides and to measure peptide fragments generated by CID. The default automatic gain control setting was used (full MS target at 3.0*e*+04, MS^n at 1*e*+04) in the linear ion trap. The 10 most intense ions above a 500-count threshold were selected for fragmentation in CID (MS^2), which was performed concurrently with a maximum ion accumulation

time of 200 ms. For CID, the activation Q was set at 0.25, isolation width (*m*/z) was 2.0, activation time was 30 ms, and normalized collision energy was 35%.

iTRAQ The protein samples were reduced by TCEP, alkylated with MMTS and digested with trypsin as previously reported[93-94]. The tryptic peptides of normoxia, hypoxia for 16 hrs, 2 hr and 24 hr reoxygenation after hypoxia were labeled with 114, 115, 116 and 117 4-plex iTRAQ tags respectively. The iTRAQ labeling of peptide samples were performed using the iTRAQ reagent multiplex kit (Applied Biosystems, Foster City, CA, USA) according to manufacturer's protocol. Peptides were labeled with respective isobaric tags, were incubated for 2 h, then combined into a single sample and vacuum centrifuged to dryness. The vacuum dried samples were reconstituted in Buffer A (10 mM KH_2PO_4, 25% acetonitrile, pH 2.85) and iTRAQ labeled peptides were fractionated using a PolySULFOETHYL A^{TM} SCX column (200 x 4.6 mm, 5 μm particle size, 200 Å pore size) by an HPLC system (Shimadzu, Japan) at a flow rate of 1.0 ml min^{-1}. The 50 mins HPLC gradient consisted of 100% buffer A (10 mM KH_2PO_4, 25% acetonitrile, pH 2.85) for 5 mins; 0-20% buffer B (10 mM KH_2PO_4, 25% ACN, 500 mM KCl, pH 3.0) for 15 mins; 20-40% buffer B for 10 mins; 40-100% buffer B for 5 mins followed by 100% buffer A for 10 mins. During sample fractionation, chromatograms were recorded at 214 nm. In total, 50 fractions were collected, concentrated to dryness using vacuum centrifuge, and then combined to 19 fractions according to the 214nm reading in the LC spectrum and reconstituted in 0.1% trifluroacetic acid and desalted with Sep-Pak Vac C18 cartridges (Waters, Milford, MA, USA). After desalting, samples were again concentrated to dryness

using vacuum centrifuge and reconstituted in 100 μL of 0.1% formic acid for LC-MS/MS analysis.

The mass spectrometric analysis of the iTRAQ labeled sample was performed using a Q-Star Elite mass spectrometer (Applied Biosystems; MDS-Sciex, USA), coupled with an online micro flow HPLC system (Shimadzu, JAPAN). Peptides were separated using a nanobored C18 column with a picofrit nanospray tip (75 μm ID x 15 cm, 5 μm particles) (New Objectives, Wuburn, MA, USA). The flow rate was maintained at 20 μL min^{-1} and the separation was performed with a splitter to get an effective flow rate of 0.2 μL min^{-1}. The MS data were acquired in the positive ion mode with a selected mass range of 300-2000 m/z. Peptides in +2 to +4 charge states were selected for MS/MS. The three most abundantly charged peptides above a 10 count threshold were selected for MS/MS and dynamically excluded for 30 sec with ±30 mDa mass tolerance. Smart information-dependent acquisition (IDA) was activated with automatic collision energy and automatic MS/MS accumulation. The fragment intensity multiplier was set to 20 and the maximum accumulation time was 2 sec. The peak areas of the iTRAQ reporter ions reflect the relative abundance of the proteins in the samples.

Mass spectrometric data analysis

Mascot data search The extract_msn (version 4.0) program found in Bioworks Browser 3.3 (Thermo Electron, Bremen, Germany) was used to extract tandem MS spectra in the dta format from the LTQ-FT ultra raw data. These dta files were then converted into the MASCOT generic file format using an in-house program. Intensity values and fragment ion *m*/*z* ratios were not manipulated. This data was used to obtain

protein identities by searching against the Refseq rat protein database (59026 sequences) by means of an in-house MASCOT server (version 2.2.03) (Matrix Science, Boston, MA, USA), 59026 decoy sequences (reverse sequences) were included in the database to estimate the false discovery rate (FDR). The search was limited to a maximum of 2 missed trypsin cleavages; $\#^{13}C$ of 2; mass tolerances of 15 ppm for peptide precursors; and 0.8 Da mass tolerance for fragment ions. Fixed modification was carbamidomethylation at Cys residue(s), whereas variable modifications were oxidation at Met residue(s) and phosphorylation on Ser, Thr and Tyr residues. The searched results including the peptide summary and the protein summary were exported as Microsoft CSV files and DAT result files. FDR of the significantly identified peptides was controlled at below 1%.

Label-free quantitation The SI_N was calculated using the Mascot search result as previously described[5]. Briefly, SI that incorporates fragment ion intensity values with spectral count and peptide number for each protein was calculated. SI was then normalized by the sum of SI of each identified protein in the experiment and further normalized by the protein length. The fragment ion intensity of the spectrum that was assigned to a specific peptide was obtained from the MS^2 section in the DAT mascot search result file by an in-house Ruby script through the spectrum title. The spectrums for SI_N were selected from the spectra list with FDR below 1%. NSAF was calculated as previously described[181-182] and emPAI measurement was automatically included in MASCOT[183].

iTRAQ data search The data acquisition was performed with the Analyst QS 2.0 software (Applied Biosystems/MDS SCIEX). Protein identification and quantification

were performed using the ProteinPilot Software 3, Revision Number: 67476 (Applied Biosystems, Foster City, CA, USA). The Paragon algorithm in the ProteinPilot software was used for the peptide identification which was further processed by the Pro Group algorithm where isoform-specific quantification was adopted to trace the differences between expressions of various isoforms. User-defined parameters were as follows: (i) Sample Type, iTRAQ 4-plex (Peptide Labeled); (ii) Cysteine alkylation, MMTS; (iii) Digestion, Trypsin; (iv) Instrument, QSTAR Elite ESI; (v) Special factors, None; (vi) Species, None; (vii) Specify Processing, Quantitate; (viii) ID Focus, biological modifications, amino acid substitutions; (ix) Database, concatenated rat database (target: Refseq rat protein database 59026 sequences; 30608194 residues) and the corresponding reverse sequence (decoy: for FDR estimation); (x) Search effort, thorough. For iTRAQ quantitation, the peptide for quantification was automatically selected by the Pro Group algorithm to calculate the reporter peak area, error factor (EF) and P-value. The resulting data was auto bias-corrected to get rid of any variations imparted due to the unequal mixing when combining different labeled samples. During bias correction, the software identifies the median average protein ratio and corrects it to unity, and then applies this factor to all quantitation results. Bias correction is only performed when there are at least 20 proteins having an average ratio. If there are fewer than 20 proteins with ratios, the sample size is too small for the median to be meaningful and no bias correction is applied.

Secreted protein determination Bioinformatics was employed to distinguish the secreted proteins and the contaminated cytoplasm protein as described in the previous studies[184]. The fasta format sequence information of the identified proteins was

submitted to web based bioinformatics tools SignalP[185], TMHMM[184], and SecretomeP[186] to determine the probability of being secreted protein; only those with probability above a certain cutoff given by the tools count. Exocarta[187], which is a database recording the proteins identified as secreted proteins from exosome in previous studies, was also used to match with the identified proteins in the present study. Text mining was employed to provide supporting information from publications. For all secreted proteins determined by SecretomeP tools, their gene IDs were used to query the NCBI gene2pubmed database. The pubmed ID related to a specific gene ID, which means the gene or protein was mentioned in the publication, was then collected and used to extract the abstract of the publication by the NCBI Esearch Entrez Utility[7]. A corpus containing the steamed vocabulary was constructed from the abstract by an in house Ruby script as described in the previous study[6]. Keywords including secretion, secreted, secreted protein, exosome, secretome were used to query the corpus. A hit indicates a publication related to the specific protein and the keywords mentioned in its abstract, which shows a higher probability that the protein may be associated with the keywords, *e.g.* secreted protein. The hit publication was then manually checked to confirm if the protein was treated as or identified as a secreted protein. The workflow is shown in figure 2.

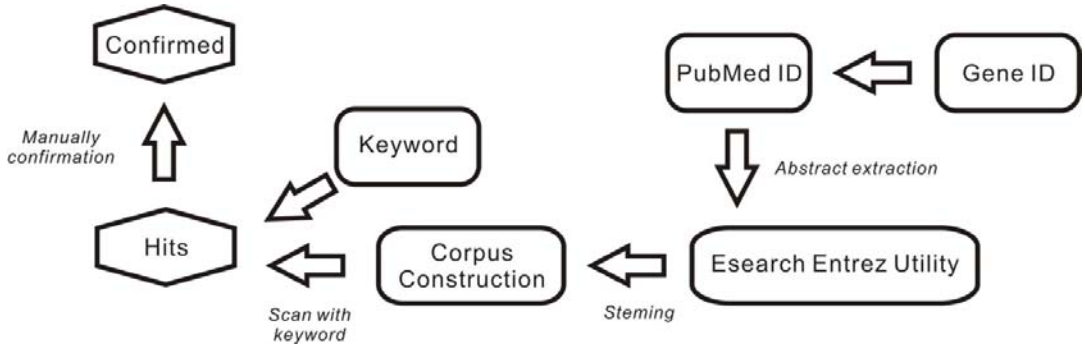

Figure 2 The work flow of text mining

Western blot

Samples were dissolved in SDS-sample buffer and heated for 10 mins at 95 ºC prior to loading to the SDS-PAGE gel. After electrophoresis, proteins on gel were blotted onto a nitrocellulose membrane. The membrane was stained with Stip1, Serpinh1, Park7, VEGF, Ppia (Santa Cruz, CA, USA) and β-actin (Millipore, MA, USA). HRP conjugated anti-mouse/anti-rabit IgG (Dako, Denmark) was used as secondary antibody.

Results and discussion

Under hypoxia, one of the responding mechanisms is to increase the expression of a subset of hypoxia-induced genes. Vascular endothelial growth factor (VEGF) is one of the most remarkably up-regulated genes[188]. The VEGF promoter contains a hypoxic response element (HRE) that can bind the transcription factor, hypoxia-inducible factor-1α (HIF-1α), and initiate transcriptional activation of the VEGF gene[189]. In this study, secreted VEGF alteration under hypoxia and 24 reoxygenation hr was detected by Western blot. Significant up-regulation of VEGF during hypoxia was observed (Figure 3), which indicates the hypoxia response of the heart myoblast H9C2.

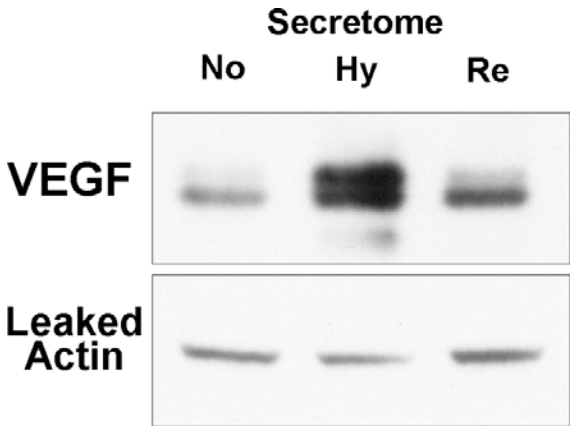

Figure 3 Secretion of VEGF from H9C2 conditioned medium measured by Western blot

Western blot was employed to measure the alteration of VEGF from condition medium generated under normoxia, hypoxia and reoxygenation. No:Normoxia, Hy: Hypoxia, Re: Reoxygenation

Rat myoblast secretome profiling

The altered H9C2 secretome between normoxia, 16 hr hypoxia and 24 hr reoxygenation was first fractionated by 1D-gel followed by LC-MS/MS profiling, and quantified by the label-free based shotgun proteomics approach as well as by stable isotope labeling using the iTRAQ-based approach. The 1D-gel based MS data were searched by MASCOT. Peptide list was generated from the DAT result file and the FDR of the result was controlled to below 1%. Peptide lists were shown in the supplemental data. 8933, 8462, 10829 peptides were identified in normoxia, hypoxia and reoxygenation respectively and in total 2007 proteins were identified. For the iTRAQ experiment, 860 proteins were identified with FDR below 1%. All proteins were identified by at least 2 peptides with 95% confidence and the unused score was above 2.08(2.0 is equivalent to 99% confident protein identification) (peptide list and protein summary are in supplemental data). As protein variation under the 2 hr

reoxygenation condition was large and also has significant bias (iTRAQ: 0.7993 comparing to normoxia), the data is not further analyzed in the iTRAQ dataset.

To select high-confidence secreted proteins for further analysis, bioinformatics tools were employed to enrich the secreted proteins. Four methods were used; the signal peptide was identified by the SignalP algorithm, proteins with transmembrane helices cleaved and released into extracellular space were recognized by TMHMM, and SecretomeP was used to identify the non-classical secreted proteins *i.e.* not signal peptide triggered protein secretion. The proteins were also screened with the Exocarta database which records the experimentally detected exosome proteins. Combined the 2007 proteins in the label free experiment with the 860 proteins in the iTRAQ experiment, 2165 proteins were identified in total. 1364 were recognized as secreted proteins by the 4 bioinformatics methods, of which 631 proteins were found in Exocarta, 540 proteins were found to have signal peptide at the N-terminus, 911 proteins were predicted to be non-classical secreted proteins and transmembrane helices section was predicted in 288 proteins (Figure 4) (supplemental data). Some secreted proteins were identified by more than one bioinformatics tools.

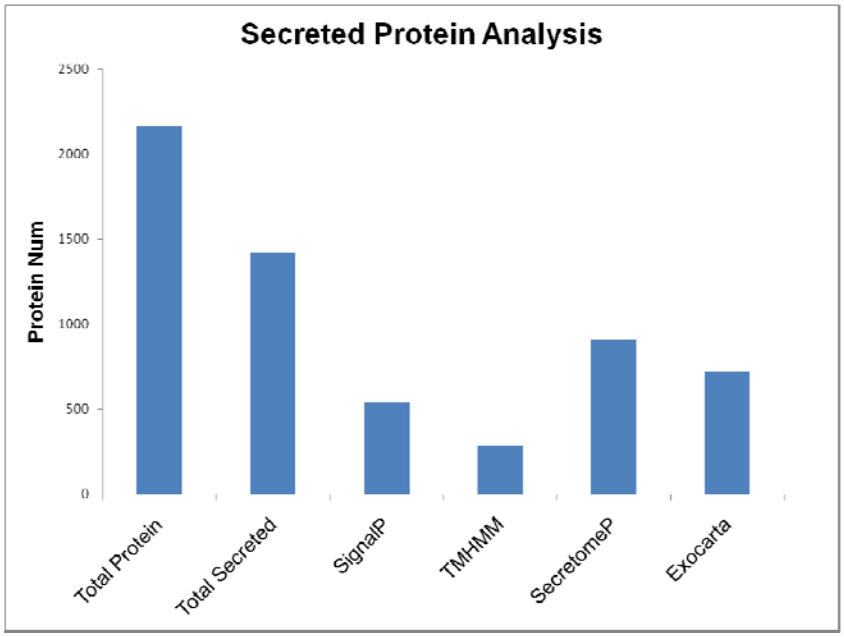

Figure 4 Secreted proteins that were recognized by SignalP, SecretomeP, TMHMM and Exocarta

To further provide supporting information to the secreted proteins, text mining technique was adopted to scan the publication that already identified these proteins in the extracellular fraction. *Gene2pubmed* database created at 2010 Jun 05 from NCBI was downloaded and used for abstract extraction. Steamed keyword "secret" stands for "secreted" or "secretion" was located in the abstract that was associated with specific proteins identified as non-classical secreted proteins in the present MS experiment. After manual checking, 10 proteins were found to be either treated as or identified as secreted proteins in the previous studies (Table 1).

GI NUM	GENE SYMBOL	UNIPROT AC	PUBMED
GI|206597443	HSPD1	P63039	19527807

GI|8393910	PEBP1	P31044	10622376
GI|293342925	NID1	P08460	10727019
GI|126723582	THOP1	P24155	15955058
GI|8394328	SOD1	P07632	17403136
GI|29293813	NAMPT	Q80Z29	20658215
GI|13591985	MIF	P30904	12297465
GI|6981026	HMGB1	P63159	11954836
GI|92373398	YBX1	P62961	19640841
GI|13592047	RNPEP	O09175	3001599

Table 1 The secreted proteins supported by the text mining result

The secreted proteins that recognized by SecretomeP algorithm only were subject to text mining to provide supportive information from previous study. 10 proteins were located in the abstract of previous published papers and confirmed to be used or considered as secreted protein in these researches. The PubMed column is the according PubMed number of the papers.

Secretion of chaperonin 60 (HSPD1) was shown to be stimulated by IL-1β and TNF-α in osteoclasts[190]. Phosphatidylethanolamine-binding protein 1 (PEBP1) was identified as a secreted protein released by adult rat hippocampal progenitor cells in a previous 2-DE coupled mass spectrometry experiment[191]. In the study conducted by Lutz Konrad *et al,* Nidogen-1 (NID1) was found to be exclusively produced and secreted by mesenchymal peritubular cells, and affected adhesion of peritubular cells in an autocrine manner[192]. The antioxidant enzyme CuZn superoxide dismutase (SOD1) was usually considered as a cytoplasmic protein, but it was also found to be secreted correlating with the depolarization-dependent calcium influx, in which may involve the soluble N-Ethyl maleimide-sensitive factor attachment protein receptor (SNARE)[193]. In a previous study, nicotinamide phosphoribosyltransferase (NAMPT) was found to be secreted by L6 rat skeletal muscle cell culture medium, indicating that it was secreted from skeletal muscle cells, supporting the view that it may be a

myokine[194]. For the rest of the proteins, it may be the first time for those proteins to be identified in the secretome fraction; therefore no literature supports were found.

SI_N label-free quantification was applied on the 1D gel based MS experiment. The SI_N value of each protein was calculated according to the method described by Griffin et al[5]. The SI_N is a value normalized by protein length and sum of abundance index of each protein in the experiment hence the relative abundance of the specific protein can be estimated. Alteration on abundance of a specific protein was estimated by comparing the relative abundance across different experiments; abundance distribution of the secretome was achieved by plotting the SI_N of each protein.

The rat myoblast H9C2 secretome including 1404 proteins generated in 16 hr normoxia was profiled by applying the SI_N calculation. As shown in figure 5, in which proteins were grouped by percentage abundance level, high-abundant proteins that account for only 12.5% of the identified protein number contribute to about 84.2% of the total abundance. Apart from the 3 proteins (Enolase 3, Eno1 protein-like, Actin, Gamma 1 propeptide-like) that were not identified as secreted protein by bioinformatics tools and text mining, the 16 high-abundant proteins in the first abundance groups were all recognized as secreted proteins. A set of proteomics data from H9C2 cytosol proteins under normoxia condition was used to estimate the protein abundance distribution of intracellular proteome (supplemental data). SI_N of each protein was calculated and compared with the secretome data (Figure 6). As shown by the figure, the variation on abundance between the normoxia secretome and the cytosol proteome indicates the intrinsic functional difference and also the limited cytosolic protein contamination. The comparisons of protein abundance distribution

between the hypoxia secretome and the cytosol proteome, the reoxygenation secretome and the cytosol proteome were shown in supplemental data, significant difference were also found in these two comparisons.

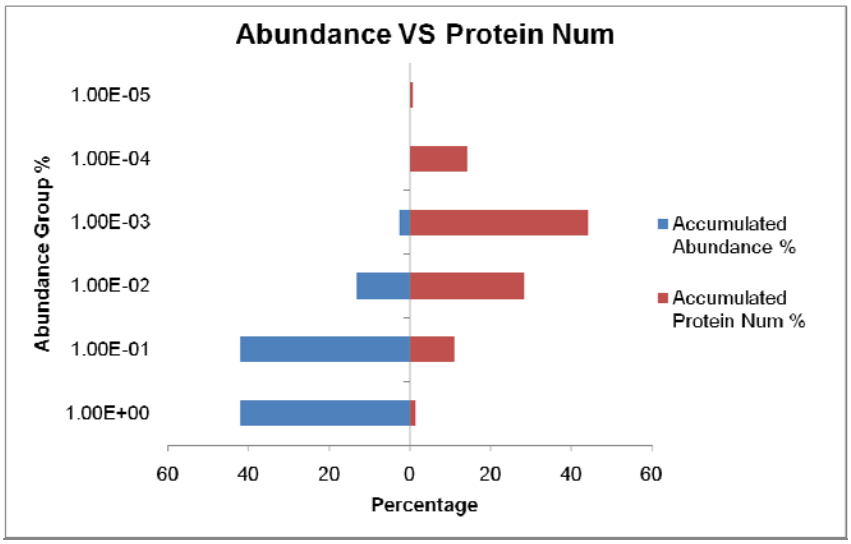

Figure 5 Distribution of the secreted protein abundance and the protein number

The distribution of accumulated secreted protein abundance and the accumulated protein number of each percentage abundance group were plot as tornado chart. The left side of the chart is the accumulated abundance; the right side is the accumulated protein number, which is represented as percentage.

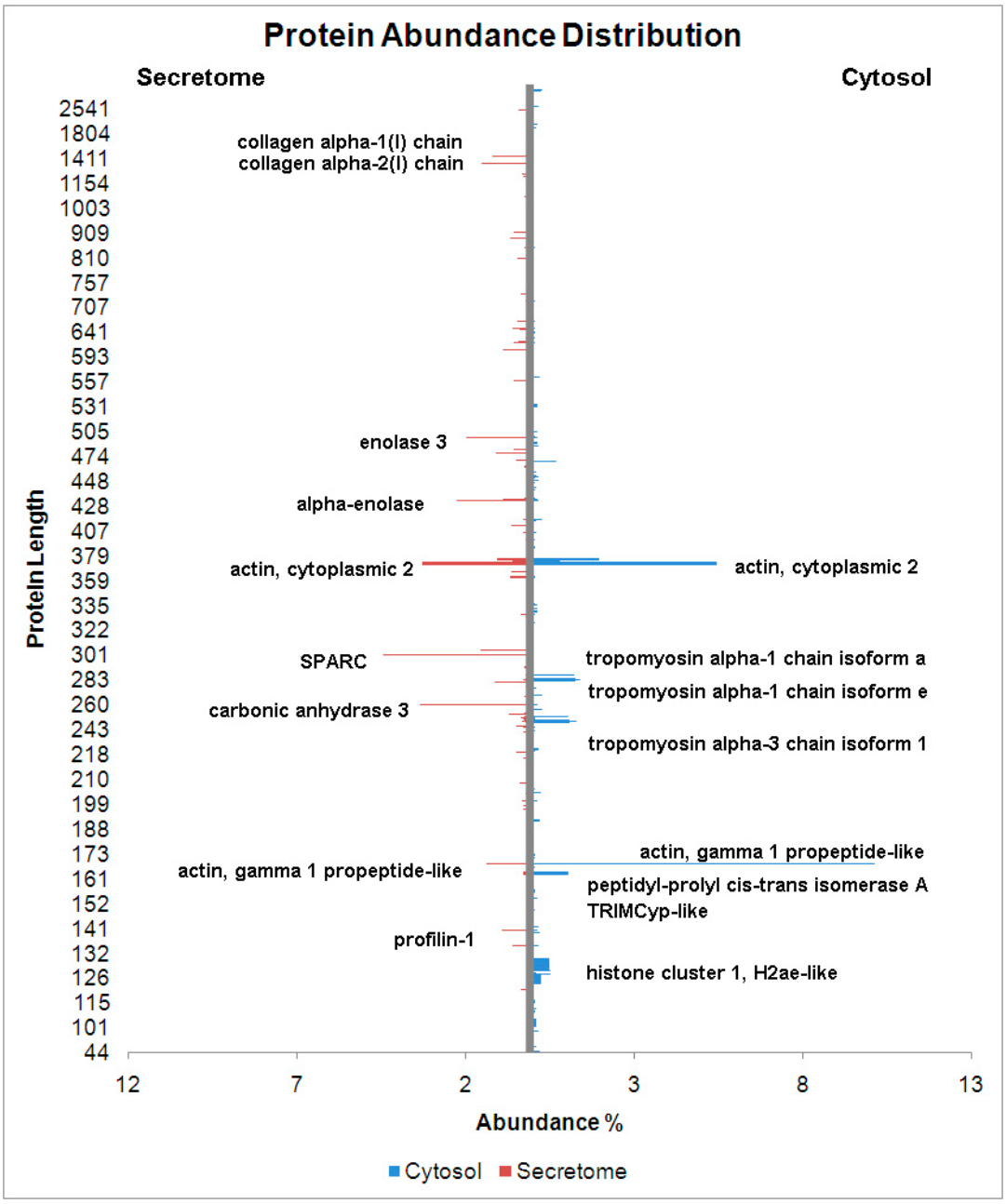

Figure 6 Abundance distribution: Secretome versus cytosolic proteome

The abundance of each secreted protein and cytosolic protein were plotted against the protein length as tornado chart. The abundance level of each protein was represented as percentage of the sum of abundance.

Quantification of the secretome under hypoxia/reoxygenation stress

Within the 860 quantified proteins in the iTRAQ experiment, 130 proteins were found to have significant changes ($P<0.05$) on abundance level under hypoxia (ratio 115/114): 87 proteins decreased and 43 proteins increased. The abundance level of 106 proteins significantly altered under 24 hr reoxygenation (ratio 117/114, $P<0.05$): 27 proteins decreased and 79 proteins increased.

For the label-free experiment, the difference in abundance between normoxia, 16 hr hypoxia and 24 hr reoxygenation was expressed as a ratio of SI_N in hypoxia versus SI_N in normoxia or SI_N in reoxygenation versus SI_N in normoxia. If the protein was not identified in either condition, the according ratio is set as N/A. In the case where a protein was identified in normoxia but not in hypoxia or reoxygenation, the abundance change is deemed as decrease; and if the protein was not identified in normoxia but in hypoxia or reoxygenation, the abundance change is deemed as increase. Besides SI_N, another two label-free quantitation methods, spectrum counting (NSAF)[195] and emPAI[196] were also applied to provide quantitative information for the 1D-gel based MS result (Supplemental data).

The label-free dataset was compared with the iTRAQ dataset to select the proteins with similar alteration trend in both experiments. Each label-free method is based on different algorithm and has its own pros and cons, hence in present study, proteins with any two or more label-free measurements that are similar to the significant iTRAQ ratio ($P<0.05$) were selected for further analysis (Table 2, 3 and supplemental data). In total, 74 and 59 secreted proteins show similar trend on abundance alteration

in the label-free and the iTRAQ experiments under hypoxia and reoxygenation, respectively.

GI	GENESYMBOL	CTRL_EMPAI	HY_EMPAI	HY/CTRL_EMPAI	CTRL_NSAF	HY_NSAF	HY/CTRL_NSAF	CTL_SIN	HY_SIN	HY/CTRL_SIN	HY/CTRL_ITRAQ	P-VALUE_ITRAQ
GI|145386553	PROS1	0.04	NA	NA	3.08E-04	0.00E+00	0.00	7.22E-07	NA	NA	0.60	1.96E-02
GI|293354593	LOC100360950	NA	NA	NA	1.24E-03	3.35E-04	0.27	2.23E-06	5.37E-07	0.24	0.63	1.56E-02
GI|157820087	HMG1L1	NA	NA	NA	8.34E-04	6.01E-04	0.72	1.23E-06	9.95E-07	0.81	0.63	7.46E-03
GI|51948384	PA2G4	0.44	0.08	0.18	4.53E-04	4.08E-04	0.90	9.03E-07	4.30E-07	0.48	0.67	8.31E-04
GI|28933457	GSTM2	1.07	0.83	0.78	6.82E-04	5.90E-04	0.87	3.01E-06	8.30E-07	0.28	0.67	2.02E-02
GI|40254752	PGK1	1.34	0.89	0.66	1.71E-03	1.16E-03	0.68	1.26E-05	4.84E-06	0.39	0.70	4.77E-05
GI|157820325	CSE1L	0.16	0.06	0.38	2.45E-04	6.62E-05	0.27	9.55E-08	5.84E-08	0.61	0.72	5.58E-03
GI|56090550	GSTO1	0.4	0.25	0.63	3.70E-04	2.67E-04	0.72	1.35E-06	5.84E-07	0.43	0.74	9.09E-03
GI|20302113	STIP1	0.29	0.16	0.55	3.83E-04	1.78E-04	0.46	4.56E-07	1.91E-07	0.42	0.75	1.28E-05
GI|62078893	UBA1	0.42	0.15	0.36	4.22E-04	1.52E-04	0.36	3.66E-07	1.42E-07	0.39	0.76	2.25E-04
GI|6981236	MYH9	0.39	0.35	0.90	7.88E-04	6.56E-04	0.83	1.13E-06	9.57E-07	0.85	0.78	3.18E-05
GI|293346337	RRBP1	0.06	NA	NA	4.09E-05	2.21E-05	0.54	3.67E-08	5.95E-09	0.16	0.78	4.19E-04
GI|77404363	NAP1L1	0.23	0.07	0.30	4.56E-04	1.65E-04	0.36	1.77E-06	2.47E-07	0.14	0.79	4.40E-04
GI|109468300	ENO1-PS1	5.19	4.19	0.81	1.05E-02	1.02E-02	0.98	8.20E-05	5.62E-05	0.69	0.80	4.38E-03
GI|29789299	XPO1	0.44	0.17	0.39	4.16E-04	2.10E-04	0.50	5.16E-07	1.92E-07	0.37	0.80	4.81E-07
GI|50657380	CLIC1	0.59	0.41	0.69	7.40E-04	4.00E-04	0.54	1.23E-06	2.34E-07	0.19	0.80	4.50E-02
GI|157821465	CARS	0.12	0.08	0.67	2.39E-04	8.60E-05	0.36	4.25E-07	2.16E-07	0.51	0.81	1.67E-02
GI|8392878	AHCY	0.49	0.3	0.61	4.13E-04	3.72E-04	0.90	7.02E-07	4.49E-07	0.64	0.82	5.15E-03
GI|18266726	PAICS	0.22	0.14	0.64	2.10E-04	1.51E-04	0.72	2.31E-07	1.28E-07	0.55	0.83	4.49E-02
GI|157786848	CCT8	0.9	0.69	0.77	1.26E-03	1.04E-03	0.82	2.20E-06	1.87E-06	0.85	0.83	2.11E-02

GI|8393381	G6PD	0.31	NA	NA	3.46E-04	1.25E-04	0.36	5.53E-07	5.85E-08	0.11	0.83	1.33E-02
GI|16758158	UFD1L	0.1	NA	NA	9.69E-05	0.00E+00	0.00	1.06E-07	NA	NA	0.83	2.14E-02
GI|71043604	SEC22B	0.13	NA	NA	1.38E-04	0.00E+00	0.00	1.41E-07	NA	NA	0.84	1.03E-02
GI|8393910	PEBP1	1.45	0.56	0.39	1.11E-03	5.16E-04	0.46	7.81E-06	3.06E-06	0.39	0.84	3.20E-02
GI|8393418	GAPDH	0.85	0.55	0.65	1.16E-03	6.76E-04	0.58	3.00E-06	2.59E-06	0.86	0.86	9.00E-03
GI|293342268	IPO5	0.56	0.45	0.80	5.22E-04	5.08E-04	0.97	1.67E-06	1.35E-06	0.81	0.86	9.34E-04
GI|54400730	CCT2	0.95	0.47	0.49	9.45E-04	5.41E-04	0.57	1.84E-06	6.28E-07	0.34	0.87	1.10E-02
GI|55741823	TARS	0.08	NA	NA	4.28E-05	0.00E+00	0.00	6.62E-08	NA	NA	0.87	3.18E-02
GI|77627971	PGM1	0.77	0.44	0.57	5.29E-04	4.01E-04	0.76	6.36E-07	5.17E-07	0.81	0.87	3.05E-02
GI|210032529	IQGAP1	0.15	0.09	0.60	2.87E-04	1.16E-04	0.41	1.66E-07	1.44E-07	0.87	0.87	4.04E-03
GI|8393610	KPNB1	0.48	0.34	0.71	7.48E-04	3.68E-04	0.49	7.23E-07	4.26E-07	0.59	0.88	5.18E-03
GI|61556967	EEF1D	0.19	0.09	0.47	3.20E-04	1.48E-04	0.46	4.73E-07	1.47E-07	0.31	0.88	3.66E-02
GI|205360969	VPS35	0.23	0.11	0.48	2.61E-04	1.62E-04	0.62	2.75E-07	1.88E-07	0.68	0.89	2.51E-02
GI|58865912	NAP1L4	0.34	0.16	0.47	4.62E-04	1.67E-04	0.36	6.04E-07	1.07E-07	0.18	0.90	2.34E-02
GI|57163991	CAPZA2	0.47	0.33	0.70	4.16E-04	3.37E-04	0.81	4.57E-07	2.74E-07	0.60	0.90	4.29E-02
GI|148491097	DYNC1H1	0.07	0.02	0.29	6.40E-05	2.77E-05	0.43	7.64E-08	3.93E-08	0.51	0.90	4.57E-02
GI|297747330	IGF2	0.34	0.16	0.47	3.11E-04	1.68E-04	0.54	1.49E-06	2.14E-07	0.14	0.93	4.88E-02
GI|18158449	COPB1	0.2	0.09	0.45	2.50E-04	1.35E-04	0.54	2.52E-07	1.40E-07	0.55	0.93	5.83E-03
GI|16758348	PRDX6	0.88	0.66	0.75	7.96E-04	5.74E-04	0.72	1.56E-06	9.47E-07	0.61	0.94	2.48E-02
GI|197386807	FLNA	1.13	1.31	1.16	1.97E-03	2.79E-03	1.42	5.45E-06	7.73E-06	1.42	1.07	8.93E-03
GI|16758780	OPLAH	0.02	0.1	5.00	2.31E-05	1.25E-04	5.41	1.38E-08	2.57E-07	18.61	1.10	4.17E-02
GI|218931161	PLOD2	0.08	0.16	2.00	1.57E-04	1.70E-04	1.08	1.25E-07	2.99E-07	2.40	1.12	3.24E-02

GI|157951709	CASQ2	1.22	1.54	1.26	4.97E-03	6.62E-03	1.33	2.71E-05	3.32E-05	1.23	1.12	1.63E-02
GI|58865670	BTD	NA	0.24	NA	5.71E-05	3.09E-04	5.41	3.51E-07	8.03E-07	2.29	1.15	1.22E-02
GI|293597511	VLDLR	0.17	0.21	1.24	2.72E-04	4.05E-04	1.49	1.81E-07	3.90E-07	2.15	1.15	4.75E-02
GI|109498802	HMCN1	0.11	0.13	1.18	1.11E-04	1.71E-04	1.55	1.32E-07	5.02E-07	3.79	1.17	8.32E-04
GI|158081739	B4GALT1	0.07	0.24	3.43	7.45E-05	2.42E-04	3.25	6.12E-08	3.38E-07	5.52	1.18	1.87E-02
GI|109482461	LOC686567	0.02	0.03	1.50	8.60E-05	1.12E-04	1.30	1.53E-07	4.35E-07	2.84	1.19	2.05E-02
GI|40254785	LAMP2	0.15	0.23	1.53	2.17E-04	3.91E-04	1.80	1.89E-07	5.24E-07	2.77	1.22	2.24E-02
GI|281306744	ODZ3	0.07	0.09	1.29	5.48E-05	9.48E-05	1.73	4.71E-08	1.54E-07	3.28	1.23	4.13E-02
GI|157820855	COL8A1	NA	0.14	NA	4.00E-05	1.73E-04	4.33	6.01E-08	4.67E-07	7.76	1.25	2.23E-02
GI|11120710	COL5A3	NA	0.04	NA	1.71E-05	5.55E-05	3.25	3.38E-08	9.31E-08	2.76	1.28	4.97E-02
GI|293342552	COL4A2	0.06	0.12	2.00	5.26E-05	1.14E-04	2.16	5.35E-08	1.22E-07	2.28	1.28	4.95E-02
GI|109505096	NID1	1.14	1.35	1.18	3.22E-03	4.80E-03	1.49	1.33E-05	2.02E-05	1.53	1.29	3.24E-02
GI|55742713	ECM1	0.05	0.1	2.00	1.06E-04	1.14E-04	1.08	1.54E-07	4.41E-07	2.86	1.30	3.24E-02
GI|198278496	C1R	0.54	0.54	1.00	6.73E-04	1.00E-03	1.49	1.13E-06	2.29E-06	2.03	1.31	3.56E-04
GI|8393057	SERPINH1	1.43	1.99	1.39	2.07E-03	2.24E-03	1.08	7.64E-06	9.17E-06	1.20	1.34	1.04E-03
GI|13786196	ATRN	0.06	0.08	1.33	6.23E-05	1.12E-04	1.80	6.18E-08	3.52E-07	5.69	1.37	6.86E-03
GI|58865820	LOXL1	0.1	0.21	2.10	1.47E-04	2.12E-04	1.44	3.11E-07	4.30E-07	1.39	1.47	6.28E-04
GI|9910214	EIF5	0.07	0.07	1.00	2.08E-04	7.50E-05	0.36	1.76E-07	5.08E-08	0.29	0.77	1.85E-02
GI|11993954	METAP2	NA	NA	NA	6.19E-05	0.00E+00	0.00	1.54E-08	NA	NA	0.77	3.27E-02
GI|61557028	TAGLN2	2.03	2.48	1.22	1.64E-03	1.29E-03	0.79	3.69E-06	3.67E-06	1.00	0.78	4.61E-04
GI|114145515	PKN3	NA	NA	NA	2.17E-04	6.71E-05	0.31	3.18E-07	6.25E-08	0.20	0.80	4.68E-03
GI|62990189	HNRNPR	0.09	0.14	1.56	1.41E-04	1.02E-04	0.72	1.20E-07	3.03E-08	0.25	0.81	3.93E-02

GI|11693142	PCNA	0.72	0.72	1.00	1.03E-03	8.63E-04	0.84	1.14E-06	9.00E-07	0.79	0.82	8.34E-03
GI|55742827	ARHGDIA	0.95	0.95	1.00	1.17E-03	9.46E-04	0.81	9.20E-06	4.62E-06	0.50	0.84	7.08E-04
GI|8392983	BGN	1.48	1.48	1.00	4.35E-03	3.49E-03	0.80	2.69E-05	1.97E-05	0.73	0.85	1.23E-02
GI|94400790	HSPB1	1.27	1.6	1.26	1.31E-03	1.26E-03	0.96	6.31E-06	3.06E-06	0.49	0.87	1.39E-02
GI|293356422	DDB1	NA	NA	NA	6.52E-04	3.39E-04	0.52	8.54E-07	7.05E-07	0.83	0.87	1.65E-03
GI|16758920	CAND1	0.63	0.75	1.19	9.43E-04	8.63E-04	0.92	3.02E-06	2.97E-06	0.98	0.87	8.75E-04
GI|93277126	MFGE8	NA	NA	NA	1.48E-03	1.33E-03	0.90	4.42E-06	2.15E-06	0.49	0.92	3.84E-02
GI|13540699	NRP2	0.06	0.06	1.00	1.93E-04	2.09E-04	1.08	2.65E-07	2.81E-07	1.06	1.10	3.68E-02
GI|16758678	PLOD1	0.12	0.12	1.00	1.23E-04	1.77E-04	1.44	1.83E-07	3.56E-07	1.95	1.12	2.40E-03
GI|300795821	FREM1	NA	NA	NA	5.38E-05	5.82E-05	1.08	4.87E-08	1.56E-07	3.20	1.12	2.78E-02
GI|110625641	FAM65B	NA	NA	NA	9.08E-05	1.96E-04	2.16	2.03E-07	1.17E-06	5.80	1.18	2.19E-03
GI|281371499	COL5A2	0.3	0.22	0.73	3.97E-04	4.51E-04	1.14	4.93E-07	9.23E-07	1.87	1.20	4.73E-04
GI|293361231	COL12A1	NA	NA	NA	3.72E-04	3.92E-04	1.05	4.18E-07	1.09E-06	2.60	1.26	2.85E-09
GI|52345385	PDIA6	0.48	0.3	0.63	4.01E-04	4.34E-04	1.08	7.39E-07	1.15E-06	1.55	1.26	1.80E-02
GI|42476116	FBLN5	0.36	0.2	0.56	5.31E-04	9.33E-04	1.76	2.23E-06	4.22E-06	1.90	1.27	1.51E-04
GI|6981324	P4HB	2.06	1.31	0.64	1.81E-03	2.09E-03	1.15	5.71E-06	5.75E-06	1.01	1.33	4.50E-03
GI|70912366	ACTR3	0.6	0.49	0.82	7.11E-04	5.39E-04	0.76	1.43E-06	1.59E-06	1.12	0.85	2.74E-02
GI|48675845	ATIC	0.28	0.22	0.79	2.51E-04	2.72E-04	1.08	2.21E-07	1.50E-07	0.68	0.89	2.72E-02
GI|11968126	PPIB	0.73	0.51	0.70	7.15E-04	6.19E-04	0.87	1.13E-06	1.42E-06	1.26	0.91	4.11E-02
GI|12018252	TKT	0.2	0.09	0.45	1.82E-04	2.95E-04	1.62	1.80E-07	1.63E-07	0.90	0.92	3.19E-02
GI|9506497	CLTC	0.63	0.45	0.71	6.57E-04	5.18E-04	0.79	1.00E-06	1.09E-06	1.09	0.93	1.51E-02
GI|210032365	HSP90B1	0.74	0.93	1.26	1.37E-03	1.44E-03	1.05	4.38E-06	4.21E-06	0.96	1.14	3.61E-03

GI|25742763	HSPA5	0.36	0.49	1.36	7.27E-04	5.90E-04	0.81	1.39E-06	1.68E-06	1.21	1.16	1.06E-03

Table 2 The significantly regulated proteins during 16 hr hypoxia detected by label free and iTRAQ

Proteins with similar trend in two or more label free measurements to iTRAQ ratio were considered as significantly regulated.

GI	GENESYMBOL	CTRL_EMPAI	RE_EMPAI	RE/CTRL_EMPAI	CTRL_NSAF	RE_NSAF	RE/CTRL_NSAF	CTL_SIN	RE_SIN	RE/CTRL_SIN	RE/CTRL_ITRAQ	P-VALUE_ITRAQ
GI|281306746	TFRC	0.12	0.08	0.67	1.56E-04	5.27E-05	0.34	2.24E-07	8.73E-08	0.39	0.72	3.03E-03
GI|17865351	VCP	0.48	0.24	0.50	6.27E-04	2.49E-04	0.40	8.06E-07	5.20E-07	0.64	0.73	5.55E-03
GI|157951709	CASQ2	1.22	1.08	0.89	4.97E-03	2.67E-03	0.54	2.71E-05	1.75E-05	0.64	0.76	9.27E-05
GI|28395795	MASP1	0.08	NA	NA	1.69E-04	0.00E+00	0.00	2.46E-07	NA	NA	0.76	1.82E-02
GI|16758666	TIMP1	1.16	1.79	1.54	1.64E-03	1.29E-03	0.79	1.21E-05	1.08E-05	0.90	0.76	3.84E-02
GI|93277126	MFGE8	NA	NA	NA	1.48E-03	6.64E-04	0.45	4.42E-06	1.72E-06	0.39	0.79	4.70E-03
GI|58865820	LOXL1	0.1	NA	NA	1.47E-04	0.00E+00	0.00	3.11E-07	NA	NA	0.80	9.29E-03
GI|29788994	TMEM132A	0.12	0.09	0.75	8.74E-05	5.89E-05	0.67	1.38E-07	1.07E-07	0.78	0.81	1.87E-02
GI|13540699	NRP2	0.06	0.1	1.67	1.93E-04	8.67E-05	0.45	2.65E-07	1.29E-07	0.49	0.81	2.04E-02
GI|13928744	TAGLN	8.1	5.01	0.62	3.70E-03	2.89E-03	0.78	1.38E-05	1.28E-05	0.93	0.83	6.93E-03
GI|46485429	GLO1	0.56	0.56	1.00	4.85E-04	3.27E-04	0.67	4.45E-07	3.66E-07	0.82	0.84	1.66E-02
GI|46485501	CDH15	0.4	0.21	0.53	4.93E-04	1.53E-04	0.31	2.14E-06	1.25E-06	0.58	0.84	9.13E-04
GI|6978723	CTSL1	0.94	0.65	0.69	9.79E-04	7.80E-04	0.80	2.52E-06	1.67E-06	0.66	0.85	2.59E-02

GI|281371499	COL5A2	0.3	0.07	0.23	3.97E-04	1.61E-04	0.40	4.93E-07	5.02E-08	0.10	0.87	3.76E-04
GI|27436861	APP	0.08	0.08	1.00	2.32E-04	1.04E-04	0.45	5.32E-07	2.09E-07	0.39	0.87	2.74E-02
GI|197333870	NID2	0.23	0.18	0.78	4.90E-04	2.01E-04	0.41	8.13E-07	3.30E-07	0.41	0.88	9.12E-03
GI|114145515	PKN3	NA	NA	NA	2.17E-04	4.18E-05	0.19	3.18E-07	7.93E-08	0.25	0.89	3.05E-02
GI|13540622	GPC1	1.51	1.38	0.91	3.41E-03	2.55E-03	0.75	2.42E-05	1.11E-05	0.46	0.91	1.34E-03
GI|209954804	PLS3	1.57	1.25	0.80	1.56E-03	1.05E-03	0.67	3.29E-06	3.74E-06	1.13	0.94	2.46E-02
GI|8394082	PSMB3	0.31	0.71	2.29	4.35E-04	7.82E-04	1.80	6.15E-07	2.07E-06	3.37	1.05	4.06E-02
GI|16758570	CDC37	NA	0.15	NA	0.00E+00	1.06E-04	NA	NA	2.13E-07	NA	1.06	3.73E-02
GI|22208848	RUVBL1	0.13	0.13	1.00	6.52E-05	1.32E-04	2.02	3.75E-08	1.63E-07	4.35	1.07	3.59E-02
GI|61556832	APRT	1.57	3.12	1.99	1.49E-03	1.89E-03	1.27	5.18E-06	4.73E-06	0.91	1.07	4.72E-02
GI|16923998	HNRNPK	0.21	0.28	1.33	2.57E-04	3.90E-04	1.52	4.81E-07	7.37E-07	1.53	1.08	2.66E-02
GI|300797978	FLNC	NA	NA	NA	7.20E-04	8.16E-04	1.13	1.29E-06	1.65E-06	1.27	1.09	1.22E-03
GI|62945366	PURB	NA	0.1	NA	0.00E+00	6.36E-05	NA	NA	4.86E-09	NA	1.11	3.92E-02
GI|16758920	CAND1	0.63	0.84	1.33	9.43E-04	8.80E-04	0.93	3.02E-06	3.34E-06	1.11	1.12	6.16E-03
GI|8392878	AHCY	0.49	0.59	1.20	4.13E-04	5.57E-04	1.35	7.02E-07	1.24E-06	1.77	1.12	2.22E-02
GI|205360969	VPS35	0.23	0.37	1.61	2.61E-04	2.27E-04	0.87	2.75E-07	3.77E-07	1.37	1.12	3.20E-02
GI|16758712	PDIA4	0.09	0.19	2.11	9.25E-05	2.81E-04	3.03	6.02E-08	1.38E-07	2.29	1.12	4.19E-02
GI|31543764	SPTAN1	0.51	0.76	1.49	5.41E-04	7.87E-04	1.45	7.42E-07	1.48E-06	2.00	1.13	1.56E-05
GI|51854227	GSN	0.16	0.25	1.56	1.91E-04	1.80E-04	0.94	2.82E-07	3.84E-07	1.36	1.14	2.46E-02
GI|8393296	EEF2	1.92	2.69	1.40	4.33E-03	3.39E-03	0.78	1.09E-05	1.25E-05	1.15	1.14	3.15E-03
GI|61557085	SPTBN1	0.19	0.31	1.63	2.14E-04	3.40E-04	1.59	2.41E-07	4.75E-07	1.97	1.14	1.22E-02
GI|25742626	AIFM1	NA	0.05	NA	0.00E+00	3.28E-05	NA	NA	5.87E-08	NA	1.14	2.79E-02

GI|61556835	THBS1	0.24	0.27	1.13	5.08E-04	4.63E-04	0.91	1.01E-06	1.60E-06	1.58	1.15	2.71E-02
GI|157817857	COL6A3	0.14	0.22	1.57	1.48E-04	1.82E-04	1.23	9.82E-08	2.74E-07	2.79	1.15	1.66E-02
GI|62652278	LRP1	0.06	0.11	1.83	9.81E-05	1.41E-04	1.44	2.18E-07	3.21E-07	1.48	1.17	3.52E-02
GI|208022685	IARS	NA	0.07	NA	0.00E+00	4.77E-05	NA	NA	6.23E-08	NA	1.17	7.21E-04
GI|157818975	FLNB	0.11	0.23	2.09	3.23E-04	4.59E-04	1.42	7.43E-07	9.63E-07	1.30	1.17	4.50E-04
GI|8393381	G6PD	0.31	0.38	1.23	3.46E-04	3.11E-04	0.90	5.53E-07	1.43E-06	2.58	1.17	2.23E-02
GI|8394072	PSMA5	0.81	0.61	0.75	4.94E-04	4.99E-04	1.01	7.04E-07	8.67E-07	1.23	1.17	3.43E-02
GI|40018616	CCT3	0.23	0.6	2.61	2.18E-04	5.15E-04	2.36	4.53E-07	1.51E-06	3.34	1.18	2.29E-04
GI|281332151	ROBO2	NA	0.04	NA	0.00E+00	2.65E-05	NA	NA	9.00E-09	NA	1.19	1.91E-02
GI|6981396	PRKAR1A	NA	0.16	NA	7.80E-05	1.05E-04	1.35	5.45E-08	3.38E-08	0.62	1.19	6.32E-03
GI|77627971	PGM1	0.77	0.77	1.00	5.29E-04	7.85E-04	1.48	6.36E-07	1.07E-06	1.68	1.19	1.69E-02
GI|77404395	SND1	0.06	0.21	3.50	6.54E-05	1.54E-04	2.36	6.56E-08	2.07E-07	3.15	1.20	6.91E-03
GI|55741823	TARS	0.08	0.13	1.63	4.28E-05	8.65E-05	2.02	6.62E-08	1.38E-07	2.09	1.21	1.91E-02
GI|293352109	LOC100360507	NA	NA	NA	2.15E-04	5.79E-04	2.70	6.04E-07	1.80E-06	2.98	1.21	4.09E-02
GI|109468300	ENO1-PS1	5.19	4.19	0.81	1.05E-02	1.24E-02	1.19	8.20E-05	1.15E-04	1.40	1.21	1.96E-02
GI|148491097	DYNC1H1	0.07	0.08	1.14	6.40E-05	5.61E-05	0.88	7.64E-08	8.62E-08	1.13	1.22	1.09E-03
GI|9507243	YWHAB	0.95	2.82	2.97	1.93E-03	3.34E-03	1.73	4.99E-06	1.09E-05	2.19	1.22	4.35E-02
GI|157823757	POSTN	2.72	3.6	1.32	5.14E-03	4.11E-03	0.80	1.89E-05	3.21E-05	1.69	1.22	1.06E-03
GI|29293811	SERPINF1	0.98	1.8	1.84	1.49E-03	1.63E-03	1.09	4.01E-06	3.87E-06	0.97	1.23	1.93E-02
GI|13929168	FAT1	0.06	0.12	2.00	5.83E-05	8.74E-05	1.50	4.95E-08	1.57E-07	3.18	1.25	3.08E-02
GI|8394009	PPIA	8.24	17.31	2.10	3.63E-03	4.89E-03	1.35	1.21E-05	3.14E-05	2.59	1.26	3.01E-02

GI|6981236	MYH9	0.39	0.55	1.41	7.88E-04	6.75E-04	0.86	1.13E-06	1.85E-06	1.65	1.27	9.29E-04
GI|40254781	GDI2	1.12	1.72	1.54	1.80E-03	2.07E-03	1.15	3.15E-06	4.18E-06	1.32	1.30	9.66E-04
GI|157818047	PTK7	0.2	0.3	1.50	1.15E-04	3.36E-04	2.92	4.30E-07	1.84E-06	4.29	1.30	4.18E-03
GI|59709467	CAP1	0.54	0.74	1.37	7.53E-04	7.61E-04	1.01	2.67E-07	1.69E-06	6.35	1.30	1.86E-03
GI|46485440	GPI	1.63	2.39	1.47	1.39E-03	2.05E-03	1.48	6.02E-06	1.40E-05	2.32	1.31	3.10E-04
GI|293597511	VLDLR	0.17	0.29	1.71	2.72E-04	3.44E-04	1.26	1.81E-07	7.54E-07	4.15	1.34	3.45E-03
GI|157824103	GLB1	0.14	0.24	1.71	1.38E-04	1.55E-04	1.12	1.44E-07	2.96E-07	2.06	1.36	2.83E-02
GI|6978487	ALDOA	3.57	5.82	1.63	6.21E-03	7.76E-03	1.25	2.76E-05	5.99E-05	2.17	1.37	5.87E-03
GI|26023949	ENO2	0.96	1.39	1.45	4.18E-03	6.51E-03	1.56	2.67E-05	5.46E-05	2.05	1.43	3.62E-02
GI|8392983	BGN	1.48	2.35	1.59	4.35E-03	4.83E-03	1.11	2.69E-05	3.10E-05	1.15	1.45	7.53E-05
GI|117935064	TPI1	2.98	7.92	2.66	2.15E-03	6.44E-03	3.00	1.44E-05	3.83E-05	2.66	1.59	7.48E-03
GI|40254752	PGK1	1.34	2.34	1.75	1.71E-03	2.16E-03	1.26	1.26E-05	2.59E-05	2.06	1.64	3.16E-10
GI|8393418	GAPDH	0.85	1.21	1.42	1.16E-03	1.63E-03	1.40	3.00E-06	8.31E-06	2.77	1.75	6.92E-03
GI|218931161	PLOD2	0.08	0.25	3.13	1.57E-04	2.64E-04	1.69	1.25E-07	4.95E-07	3.97	2.00	1.81E-03
GI|293354593	LOC100360950	NA	NA	NA	1.24E-03	1.88E-03	1.52	2.23E-06	4.88E-06	2.19	2.82	3.20E-03

Table 3 The significantly regulated proteins during 24 hr reoxygenation detected by label free and iTRAQ

Proteins with similar trend in two or more label free measurements to iTRAQ ratio were considered as significantly regulated.

To gain a systemic view of the modulated secreted proteins under hypoxia and reoxygenation, overrepresentation ($P<0.05$) of biological process terms were detected using DAVID tools. 85 biological processes were enriched by the modulated secreted proteins (Figure 7 and supplemental data). The proteins up-regulated in hypoxia were associated with biological processes such as extracellular matrix organization, cell adhesion, collagen fibril organization. It is shown by these associated biological processes that ECM remodeling began in the hypoxia stage and the cell adhesion was modulated. The declined proteins in hypoxia are related to positive regulation of cellular component organization, intracellular transport, establishment of protein localization etc. During the reoxygenation stage, the increased proteins in the secretome are involved in metabolism, establishment or maintenance of cell polarity, regulation of protein complex assembly etc. Whereas the own-regulated proteins are related to several biological processes such as cell adhesion, regulation of programmed cell death, and regulation of apoptosis. The proteins that were modulated during hypoxia and reoxygenation were further discussed below. The fold change of specific protein is represented by the iTRAQ ratio.

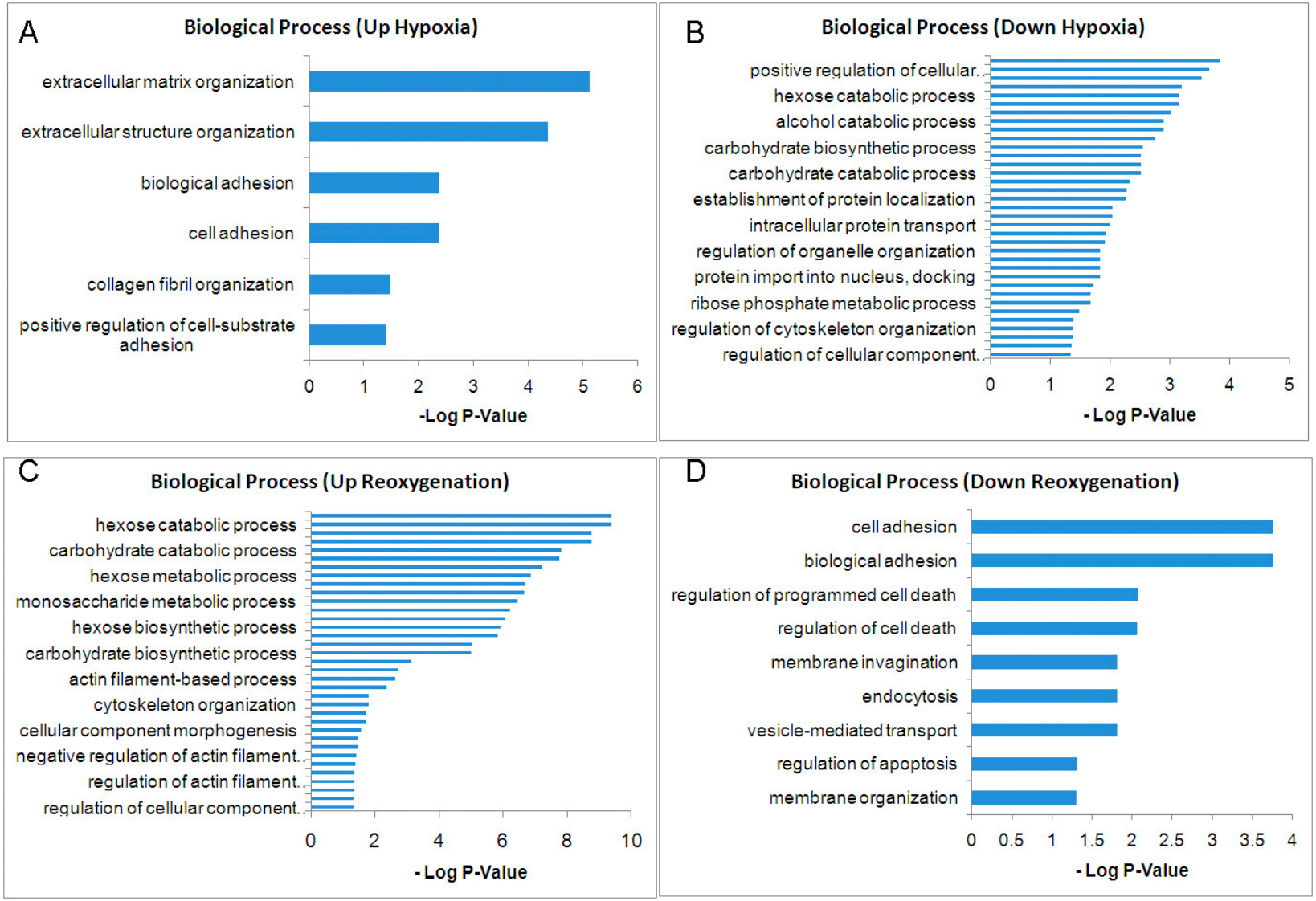
A
Biological Process (Up Hypoxia)
extracellular matrix organization
extracellular structure organization
biological adhesion
cell adhesion
collagen fibril organization
positive regulation of cell-substrate adhesion
0 1 2 3 4 5 6
-Log P-Value
B
Biological Process (Down Hypoxia)
positive regulation of cellular..
hexose catabolic process
alcohol catabolic process
carbohydrate biosynthetic process
carbohydrate catabolic process
establishment of protein localization
intracellular protein transport
regulation of organelle organization
protein import into nucleus, docking
ribose phosphate metabolic process
regulation of cytoskeleton organization
regulation of cellular component..
0 1 2 3 4 5
- Log P-Value
C
Biological Process (Up Reoxygenation)
hexose catabolic process
carbohydrate catabolic process
hexose metabolic process
monosaccharide metabolic process
hexose biosynthetic process
carbohydrate biosynthetic process
actin filament-based process
cytoskeleton organization
cellular component morphogenesis
negative regulation of actin filament..
regulation of actin filament..
regulation of cellular component..
0 2 4 6 8 10
- Log P-Value
D
Biological Process (Down Reoxygenation)
cell adhesion
biological adhesion
regulation of programmed cell death
regulation of cell death
membrane invagination
endocytosis
vesicle-mediated transport
regulation of apoptosis
membrane organization
0 0.5 1 1.5 2 2.5 3 3.5 4
- Log P-Value

Figure 7 The enriched biological processes of the secreted proteins changed under hypoxia and reoxygenation

Biological process enriched by the proteins that were: A. Up-regulated during 16 hr hypoxia B. Down-regulated during 16 hr hypoxia C. Up-regulated during 24 hr reoxygenation D. Down-regulated during 24 hr reoxygenation. The keywords with P-values below 0.05 were plot. The P-value was transformed to -Log (P-value), hence the higher the more confident of the keyword enrichment.

ECM remodeling, angiogenesis and inflammation response during hypoxia

Extracellular matrix related proteins were modulated during hypoxia. Serpin H1 (SERPINH1) binds specifically to collagen. It could be involved as a chaperone in the biosynthetic pathway of collagen. A previous study showed that modest reduction in SERPINH1 by antisense oligonucleotides led to significant decrease in procollagen synthesis[197], which indicated the important role of SERPINH1 in ECM regulation. Cell-surface expression of Serpinh1 was also reported[198-199]. Due to its collagen binding function, inhibition of SERPINH1 abolished platelet aggregation in response to collagen [199]. It is not clear how SERPINH1, which is considered to locate in endoplasmic reticulum, is secreted into peripheral blood, while SERPINH1 antigen and autoantibodies to SERPINH1 were detected in sera of patients with mixed connective tissue disease[200]. In our study, secreted SERPINH1 was found to be up-regulated (1.34 fold P=1.04E-3) after hypoxia. The up-regulation of SERPINH1 may contribute to collagen deposition. Hypoxia stimulates the gene expression of a cluster of hydroxylases that are indispensible for collagen fiber formation[201]. Up-regulation of Procollagen-lysine, 2-oxoglutarate 5-dioxygenase 1/2 (PLOD1, PLOD2) was detected under hypoxia (1.12 fold P=2.40E-3, 1.12 fold P=3.24E-2) and was supported by a previous study[201]. The expressions of these 2 proteins are coordinated by HIF-1[201].

PLOD1 and PLOD2 form hydroxylysine residues in -Xaa-Lys-Gly- sequences in collagens. These hydroxylysines serve as sites of attachment for carbohydrate units and are essential for the stability of the intermolecular collagen cross-links. Enhanced collagen deposition under hypoxia was observed in the present study corresponding to the increased secretion of SERPINH1 and PLOD1/2. Collagen alpha-1(VIII) chain (COL8A1), collagen alpha-1(XII) chain (COL12A1), collagen type IV alpha 2 (COL4A2), collagen type V alpha 2 (COL5A2) and collagen alpha-3(V) chain (COL5A3) have increased 1.25 (P=2.23E-2), 1.26 (P=2.85E-9), 1.28 (P=4.95E-2), 1.20 (P=4.73E-4), 1.28 (P=4.97E-2) fold during hypoxia. The collagen deposition represents the ECM remodeling response of cardiac myocytes under ischemia/hypoxia stress. Raised collagen secretion after ischemia and reperfusion injury was observed by previous studies. Formation of collagen-based scar provides mechanical support to the injured myocardium[154]. Increased abundance of Lysyl oxidase homolog1 (LOXL1, 1.47 fold P=6.28E-4) was also detected under hypoxia. Expression of cross-linking enzymes, such as LOXL1, increased to induce the matrix cross-linking in the infarcted myocardium as the scar matures[170]. Dense cross-linked collagen in the mature scar enhances tensile strength of the infarct while increasing passive stiffness and resulting in diastolic dysfunction.

During hypoxia, oxygen supply is limited. Angiogenesis is hence elicited to cope with the stress. Extracellular matrix protein 1 (ECM1) was found to be up-regulated (1.30 fold P=3.24E-2) under 16 hr hypoxia. ECM1 was reported to interact with perlecan domain V[202], which is a potent anti-angiogenic factor[203]. A previous study found that the expression level of ECM1 has a high positive association with the growth,

metastasis and angiogenesis of laryngeal carcinoma[204]. The increased secretion of ECM1 by H9C2 during hypoxia may be part of the angiogenesis process.

Attractin (ATRN) was another up-regulated (1.37 fold P=6.86E-3) protein during hypoxia. This protein is an ectoenzyme, the circulating levels of which are related to the ability of peripheral blood mononuclear cells (PBMC) to react *in vitro* to recall antigens like tetanus toxoid[205]. It is reported by a previous study that recombinant ATRN mediates monocyte/macrophage spreading and T cell clustering[206]. Another study also found rapid up-regulation of ATRN by activated T cells[207]. These discoveries suggest a significant role of ATRN in the immune response *in vivo*. Death of cardiomyocyte during hypoxia triggers a cascade of inflammatory pathways that work to clear dead cells and matrix debris, as well as to repair and heal damaged tissues. The increase of ATRN during hypoxia/ischemia may be involved in the inflammatory process to interact with the monocytes and macrophages.

Biglycan, vitamin k-dependent protein s and stress-induced-phosphoprotein 1 were modulated during hypoxia

Biglycan (BGN) is a member of the small leucine-rich proteoglycan family that regulates fibrillogenesis of collagen and the fibril diameter [208]. The expression of biglycan increases at 3, 7 and 14 days after MI in wild type mice; and collagen matrix formation of infarct scars was impaired in knockout mice [209]. Exogenous administration of biglycan protects myocardial cells from hypoxia/reoxygenation injury via an NO-dependent mechanism [210]. Down-regulation (0.85 fold P=1.23E-2) of Bgn observed in our experiment after hypoxia reflects a deficiency of the cardio protection. Vitamin k-dependent protein s (PROS1) is an anticoagulant plasma protein.

The deficiency of which has been associated with MI. An increased tendency of arterial thrombosis due to PROS1 deficiency has also been suggested[211-212]. After 16 hr hypoxia, decreased secreted PROS1 level was detected (0.60 fold P=1.96E-2), which suggests an elevated risk of thrombosis after ischemia *in vivo*.

Stress-induced-phosphoprotein 1 (STIP1) is an adaptor protein that coordinates the functions of HSP70 and HSP90. According to the UniProt gene ontology annotation, Stip1 locates in the cytoplasm and nucleus. However, it is also found at the cell membrane besides in the cytoplasm in a previous study[213] even though no transmembrane helices were predicted on stip1 by the TMHMM algorithm. STIP1 was detected in the secreted proteome in our study and found in the exosome fraction in a previous study[214] recorded by the Exocarta database. Under hypoxia declined abundance of Stip1 (0.75 fold P=1.28E-5) was observed.

Increase of cell adhesion proteins during reoxygenation stage

Abundance of several extracellular proteins related to cell adhesion increased under reoxygenation. Roundabout 2 (ROBO2), POSTN, Thrombospondin 1 (THBS1), Protocadherin Fat1 (FAT1) increased 1.19 (P=1.91E-2), 1.22 (P=1.06E-3), 1.15 (P=2.71E-2), 1.25 (P=3.08E-2) fold under reoxygenation, respectively. ROBO is a novel member of the Ig superfamily of cell adhesion molecules (CAM)[215]. Three vertebrate Robo homologues including Robo1, Robo2 and Rig1 have been cloned. Robo shows a high level of homology to other CAMs including NCAM, L1 and DCC[216-217]. Vertebrate Robo1 and Robo2 can interact both homophilically and heterophilically to promote neurite outgrowth[215]. POSTN is an ECM protein significantly related to fibrosis and ECM metabolism in a range of disease conditions,

including cardiovascular disease and cancer[165] and also has genomic associations with ventricular hypertrophy[166] and heart failure[167]. POSTN was found to be significantly over-expressed under the myocardial pressure overload and significantly under-expressed in relief of pressure overload and its expression was found to be associated with greater dysfunction in ventricular remodeling[218]. Abundant expression of POSTN was found in the border zone in both mouse and human myocardial infarction and significantly modulated the phenotype and function of fibroblast in the infarcted myocardium[168]. POSTN null mice had impaired healing and higher risk of cardiac rupture[168-169]. However, surviving mice had less fibrosis and considerably better cardiac performance which suggests that POSTN depletion attenuated adverse remodeling[169]. THBS1 is an adhesive glycoprotein that mediates cell-cell and cell-matrix interactions. Expression of Thbs1 was reported to be stimulated by stabilized HIF-1α under hypoxia. It was shown that hypoxia contributed to the progression of fibrosis in patients with systemic sclerosis by increasing release of major extracellular matrix proteins including Thbs1[219]. THBS1 was also found to promote migration of human coronary artery smooth muscle cells under hypoxia which is a vital cause of arterial wall thickening[220]. Re-endothelialization and reduced neointimal formation in balloon-injured rat arteries can be significantly accelerated by antibody against Thbs1[221]. Moreover, THBS1 is an activator of transforming growth factor beta (TGFβ). A previous study found that Thbs1 is induced in myocardial infarct healing and participates in suppressing the post-infarction inflammatory response, inhibiting local angiogenesis, and limiting expansion of granulation tissue into the non-infarcted area[158]. FAT1 is annotated as a cell membrane protein by cellular component in

Uniprot; signal peptide was detected by SignalP and transmembrane helices by TMHMM in the present study. Previous studies reported that Fat1 was localized at filopodial tips, lamellipodial edges, and cell-cell boundaries. Knockdown of FAT1 mediated by RNA interference resulted in disorganization of cell junction-associated F-actin and other actin fibers/cables, disturbance of cell-cell contacts, and also cell polarity formation inhibition at wound margins[222]. In an epithelial cell wound model, FAT1 knockdown decreased recruitment of endogenous vasodilator-stimulated phosphoprotein (VASP) to the leading edge and led to lamellipodial dynamics impairment, polarization failure, and cell migration attenuation [223]. The increased abundance of these proteins contributes to cell-ECM interaction, cell adhesion, anti-inflammation response and ECM remodeling regulation during the reoxygenation stage.

Proteins relate to cell survival were regulated during reoxygenation

Different from hypoxia, when it was down-regulated, secreted form of BGN was 1.45 fold up-regulated (P=7.53E-5) after reoxygenation, the cytoplasmic form of which was also reported to be increased in the mice myocardial infarction model[209]. The increased BGN may exert its cardioprotective effect under stress[210].

Peptidyl-prolyl cis-trans isomerase (PPIA) is an 18 kDa protein possessing multiple functions. A previous study indicated its role as a secreted redox-sensitive mediator and vascular smooth muscle cell growth factor which stimulates cell growth and inhibits apoptosis[132]. Under hypoxia/reoxygenation, secreted PPIA plays a role in protecting cardiac myocytes against oxidative stress-induced apoptosis via all autocrine fashion[133]. PPIA is also a molecular chaperone that acts as an acceleration

factor in protein folding and assembly[134]. Expression of PPIA was found to increase in rat cardiac myocytes under hypoxia and reoxygenation[133]. Moreover, overexpression of PPIA in cancer cells renders resistance to hypoxia- and cisplatin-induced cell death[135]. It is shown in the dataset that PPIA was up-regulated (1.26 fold P=3.01E-2) after 24 hr reoxygenation. The increased secretion of PPIA by cardiac myocytes under reoxygenation stress after hypoxia has been observed by a previous study[133] and our observation confirmed the finding.

Significantly down-regulated proteins during 24 hr reoxygenation including glyoxalase I (GLO1), transmembrane protein 132A (TMEM132A), and metalloproteinase inhibitor 1 (TIMP1) were classified into the biological process of programmed cell death regulation. These proteins were studied before and found to have anti-apoptosis function. Overexpression of Glo1 reduces renal ischemia-reperfusion injury in rats[224]. Knockdown of TMEM132A by RNA interference facilitates serum starvation-induced cell death in Neuro2a cells[225]. TIMP1 was found to prevent radiation-induced apoptosis of capillary endothelial cells[226]. The declined secretion of these anti-apoptosis proteins indicates the pro-apoptosis trend of the modulation under reoxygenation stress.

Besides its anti-apoptosis function, TIMP1 also inhibits the activity of metalloproteinases. Decrease of TIMP1 secreted by carcinoma cells under hypoxia and reoxygenation was reported by a previous study[227]. Reduced secretion of TIMP1 leads to diminished inhibition on the matrix metalloproteinase, which plays an important role in degrading the collagens. The cardiac collagen deposition and degradation is a dynamic balance under pathological situation and is part of the ECM

remodeling[228]. Moreover decrease of COL5A2 (0.87 fold P=3.76E-4) as well as LOXL1 (0.80 fold P=9.29E-3) was detected under reoxygenation accordingly.

Validation of the regulation on secreted proteins by Western blot

Alterations of selected secreted protein during hypoxia and reoxygenation were validated by western blot. STIP1, SERPINH1, PPIA and Protein DJ-1(PARK7) which had no significant change after hypoxia and reoxygenation were blotted (Figure 8). From the western result it is found that the alteration on STIP1, and SERPINH1 after hypoxia agreed with the proteomics data. PPIA showed significant up-regulation after reoxygenation. No significant change was found on PARK7 after hypoxia and reoxygenation, which also agreed with the proteomics data.

To further prove that the regulation was due to secretion but not change on the expression level, western blot was also carried out on the cell lysate samples that were subjected to normoxia, hypoxia and reoxygenation. No significant regulation (STIP1, SERPINH1) or different regulation (PPIA) was identified in cell lysates, indicating that the regulation was due to secretion but not the expression level change (Figure 8). Secreted and cytosol SERPINH1, PARK7 were blotted and exposed for the same duration on the same membrane; SERPINH1 showed stronger signal than Park7 in the cell lysate, however, the situation is the opposite in the secretome (Figure 8). This difference indicates that the proteome composition of the secretome sample differs from the cell lysate, which provides an indirect proof of limited cytosol contamination.

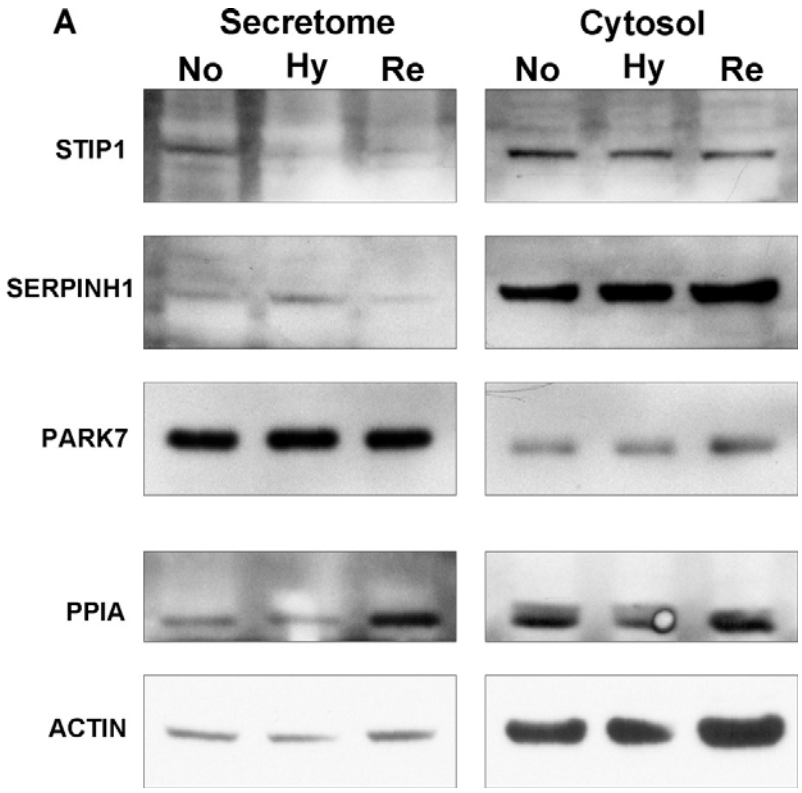

Figure 8 Western blot of Stip1, SerpinH1, Park7, and Ppia from secretome and cytosol proteome

Conclusion

In the present study, secretome from rat heart myoblast H9C2 under 16 hr normoxia, 16 hr hypoxia and 24 hr reoxygenation stress were profiled and quantified by the label-free MS approach and the stable isotope-labeling iTRAQ-based method to select high confident modulated proteins for further analysis. Selected proteins' differentiated secretion levels were further confirmed by Western blot.

Large numbers of proteins were identified as secreted proteins besides those well known secreted proteins such as collagen, SPARC and Fibronectin. These newly identified proteins passed bioinformatics filters and were recognized as exosome

proteins, proteins with signal peptide or transmembrane helices and proteins which were secreted by non-classical secretion pathways. By applying the SI_N label-free method protein abundance distribution was obtained. The normoxia secreted proteome shows different abundance distribution comparing to the whole proteome under the same condition. The differential abundance distribution was also shown by Western blot on PARK7 and SERPINH1 from the secretome and cell lysate. These data indicate the intrinsic difference of characteristic between the secretome and the cytosol proteome.

Label-free quantitation is an alternative choice to the stable isotope labeling approach for quantitative proteomics analysis. No additional chemistry or sample preparation steps are required for the label-free approach that can be performed in almost any types of LC-MS/MS instruments. However, more variation is introduced during the sample preparation and MS analysis steps. Several algorithms such as area under curve (AUC), NSAF, emPAI, SI_N, Spectral TIC are available for quantitation and bias correction; each has its pros and cons under different experimental situations[229]. Labeling strategies like iTRAQ are often considered to be more accurate in quantitating protein abundances. In a previous study, iTRAQ was used as validation for the label free experiment[230]. However, the number of samples that can be analyzed in a single experiment is limited. Moreover, the abundance alteration amplitude may sometimes be compressed by isotope labeling quantitation but not the label-free methods[231]. In the present study, we quantified the hypoxic/reoxygenated secretome from cardiomyocyte H9C2 by applying both stable-isotope labeling and three label-free semi quantitative methods to achieve a more-confident quantitative result.

Label-free methods including emPAI, NSAF and SI_N were applied on the 1D gel based MS dataset to quantify the identified proteins from normoxia, hypoxia and reoxygenation. The emPAI calculation is automatically included in MASCOT[183]. NSAF and SI_N were calculated from the DAT result from the MASCOT search result. The quantified dataset was compared with the iTRAQ dataset. iTRAQ labeled proteins with significant abundance change ($P<0.05$) were selected for comparison. Proteins with similar trend in at least two or more label-free quantitation to the iTRAQ ratio were considered as modulated proteins in the according condition.

Analysis on the quantitative dataset reveals ECM remodeling during hypoxia including increased SERPINH1, PLOD1/2 and collagen deposition, which is the cellular response to the damage caused by hypoxia's attempting to provide a scaffold for inflammatory cells to migrate in and to clean up dead cells. Increased secretion of LOXL1 was also observed during the stage of hypoxia, which cross-links the collagen to form a mature scar. The ECM turnover is regulated by the ECM protein deposition and degradation which is carried out by the matrix metalloproteinase. At the reoxygenation stage, we observed decrease of TIMP1, which irreversibly inactivates matrix metalloproteinase by binding to their catalytic zinc cofactor; and decrease of COL5A and LOXL1, which may be due to the shift of the balance from deactivation to activation of the matrix metalloproteinase.

During reoxygenation, secretion of a group of cell adhesion proteins including ROBO2, POSTN, THBS1 and FAT1 increased. Such cell adhesion proteins are involved in cell-cell interaction or cell-matrix adhesion. Especially, POSTN exerts modulation on the ECM remodeling and the healing process; THBS1 limits the

inflammation response via TGFβ activation and regulates the infarct healing through its angiostatic effects by applying direct anti-inflammatory actions or by mediating MMP activation[171]. There is limited information that relates ROBO2 and FAT1 to cardiovascular events and none to cardiac ischemia/reperfusion. The abundance rise of these two secreted proteins under hypoxia/reoxygenation is a novel observation and their functions in the scenario are yet to be clarified. Pro-apoptotic response was observed during reoxygenation as decrease of several anti-apoptosis proteins including GLO1, TMEM132A and TIMP1 was detected.

By using the label-free and iTRAQ-based method, we identified modulated subproteome of the secreteome of cardiomyocytes under hypoxia and reoxygenation. The detected modulation of secretome that participates in or regulates ECM composition as well as those secreted proteins such as ECM1, ATRN, STIP1 that have not been observed under the pathological situation before provides a systemic view of the molecular events and novel information to understand the underlying mechanism involved in cardiac hypoxia and reoxygenation.

Chapter 4. Conclusions

In chapter 2, we demonstrate a study on proteome alteration during cardiac ischemia and reperfusion in a mice model by the iTRAQ quantitative approach. Important functional groups of proteins were found to be regulated which indicate the perturbation caused by the oxygen and energy depletion circumstance. Figure 1 summarized the proteomics study on both *in vivo* and *in vitro* models.

As shown by analysis on the modulation of energy production protein groups and decrease of the anti-oxidative proteins, ROS imbalance may be involved. Declined protein abundance of oxidative stress sensing protein PARK7 during the ischemia and reperfusion stage was detected. The antioxidant transcriptional master regulator NRF2, which is protected by PARK7 from degradation, was also decreased along with its downstream gene products shown in the iTRAQ data. To further study the role of PARK7 under ischemia/hypoxia, FLAG-tagged Park7 was cloned and expressed in the rat heart myoblast H9C2 cell line. Increase on the protein level of NRF2 as well as on the *Sod1* and *Sod2* mRNAs levels were observed in the expressed cell line under hypoxia. Cell survival under hypoxia stress was also improved for the expressed cells. This *in vitro* experiment shows that the protein level of PARK7 affects NRF2 protein and the transcriptional level of its downstream anti-oxidative stress proteins, and implies the importance of PARK7 under ischemia and reperfusion.

Under hypoxia, protein folding in endoplasmic reticulum (ER) is interrupted and the unfolded polypeptides or improperly folded proteins cause ER stress and unfolded protein response (UPR). Protein maturation is important especially when the cells are

stressed. The folding assisting protein PPIA is found to be up-regulated/increased during cardiac ischemia and reperfusion. The interactome of PPIA was studied by IP-MS in FLAG-tagged PPIA expressed H9C2 cells. Some of the interaction partners are related to protein folding and stabilization, which is coincident with the function of cytoplasmic PPIA. Interactome variation between normoxia and hypoxia was also acquired by the label-free IP-MS approach. It is shown that Chaperonin containing TCP1 complex and USP47 have higher binding efficiency to PPIA under hypoxia. This indicates that PPIA may help to increase the protein folding capacity when unfolded protein stress was induced by hypoxia. Further, proteins involved in important biological processes were found to locate within the interaction network of PPIA by using bioinformatics techniques. The functional study of PPIA interactome indicates that up-regulation of PPIA during ischemia and reperfusion helps to cope with the accumulated unfolded polypeptide stress.

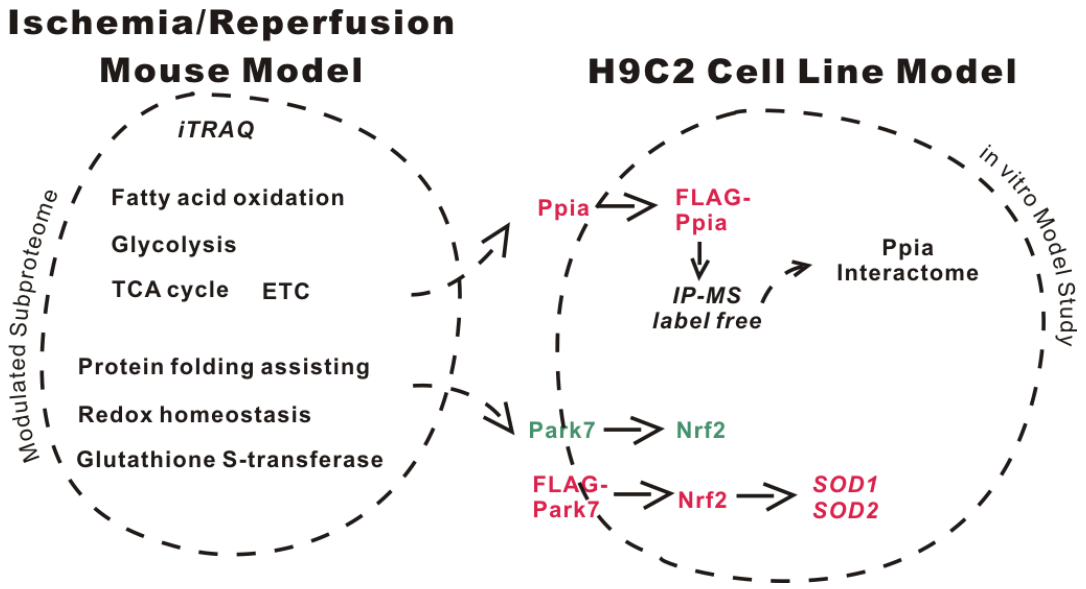

Figure 1 Ischemia/reperfusion injury study on in vivo mouse model by iTRAQ-MS approach. Regulated proteins were further studied on in vitro heart myoblast H9C2 cell line model.

The microenvironment of cardiac infarction area undergoes dynamic changes and the infarct healing process can be regulated by the secreted proteins within the niche. Hence the profile of the secretion from cardiac myocytes will be of great interest to achieve better understanding of the mechanism of I/R injury or stem cells transplantation therapy. To provide a systemic view of the modulation on secreted proteome under hypoxia and the following reoxygenation, secretome from H9C2 cells under 16 hr normoxia, 16 hr hypoxia and 24 hr reoxygenation stressed were profiled and quantified by label-free MS approach and stable-isotopelabeling iTRAQ-based method (chapter 3).

Large numbers of proteins were identified as secreted proteins besides those well known secreted proteins such as collagen, SPARC and fibronectin. These newly identified proteins passed bioinformatics filters and were recognized as exosome proteins, proteins with signal peptide or transmembrane helices and proteins which were secreted by non-classical secretion pathway. By applying the SI_N label free method protein abundance distribution was obtained. The difference on abundance distribution shown by comparing the normoxia secreted proteome to the cytosol proteome under same condition indicates the intrinsic difference of the characteristics of the two proteomes.

The hypoxic/reoxygenated secretome from cardiomyoblast H9C2 was quantified by applying both the stable-isotope labeling method iTRAQ and label-free semi-

quantitative methods to achieve a higher-confident of quantitative result. Analysis on the quantitative dataset reveals ECM remodeling during hypoxia including increased SERPINH1, PLOD1/2 and collagen deposition. Increased secretion of LOXL1 was observed during the hypoxia stage, which cross-links the collagen to form a mature scar. Rise of inflammatory response were also detected at the hypoxia stage. Whereas proteins involved in redox-homeostasis, cardioprotection and anticoagulant process were down-regulated. At the reoxygenation stage, we observed decrease of TIMP1, which irreversibly inactivates matrix metalloproteinase by binding to their catalytic zinc cofactor; and decrease of COL5A and LOXL1, which may be due to the shift of the balance from deactivation to activation of the matrix metalloproteinase. During reoxygenation, secretion of a group of cell adhesion proteins including ROBO2, POSTN, THBS1 and FAT1 increased. Especially, POSTN exerts modulation on the ECM remodeling and the healing process; THBS1 limits the inflammation response via TGFβ activation and regulates the infarct healing through its angiostatic effects by apply direct anti-inflammatory actions or by mediating MMP activation[171]. The abundance rise of these ROBO2 and FAT1 under hypoxia/reoxygenation is a novel observation and their functions in the scenario are yet to be clarified. Pro-apoptotic response was observed during reoxygenation as decrease of several anti-apoptosis proteins including GLO1, TMEM132A and TIMP1 were detected.

The analysis of the secreteome modulation under hypoxia and reoxygenation were summarized in figure 2.

Despite the intrinsic difference between the *in vivo* and *in vitro* model, regulation on similar functional groups of proteins were observed in both experiments. During

ischemia and reperfusion proteins relate to redox homeostasis and detoxification such as PRDX1/3/5, GSTP1, and GSTM2 etc in the myocardium were down regulated. Likewise, GSTM2, GSTO1 and PRDX5 declined in the secretome from the H9C2 heart myoblast under hypoxia. The similarity observed in the two experiments indicates significant dysregulation on the antioxidative stress function of the cellular system. Additionally, PPIA in the cytoplasm was up regulated during ischemia/reperfusion(*in vivo* model) and increased in secretion to extracellular environment as revealed in the *in vitro* model. Cytosolic PPIA responses to the misfolded proteins accumulated during low oxygen condition and to the rapid protein turnover. Secreted PPIA promotes vascular smooth muscle cell growth and inhibits apoptosis which protects cardiac myocytes from oxidative stress. The up regulation of PPIA in both cytosolic and extracellular environment when cardiac cells confront the lowered oxygen challenge exerts positive effects, suggesting a protective response of the myocardium through multiple pathways by a single protein.

The two studies also provide a systemic view of both cellular and extracellular molecular events that response to similar challenges. Metabolic modulation to adapt to the stress inside the cell during ischemia and reperfusion is accompanied by the inflammation response and scar formation, which facilitates to remove the dead cells and reconstitutes the mechanic strength of the heart once the stressed myocyte failed to survive. Besides the scar formation process, ECM is remodeled with increase of several cell adhesion proteins during the reoxygenation stage. The ECM remodeling contributes to fibrosis and thickening of the arterial wall which has adverse effect on the cardiac performance. Moreover, ROS imbalance inside the cells caused by

ischemia and extended to reperfusion stage is accompanied by angiogenesis response in the extracellular location (increase of ECM1), indicating that the cardiac myocyte system responds to relieve the depleted oxygen stress.

In conclusion, by utilizing the power of mass spectrometry-based proteomics, proteome modulation under ischemia and reperfusion in a mouse model was analyzed. Abundance level of essential protein functional groups were found to be altered, which indicates metabolic adaption of the myocardium to the stress and the refractory period of reversing the proteome modulation upon reperfusion. An *in vitro* cell line model was adopted to further study the regulated proteins under stress to obtain novel knowledge about the pathological process. Secretomes from H9C2 under hypoxia and reoxygenation were analyzed by the label-free and iTRAQ approaches to provide a systemic view of the extracellular molecular events under stress. A large number of secreted proteins were identified and the modulation on the abundance level of the subproteome reveals detailed information related to the extracellular matrix (ECM) remodeling, angiogenesis, inflammation response etc. Many secreted proteins were detected to be regulated under hypoxia and reoxygenation for the first time. The proteomics study in this thesis potentially advances our understanding of the cardiac biology, facilitating the follow-up investigations on the ischemia/reperfusion injury and therapeutic method development. In the future, functional study of the regulated secreted proteins can be performed to elucidate their roles under hypoxia and reoxygenation. Many of these proteins were found to be modulated under the stress conditions for the first time, which makes them novel research targets for follow up cell biology study. In addition, researches focusing on the mechanism of PARK7

down-regulation and PPIA up-regulation may help to understand the pathophysiology of ischemia heart disease.

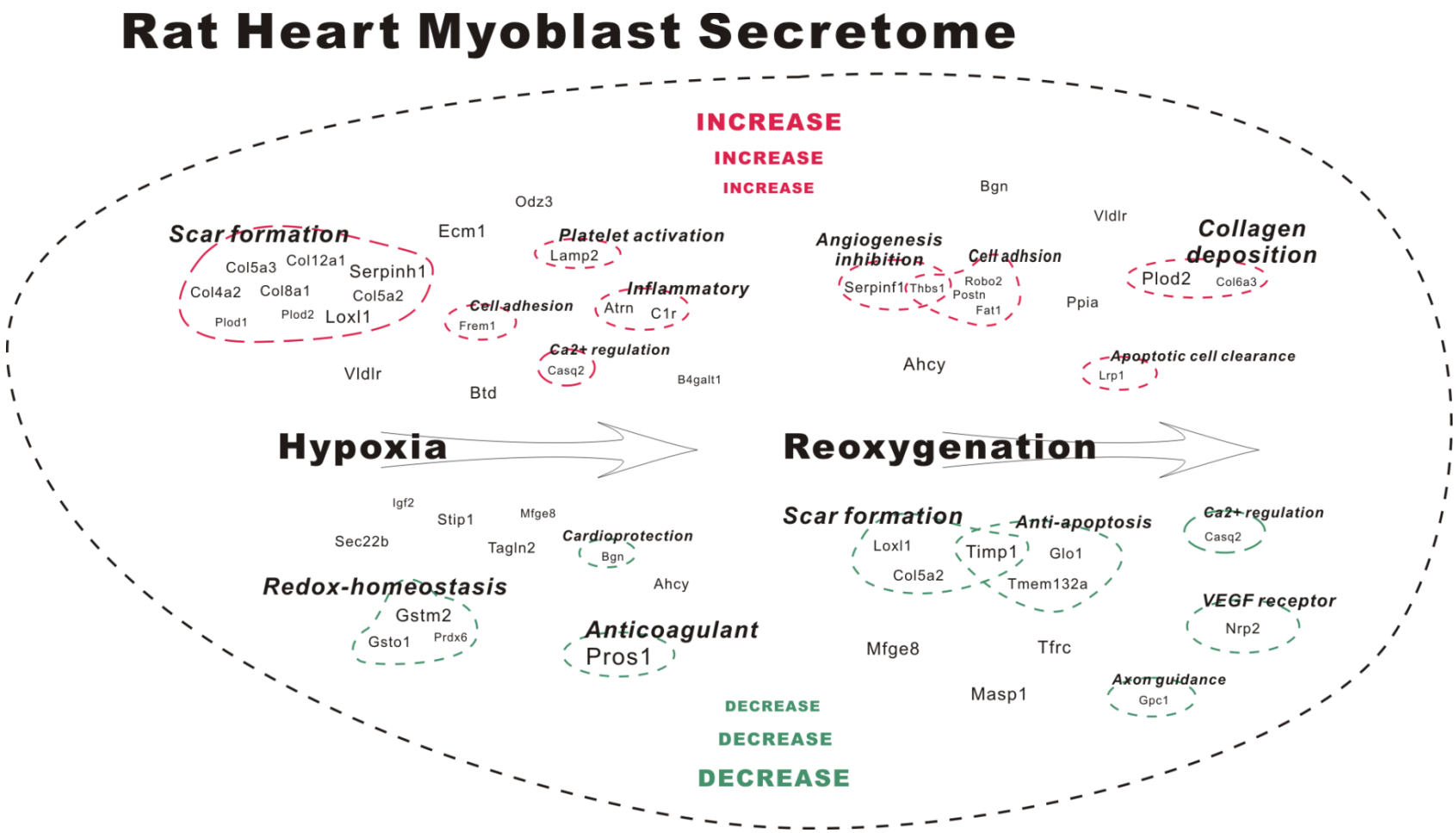

Figure *2 Summary of the secretome study on conditioned media generated from H9C2 cells under hypoxia and reoxygenation*

References

1. Van Eyk, J. E., Overview: The maturing of proteomics in cardiovascular research. *Circulation Research* **2011,** 108, (4), 490-498.
2. Tran, J. C.; Doucette, A. A., Gel-eluted liquid fraction entrapment electrophoresis: An electrophoretic method for broad molecular weight range proteome separation. *Analytical Chemistry* **2008,** 80, (5), 1568-1573.
3. Tran, J. C.; Doucette, A. A., Multiplexed size separation of intact proteins in solution phase for mass spectrometry. *Analytical Chemistry* **2009,** 81, (15), 6201-6209.
4. Chen, C. H.; Budas, G. R.; Churchill, E. N.; Disatnik, M. H.; Hurley, T. D.; Mochly-Rosen, D., Activation of aldehyde dehydrogenase-2 reduces ischemic damage to the heart. *Science* **2008,** 321, (5895), 1493-1495.
5. Griffin, N. M.; Yu, J.; Long, F.; Oh, P.; Shore, S.; Li, Y.; Koziol, J. A.; Schnitzer, J. E., Label-free, normalized quantification of complex mass spectrometry data for proteomic analysis. *Nature Biotechnology* **2010,** 28, (1), 83-89.
6. Leong, H. S.; Kipling, D., Text-based over-representation analysis of microarray gene lists with annotation bias. *Nucleic Acids Research* **2009,** 37, (11).
7. Maglott, D.; Ostell, J.; Pruitt, K. D.; Tatusova, T., Entrez gene: Gene-centered information at NCBI. *Nucleic Acids Research* **2011,** 39, (SUPPL. 1), D52-D57.
8. Charbonnier, S.; Gallego, O.; Gavin, A. C., The social network of a cell: Recent advances in interactome mapping. In 2008; Vol. 14, pp 1-28.
9. Bader, S.; Kühner, S.; Gavin, A. C., Interaction networks for systems biology. *FEBS Letters* **2008,** 582, (8), 1220-1224.
10. Kar, G.; Gursoy, A.; Keskin, O., Human cancer protein-protein interaction network: A structural perspective. *PLoS computational biology* **2009,** 5, (12).
11. Paris, L.; Bazzoni, G., The protein interaction network of the epithelial junctional complex: A system-level analysis. *Molecular Biology of the Cell* **2008,** 19, (12), 5409-5421.
12. Zaidel-Bar, R.; Itzkovitz, S.; Ma'ayan, A.; Iyengar, R.; Geiger, B., Functional atlas of the integrin adhesome. *Nature Cell Biology* **2007,** 9, (8), 858-867.
13. Watts, D. J.; Strogatz, S. H., Collective dynamics of 'small-world' networks. *Nature* **1998,** 393, (6684), 440-442.
14. Chavez, J. D.; Hoopmann, M. R.; Weisbrod, C. R.; Takara, K.; Bruce, J. E., Quantitative proteomic and interaction network analysis of cisplatin resistance in HeLa cells. *PLoS ONE* **2011,** 6, (5).
15. Albert, R.; Barabási, A. L., Statistical mechanics of complex networks. *Reviews of Modern Physics* **2002,** 74, (1), 47-97.
16. Jeong, H.; Mason, S. P.; Barabási, A. L.; Oltvai, Z. N., Lethality and centrality in protein networks. *Nature* **2001,** 411, (6833), 41-42.
17. Winzeler, E. A.; Shoemaker, D. D.; Astromoff, A.; Liang, H.; Anderson, K.; Andre, B.; Bangham, R.; Benito, R.; Boeke, J. D.; Bussey, H.; Chu, A. M.; Connelly, C.; Davis, K.; Dietrich, F.; Dow, S. W.; El Bakkoury, M.; Foury, F.; Friend, S. H.; Gentalen, E.; Giaever, G.; Hegemann, J. H.; Jones, T.; Laub, M.; Liao, H.; Liebundguth, N.; Lockhart, D. J.; Lucau-Danila, A.; Lussier, M.; M'Rabet, N.; Menard, P.; Mittmann, M.; Pai, C.; Rebischung, C.; Revuelta, J. L.; Riles, L.; Roberts, C. J.; Ross-MacDonald, P.; Scherens, B.; Snyder, M.; Sookhai-Mahadeo, S.; Storms, R. K.;

Véronneau, S.; Voet, M.; Volckaert, G.; Ward, T. R.; Wysocki, R.; Yen, G. S.; Yu, K.; Zimmermann, K.; Philippsen, P.; Johnston, M.; Davis, R. W., Functional characterization of the S. cerevisiae genome by gene deletion and parallel analysis. *Science* **1999,** 285, (5429), 901-906.
18. Ross-Macdonald, P.; Coelho, P. S. R.; Roemer, T.; Agarwal, S.; Kumar, A.; Jansen, R.; Cheung, K. H.; Sheehan, A.; Symonlatis, D.; Umansky, L.; Heldtman, M.; Nelson, F. K.; Iwasaki, H.; Hager, K.; Gerstein, M.; Miller, P.; Roeder, G. S.; Snyder, M., Large-scale analysis of the yeast genome by transposon tagging and gene disruption. *Nature* **1999,** 402, (6760), 413-418.
19. Ori, A.; Wilkinson, M. C.; Fernig, D. G., A systems biology approach for the investigation of the heparin/heparan sulfate interactome. *Journal of Biological Chemistry* **2011,** 286, (22), 19892-19904.
20. Lopez, A. D.; Mathers, C. D.; Ezzati, M.; Jamison, D. T.; Murray, C. J., Global and regional burden of disease and risk factors, 2001: systematic analysis of population health data. *Lancet* **2006,** 367, (9524), 1747-57.
21. Beaglehole, R.; Bonita, R., Global public health: a scorecard. *The Lancet* **2008,** 372, (9654), 1988-1996.
22. Faster, B.; Kelly, B. B., *Promoting Cardiovascular Health in the Developing World: A Critical Challenge to Achieve Global Health* **2010**.
23. Bassand, J. P.; Danchin, N.; Filippatos, G.; Gitt, A.; Hamm, C.; Silber, S.; Tubaro, M.; Weidinger, F., Implementation of reperfusion therapy in acute myocardial infarction. A policy statement from the European Society of Cardiology. *Eur Heart J* **2005,** 26, (24), 2733-41.
24. Bleumink, G. S.; Knetsch, A. M.; Sturkenboom, M. C. J. M.; Straus, S. M. J. M.; Hofman, A.; Deckers, J. W.; Witteman, J. C. M.; Stricker, B. H. C., Quantifying the heart failure epidemic: prevalence, incidence rate, lifetime risk and prognosis of heart failure. *European Heart Journal* **2004,** 25, (18), 1614-1619.
25. Jennings, R. B.; Sommers, H. M.; Smyth, G. A.; Flack, H. A.; Linn, H., Myocardial necrosis induced by temporary occlusion of a coronary artery in the dog. *Arch Pathol* **1960,** 70, 68-78.
26. Knight, D. R., Editorial overview: cardioprotective drugs for myocardial ischemic injury--a therapeutic area at risk. *Curr Opin Investig Drugs* **2007,** 8, (3), 190-2.
27. Ananthakrishnan, R.; Kaneko, M.; Hwang, Y. C.; Quadri, N.; Gomez, T.; Li, Q.; Caspersen, C.; Ramasamy, R., Aldose reductase mediates myocardial ischemia-reperfusion injury in part by opening mitochondrial permeability transition pore. *American Journal of Physiology - Heart and Circulatory Physiology* **2009,** 296, (2), H333-H341.
28. Crompton, M., The mitochondrial permeability transition pore and its role in cell death. *The Biochemical journal* **1999,** 341, Pt 2/.
29. Griffiths, E. J.; Halestrap, A. P., Mitochondrial non-specific pores remain closed during cardiac ischaemia, but open upon reperfusion. *Biochemical Journal* **1995,** 307, (1), 93-98.
30. Wang, C.; Youle, R. J., The role of mitochondria in apoptosis In 2010; Vol. 43, pp 95-118.
31. Di Lisa, F.; Menabò, R.; Canton, M.; Barile, M.; Bernardi, P., Opening of the Mitochondrial Permeability Transition Pore Causes Depletion of Mitochondrial and Cytosolic NAD+ and Is a Causative Event in the Death of Myocytes in Postischemic Reperfusion of the Heart. *Journal of Biological Chemistry* **2001,** 276, (4), 2571-2575.

32. Griffiths, E. J.; Halestrap, A. P., Protection by cyclosporin A of ischemia/reperfusion-induced damage in isolated rat hearts. *Journal of Molecular and Cellular Cardiology* **1993,** 25, (12), 1461-1469.
33. Gunter, T. E.; Pfeiffer, D. R., Mechanisms by which mitochondria transport calcium. *American Journal of Physiology - Cell Physiology* **1990,** 258, (5 27-5), C755-C786.
34. Halestrap, A. R.; Connern, C. R.; Griffiths, E. J.; Kerr, P. M., Cyclosporin A binding to mitochondrial cyclophilin inhibits the permeability transition pore and protects hearts from ischaemia/reperfusion injury. *Molecular and Cellular Biochemistry* **1997,** 174, (1-2), 167-172.
35. Hardy, L.; Clark, J. B.; Darley-Usmar, V. M.; Smith, D. R.; Stone, D., Reoxygenation-dependent decrease in mitochondrial NADH:CoQ reductase (Complex I) activity in the hypoxic/reoxygenated rat heart. *Biochemical Journal* **1991,** 274, (1), 133-137.
36. Hausenloy, D. J.; Maddock, H. L.; Baxter, G. F.; Yellon, D. M., Inhibiting mitochondrial permeability transition pore opening: A new paradigm for myocardial preconditioning? *Cardiovascular Research* **2002,** 55, (3), 534-543.
37. Javadov, S. A.; Lim, K. H. H.; Kerr, P. M.; Suleiman, M. S.; Angelini, G. D.; Halestrap, A. P., Protection of hearts from reperfusion injury by propofol is associated with inhibition of the mitochondrial permeability transition. *Cardiovascular Research* **2000,** 45, (2), 360-369.
38. Kerr, P. M.; Suleiman, M. S.; Halestrap, A. P., Reversal of permeability transition during recovery of hearts from ischemia and its enhancement by pyruvate. *American Journal of Physiology - Heart and Circulatory Physiology* **1999,** 276, (2 45-2), H496-H502.
39. Rajesh, K. G.; Sasaguri, S.; Zhitian, Z.; Suzuki, R.; Asakai, R.; Maeda, H., Second window of ischemic preconditioning regulates mitochondrial permeability transition pore by enhancing Bcl-2 expression. *Cardiovascular Research* **2003,** 59, (2), 297-307.
40. Arslan, F.; Smeets, M. B.; O'Neill, L. A. J.; Keogh, B.; McGuirk, P.; Timmers, L.; Tersteeg, C.; Hoefer, I. E.; Doevendans, P. A.; Pasterkamp, G.; De Kleijn, D. P. V., Myocardial ischemia/reperfusion injury is mediated by leukocytic toll-like receptor-2 and reduced by systemic administration of a novel anti-toll-like receptor-2 antibody. *Circulation* **2010,** 121, (1), 80-90.
41. Jennings, R. B.; Reimer, K. A., The cell biology of acute myocardial ischemia. *Annual Review of Medicine* **1991,** 42, 225-246.
42. Di Lisa, F.; Menabò, R.; Canton, M.; Petronilli, V., The role of mitochondria in the salvage and the injury of the ischemic myocardium. *Biochimica et Biophysica Acta - Bioenergetics* **1998,** 1366, (1-2), 69-78.
43. Piper, H. M.; Abdallah, Y.; Schäfer, C., The first minutes of reperfusion: A window of opportunity for cardioprotection. *Cardiovascular Research* **2004,** 61, (3), 365-371.
44. Inserte, J.; Garcia-Dorado, D.; Hernando, V.; Barba, I.; Soler-Soler, J., Ischemic preconditioning prevents calpain-mediated impairment of Na+/K+-ATPase activity during early reperfusion. *Cardiovascular Research* **2006,** 70, (2), 364-373.
45. Varadarajan, S. G.; An, J.; Novalija, E.; Smart, S. C.; Stowe, D. F., Changes in [Na+]i, compartmental [Ca2+], and nadh with dysfunction after global ischemia in intact hearts. *American Journal of Physiology - Heart and Circulatory Physiology* **2001,** 280, (1 49-1), H280-H293.
46. Murphy, E.; Steenbergen, C., Ion transport and energetics during cell death and protection. *Physiology* **2008,** 23, (2), 115-123.

47. Inserte, J.; Garcia-Dorado, D.; Ruiz-Meana, M.; Padilla, F.; Barrabés, J. A.; Pina, P.; Agulló, L.; Piper, H. M.; Soler-Soler, J., Effect of inhibition of Na+/Ca2+ exchanger at the time of myocardial reperfusion on hypercontracture and cell death. *Cardiovascular Research* **2002,** 55, (4), 739-748.
48. Bernardi, P., Mitochondrial transport of cations: Channels, exchangers, and permeability transition. *Physiological Reviews* **1999,** 79, (4), 1127-1155.
49. Turrens, J. F., Mitochondrial formation of reactive oxygen species. *Journal of Physiology* **2003,** 552, (2), 335-344.
50. Kevin, L. G.; Camara, A. K. S.; Riess, M. L.; Novalija, E.; Stowe, D. F., Ischemic preconditioning alters real-time measure of O2 radicals in intact hearts with ischemia and reperfusion. *American Journal of Physiology - Heart and Circulatory Physiology* **2003,** 284, (2 53-2), H566-H574.
51. Sebbag, L.; Verbinski, S. G.; Reimer, K. A.; Jennings, R. B., Protection of ischemic myocardium in dogs using intracoronary 2,3-butanedione monoxime (BDM). *Journal of Molecular and Cellular Cardiology* **2003,** 35, (2), 165-176.
52. Halestrap, A. P.; Clarke, S. J.; Javadov, S. A., Mitochondrial permeability transition pore opening during myocardial reperfusion - A target for cardioprotection. *Cardiovascular Research* **2004,** 61, (3), 372-385.
53. Juhaszova, M.; Wang, S.; Zorov, D. B.; Bradley Nuss, H.; Gleichmann, M.; Mattson, M. P.; Sollott, S. J., The identity and regulation of the mitochondrial permeability transition pore: where the known meets the unknown. In 2008; Vol. 1123, pp 197-212.
54. Di Lisa, F.; Bernardi, P., A CaPful of mechanisms regulating the mitochondrial permeability transition. *Journal of Molecular and Cellular Cardiology* **2009,** 46, (6), 775-780.
55. Murry, C. E.; Jennings, R. B.; Reimer, K. A., Preconditioning with ischemia: A delay of lethal cell injury in ischemic myocardium. *Circulation* **1986,** 74, (5), 1124-1136.
56. Downey, J. M.; Krieg, T.; Cohen, M. V., Mapping preconditioning's signaling pathways: an engineering approach. In 2008; Vol. 1123, pp 187-196.
57. Oldenburg, O.; Cohen, M. V.; Downey, J. M., Mitochondrial KATP channels in preconditioning. *Journal of Molecular and Cellular Cardiology* **2003,** 35, (6), 569-575.
58. Costa, A. D. T.; Pierre, S. V.; Cohen, M. V.; Downey, J. M.; Garlid, K. D., cGMP signalling in pre- and post-conditioning: The role of mitochondria. *Cardiovascular Research* **2008,** 77, (2), 344-352.
59. Kuno, A.; Critz, S. D.; Cui, L.; Solodushko, V.; Yang, X. M.; Krahn, T.; Albrecht, B.; Philipp, S.; Cohen, M. V.; Downey, J. M., Protein kinase C protects preconditioned rabbit hearts by increasing sensitivity of adenosine A2b-dependent signaling during early reperfusion. *Journal of Molecular and Cellular Cardiology* **2007,** 43, (3), 262-271.
60. Andrukhiv, A.; Costa, A. D.; West, I. C.; Garlid, K. D., Opening mitoKATP increases superoxide generation from complex I of the electron transport chain. *American Journal of Physiology - Heart and Circulatory Physiology* **2006,** 291, (5), H2067-H2074.
61. Gomez, L.; Paillard, M.; Thibault, H.; Derumeaux, G.; Ovize, M., Inhibition of GSK3β by postconditioning is required to prevent opening of the mitochondrial permeability transition pore during reperfusion. *Circulation* **2008,** 117, (21), 2761-2768.
62. Costa, A. D. T.; Garlid, K. D., Intramitochondrial signaling: Interactions among mitoKATP, PKCε, ROS, and MPT. *American Journal of Physiology - Heart and Circulatory Physiology* **2008,** 295, (2), H874-H882.

63. Heinen, A.; Camara, A. K. S.; Aldakkak, M.; Rhodes, S. S.; Riess, M. L.; Stowe, D. F., Mitochondrial Ca2+-induced K+ influx increases respiration and enhances ROS production while maintaining membrane potential. *American Journal of Physiology - Cell Physiology* **2007,** 292, (1), C148-C156.
64. Stowe, D. F.; Aldakkak, M.; Camara, A. K. S.; Riess, M. L.; Heinen, A.; Varadarajan, S. G.; Jiang, M. T., Cardiac mitochondrial preconditioning by Big Ca2+-sensitive K+ channel opening requires superoxide radical generation. *American Journal of Physiology - Heart and Circulatory Physiology* **2006,** 290, (1), H434-H440.
65. Nishida, H.; Sato, T.; Miyazaki, M.; Nakaya, H., Infarct size limitation by adrenomedullin: Protein kinase A but not PI3-kinase is linked to mitochondrial KCa channels. *Cardiovascular Research* **2008,** 77, (2), 398-405.
66. Liew, F. Y.; Xu, D.; Brint, E. K.; O'Neill, L. A. J., Negative regulation of toll-like receptor-mediated immune responses. *Nature Reviews Immunology* **2005,** 5, (6), 446-458.
67. Baldwin Iii, W. M.; Larsen, C. P.; Fairchild, R. L., Innate immune responses to transplants: A significant variable with cadaver donors. *Immunity* **2001,** 14, (4), 369-376.
68. Halloran, P. F.; Autenried, P.; Ramassar, V.; Urmson, J.; Cockfield, S., Local T cell responses induce widespread MHC expression: Evidence that IFN-γ induces its own expression in remote sites. *Journal of Immunology* **1992,** 148, (12), 3837-3846.
69. Weiser, M. R.; Williams, J. P.; Moore Jr, F. D.; Kobzik, L.; Ma, M.; Hechtman, H. B.; Carroll, M. C., Reperfusion injury of ischemic skeletal muscle is mediated by natural antibody and complement. *Journal of Experimental Medicine* **1996,** 183, (5), 2343-2348.
70. Weisman, H. F.; Bartow, T.; Leppo, M. K.; Marsh Jr, H. C.; Carson, G. R.; Concino, M. F.; Boyle, M. P.; Roux, K. H.; Weisfeldt, M. L.; Fearon, D. T., Soluble human complement receptor type 1: In vivo inhibitor of complement suppressing post-ischemic myocardial inflammation and necrosis. *Science* **1990,** 249, (4965), 146-151.
71. Zhao, P.; Wang, J.; He, L.; Ma, H.; Zhang, X.; Zhu, X.; Dolence, E. K.; Ren, J.; Li, J., Deficiency in TLR4 signal transduction ameliorates cardiac injury and cardiomyocyte contractile dysfunction during ischemia. *Journal of Cellular and Molecular Medicine* **2009,** 13, (8 A), 1513-1525.
72. Hansen, P. R., Role of neutrophils in myocardial ischemia and reperfusion. *Circulation* **1995,** 91, (6), 1872-1885.
73. Sakata, Y.; Dong, J. W.; Vallejo, J. G.; Huang, C. H.; Baker, J. S.; Tracey, K. J.; Tacheuchi, O.; Akira, S.; Mann, D. L., Toll-like receptor 2 modulates left ventricular function following ischemia-reperfusion injury. *American Journal of Physiology - Heart and Circulatory Physiology* **2007,** 292, (1), H503-H509.
74. Favre, J.; Musette, P.; Douin-Echinard, V.; Laude, K.; Henry, J. P.; Arnal, J. F.; Thuillez, C.; Richard, V., Toll-like receptors 2-deficient mice are protected against postischemic coronary endothelial dysfunction. *Arteriosclerosis, Thrombosis, and Vascular Biology* **2007,** 27, (5), 1064-1071.
75. Rosano, G. M. C.; Fini, M.; Caminiti, G.; Barbaro, G., Cardiac metabolism in myocardial ischemia. *Current Pharmaceutical Design* **2008,** 14, (25), 2551-2562.
76. Garnier, A.; Fortin, D.; Deloménie, C.; Momken, I.; Veksler, V.; Ventura-Clapier, R., Depressed mitochondrial transcription factors and oxidative capacity in rat failing cardiac and skeletal muscles. *Journal of Physiology* **2003,** 551, (2), 491-501.

77. Gurusamy, N.; Goswami, S.; Malik, G.; Das, D. K., Oxidative injury induces selective rather than global inhibition of proteasomal activity. *Journal of Molecular and Cellular Cardiology* **2008,** 44, (2), 419-428.
78. Callipo, L.; Capriotti, A. L.; Cavaliere, C.; Gubbiotti, R.; Samperi, R.; Laganà, A., Evaluation of different two-dimensional chromatographic techniques for proteomic analysis of mouse cardiac tissue. *Biomedical Chromatography* **2011,** 25, (5), 594-599.
79. Zong, C.; Gomes, A. V.; Drews, O.; Li, X.; Young, G. W.; Berhane, B.; Qiao, X.; French, S. W.; Bardag-Gorce, F.; Ping, P., Regulation of murine cardiac 20S proteasomes: Role of associating partners. *Circulation Research* **2006,** 99, (4), 372-380.
80. Deng, N.; Zhang, J.; Zong, C.; Wang, Y.; Lu, H.; Yang, P.; Wang, W.; Young, G. W.; Korge, P.; Lotz, C.; Doran, P.; Liem, D. A.; Apweiler, R.; Weiss, J. N.; Duan, H.; Ping, P., Phosphoproteome analysis reveals regulatory sites in major pathways of cardiac mitochondria. *Molecular and Cellular Proteomics* **2011,** 10, (2).
81. Warren, C. M.; Geenen, D. L.; Helseth Jr, D. L.; Xu, H.; Solaro, R. J., Sub-proteomic fractionation, iTRAQ, and OFFGEL-LC-MS/MS approaches to cardiac proteomics. *Journal of Proteomics* **2010,** 73, (8), 1551-1561.
82. Wong, R.; Aponte, A. M.; Steenbergen, C.; Murphy, E., Cardioprotection leads to novel changes in the mitochondrial proteome. *American Journal of Physiology - Heart and Circulatory Physiology* **2010,** 298, (1), H75-H91.
83. Feng, L. X.; Jing, C. J.; Tang, K. L.; Tao, L.; Cao, Z. W.; Wu, W. Y.; Guan, S. H.; Jiang, B. H.; Yang, M.; Liu, X.; Guo, D. A., Clarifying the signal network of salvianolic acid B using proteomic assay and bioinformatic analysis. *Proteomics* **2011,** 11, (8), 1473-1485.
84. Xie, L.; Terrand, J.; Xu, B.; Tsaprailis, G.; Boyer, J.; Chen, Q. M., Cystatin C increases in cardiac injury: A role in extracellular matrix protein modulation. *Cardiovascular Research* **2010,** 87, (4), 628-635.
85. Chou, H. C.; Chen, Y. W.; Lee, T. R.; Wu, F. S.; Chan, H. T.; Lyu, P. C.; Timms, J. F.; Chan, H. L., Proteomics study of oxidative stress and Src kinase inhibition in H9C2 cardiomyocytes: a cell model of heart ischemia-reperfusion injury and treatment. *Free Radical Biology and Medicine* **2010,** 49, (1), 96-108.
86. Thu, V. T.; Kim, H. K.; Ha, S. H.; Yoo, J. Y.; Park, W. S.; Kim, N.; Oh, G. T.; Han, J., Glutathione peroxidase 1 protects mitochondria against hypoxia/ reoxygenation damage in mouse hearts. *Pflugers Archiv European Journal of Physiology* **2010,** 460, (1), 55-68.
87. Liu, L.; Zhang, X. J.; Jiang, S. R.; Ding, Z. N.; Ding, G. X.; Huang, J.; Cheng, Y. L., Heat shock protein 27 regulates oxidative stress-induced apoptosis in cardiomyocytes: Mechanisms via reactive oxygen species generation and Akt activation. *Chinese Medical Journal* **2007,** 120, (24), 2271-2277.
88. Hollander, J. M.; Martin, J. L.; Belke, D. D.; Scott, B. T.; Swanson, E.; Krishnamoorthy, V.; Dillmann, W. H., Overexpression of wild-type heat shock protein 27 and a nonphosphorylatable heat shock protein 27 mutant protects against ischemia/reperfusion injury in a transgenic mouse model. *Circulation* **2004,** 110, (23), 3544-3552.
89. Lai, R. C.; Arslan, F.; Lee, M. M.; Sze, N. S. K.; Choo, A.; Chen, T. S.; Salto-Tellez, M.; Timmers, L.; Lee, C. N.; El Oakley, R. M.; Pasterkamp, G.; de Kleijn, D. P. V.; Lim, S. K., Exosome secreted by MSC reduces myocardial ischemia/reperfusion injury. *Stem Cell Research* **2010,** 4, (3), 214-222.
90. Lai, R. C.; Arslan, F.; Tan, S. S.; Tan, B.; Choo, A.; Lee, M. M.; Chen, T. S.; Teh, B. J.; Eng, J. K. L.; Sidik, H.; Tanavde, V.; Hwang, W. S.; Lee, C. N.; Oakley, R. M. E.; Pasterkamp, G.; de Kleijn, D. P. V.; Tan, K. H.; Lim, S. K., Derivation and

characterization of human fetal MSCs: An alternative cell source for large-scale production of cardioprotective microparticles. *Journal of Molecular and Cellular Cardiology* **2010,** 48, (6), 1215-1224.
91. Timmers, L.; Lim, S. K.; Arslan, F.; Armstrong, J. S.; Hoefer, I. E.; Doevendans, P. A.; Piek, J. J.; El Oakley, R. M.; Choo, A.; Lee, C. N.; Pasterkamp, G.; de Kleijn, D. P. V., Reduction of myocardial infarct size by human mesenchymal stem cell conditioned medium. *Stem Cell Research* **2008,** 1, (2), 129-137.
92. Redel, A.; Jazbutyte, V.; Smul, T. M.; Lange, M.; Eckle, T.; Eltzschig, H.; Roewer, N.; Kehl, F., Impact of ischemia and reperfusion times on myocardial infarct size in mice in vivo. *Experimental Biology and Medicine* **2008,** 233, (1), 84-93.
93. Datta, A.; Park, J. E.; Li, X.; Zhang, H.; Ho, Z. S.; Heese, K.; Lim, S. K.; Tam, J. P.; Sze, S. K., Phenotyping of an in vitro model of ischemic penumbra by iTRAQ-based shotgun quantitative proteomics. *Journal of proteome research* **2010,** 9, (1), 472-484.
94. Guo, T.; Gan, C. S.; Zhang, H.; Zhu, Y.; Kon, O. L.; Sze, S. K., Hybridization of pulsed-Q dissociation and collision-activated dissociation in linear ion trap mass spectrometer for iTRAQ quantitation. *Journal of proteome research* **2008,** 7, (11), 4831-4840.
95. Zhang, H.; Guo, T.; Li, X.; Datta, A.; Park, J. E.; Yang, J.; Lim, S. K.; Tam, J. P.; Sze, S. K., Simultaneous characterization of glyco- and phosphoproteomes of mouse brain membrane proteome with electrostatic repulsion hydrophilic interaction chromatography. *Molecular and Cellular Proteomics* **2010,** 9, (4), 635-647.
96. Keshava Prasad, T. S.; Goel, R.; Kandasamy, K.; Keerthikumar, S.; Kumar, S.; Mathivanan, S.; Telikicherla, D.; Raju, R.; Shafreen, B.; Venugopal, A.; Balakrishnan, L.; Marimuthu, A.; Banerjee, S.; Somanathan, D. S.; Sebastian, A.; Rani, S.; Ray, S.; Harrys Kishore, C. J.; Kanth, S.; Ahmed, M.; Kashyap, M. K.; Mohmood, R.; Ramachandra, Y. I.; Krishna, V.; Rahiman, B. A.; Mohan, S.; Ranganathan, P.; Ramabadran, S.; Chaerkady, R.; Pandey, A., Human Protein Reference Database - 2009 update. *Nucleic Acids Research* **2009,** 37, (SUPPL. 1), D767-D772.
97. Aranda, B.; Achuthan, P.; Alam-Faruque, Y.; Armean, I.; Bridge, A.; Derow, C.; Feuermann, M.; Ghanbarian, A. T.; Kerrien, S.; Khadake, J.; Kerssemakers, J.; Leroy, C.; Menden, M.; Michaut, M.; Montecchi-Palazzi, L.; Neuhauser, S. N.; Orchard, S.; Perreau, V.; Roechert, B.; van Eijk, K.; Hermjakob, H., The IntAct molecular interaction database in 2010. *Nucleic Acids Research* **2009,** 38, (SUPPL.1), D525-D531.
98. Cline, M. S.; Smoot, M.; Cerami, E.; Kuchinsky, A.; Landys, N.; Workman, C.; Christmas, R.; Avila-Campilo, I.; Creech, M.; Gross, B.; Hanspers, K.; Isserlin, R.; Kelley, R.; Killcoyne, S.; Lotia, S.; Maere, S.; Morris, J.; Ono, K.; Pavlovic, V.; Pico, A. R.; Vailaya, A.; Wang, P. L.; Adler, A.; Conklin, B. R.; Hood, L.; Kuiper, M.; Sander, C.; Schmulevich, I.; Schwikowski, B.; Warner, G. J.; Ideker, T.; Bader, G. D., Integration of biological networks and gene expression data using Cytoscape. *Nature protocols* **2007,** 2, (10), 2366-2382.
99. Lopaschuk, G. D.; Ussher, J. R.; Folmes, C. D. L.; Jaswal, J. S.; Stanley, W. C., Myocardial fatty acid metabolism in health and disease. *Physiological Reviews* **2010,** 90, (1), 207-258.
100. Stanley, W. C.; Recchia, F. A.; Lopaschuk, G. D., Myocardial substrate metabolism in the normal and failing heart. *Physiological Reviews* **2005,** 85, (3), 1093-1129.
101. Lewandowski, E. D.; White, L. T., Pyruvate dehydrogenase influences postischemic heart function. *Circulation* **1995,** 91, (7), 2071-2079.

102. Krause, G. S.; Tiffany, B. R.; Nowak Jr, T. S., Suppression of protein synthesis in the reperfused brain. *Stroke* **1993,** 24, (5), 747-756.
103. Turrens, J. F., Superoxide production by the mitochondrial respiratory chain. *Bioscience Reports* **1997,** 17, (1), 3-8.
104. Muller, F. L.; Roberts, A. G.; Bowman, M. K.; Kramer, D. M., Architecture of the Q-o site of the cytochrome bc1 complex probed by superoxide production. *Biochemistry* **2003,** 42, (21), 6493-6499.
105. Aldakkak, M.; Stowe, D. F.; Chen, Q.; Lesnefsky, E. J.; Camara, A. K. S., Inhibited mitochondrial respiration by amobarbital during cardiac ischaemia improves redox state and reduces matrix Ca2+ overload and ROS release. *Cardiovascular Research* **2008,** 77, (2), 406-415.
106. Ott, M.; Robertson, J. D.; Gogvadze, V.; Zhivotovsky, B.; Orrenius, S., Cytochrome c release from mitochondria proceeds by a two-step process. *Proceedings of the National Academy of Sciences of the United States of America* **2002,** 99, (3), 1259-1263.
107. Chen, Q.; Moghaddas, S.; Hoppel, C. L.; Lesnefsky, E. J., Reversible blockade of electron transport during ischemia protects mitochondria and decreases myocardial injury following reperfusion. *Journal of Pharmacology and Experimental Therapeutics* **2006,** 319, (3), 1405-1412.
108. Jiang, W. L.; Fu, F. H.; Xu, B. M.; Tian, J. W.; Zhu, H. B.; Jian, H., Cardioprotection with forsythoside B in rat myocardial ischemia-reperfusion injury: Relation to inflammation response. *Phytomedicine* **2009**.
109. Piao, C. S.; Gao, S.; Lee, G. H.; Kim, D. S.; Park, B. H.; Chae, S. W.; Chae, H. J.; Kim, S. H., Sulforaphane protects ischemic injury of hearts through antioxidant pathway and mitochondrial KATP channels. *Pharmacological Research* **2009**.
110. Baudry, N.; Laemmel, E.; Vicaut, E., In vivo reactive oxygen species production induced by ischemia in muscle arterioles of mice: Involvement of xanthine oxidase and mitochondria. *American Journal of Physiology - Heart and Circulatory Physiology* **2008,** 294, (2), H821-H828.
111. Hori, M.; Nishida, K., Oxidative stress and left ventricular remodelling after myocardial infarction. *Cardiovascular Research* **2009,** 81, (3), 457-464.
112. Zorov, D. B.; Filburn, C. R.; Klotz, L. O.; Zweier, J. L.; Sollott, S. J., Reactive oxygen species (ROS)-induced ROS release: A new phenomenon accompanying induction of the mitochondrial permeability transition in cardiac myocytes. *Journal of Experimental Medicine* **2000,** 192, (7), 1001-1014.
113. Aleyasin, H.; Rousseaux, M. W. C.; Phillips, M.; Kim, R. H.; Bland, R. J.; Callaghan, S.; Slack, R. S.; During, M. J.; Mak, T. W.; Park, D. S., The Parkinson's disease gene DJ-1 is also a key regulator of stroke-induced damage. *Proceedings of the National Academy of Sciences of the United States of America* **2007,** 104, (47), 18748-18753.
114. Mitsumoto, A.; Nakagawa, Y., DJ-1 is an indicator for endogenous reactive oxygen species elicited by endotoxin. *Free Radical Research* **2001,** 35, (6), 885-893.
115. Mitsumoto, A.; Nakagawa, Y.; Takeuchi, A.; Okawa, K.; Iwamatsu, A.; Takanezawa, Y., Oxidized forms of peroxiredoxins and DJ-1 on two-dimensional gels increased in response to sublethal levels of paraquat. *Free Radical Research* **2001,** 35, (3), 301-310.
116. Junn, E.; Taniguchi, H.; Jeong, B. S.; Zhao, X.; Ichijo, H.; Mouradian, M. M., Interaction of DJ-1 with Daxx inhibits apoptosis signal-regulating kinase 1 activity and cell death. *Proceedings of the National Academy of Sciences of the United States of America* **2005,** 102, (27), 9691-9696.

117. da Costa, C. A., DJ-1: A new comer in Parkinson's disease pathology. *Current Molecular Medicine* **2007,** 7, (7), 650-657.
118. Clements, C. M.; McNally, R. S.; Conti, B. J.; Mak, T. W.; Ting, J. P. Y., DJ-1, a cancer- and Parkinson's disease-associated protein, stabilizes the antioxidant transcriptional master regulator Nrf2. *Proceedings of the National Academy of Sciences of the United States of America* **2006,** 103, (41), 15091-15096.
119. Cullinan, S. B.; Gordan, J. D.; Jin, J.; Harper, J. W.; Diehl, J. A., The Keap1-BTB protein is an adaptor that bridges Nrf2 to a Cul3-based E3 ligase: Oxidative stress sensing by a Cul3-Keap1 ligase. *Molecular and Cellular Biology* **2004,** 24, (19), 8477-8486.
120. Kobayashi, A.; Kang, M. I.; Okawa, H.; Ohtsuji, M.; Zenke, Y.; Chiba, T.; Igarashi, K.; Yamamoto, M., Oxidative stress sensor Keap1 functions as an adaptor for Cul3-based E3 ligase to regulate proteasomal degradation of Nrf2. *Molecular and Cellular Biology* **2004,** 24, (16), 7130-7139.
121. Zhang, D. D.; Lo, S. C.; Cross, J. V.; Templeton, D. J.; Hannink, M., Keap1 is a redox-regulated substrate adaptor protein for a Cul3-dependent ubiquitin ligase complex. *Molecular and Cellular Biology* **2004,** 24, (24), 10941-10953.
122. Furukawa, M.; Xiong, Y., BTB protein keap1 targets antioxidant transcription factor Nrf2 for ubiquitination by the cullin 3-Roc1 ligase. *Molecular and Cellular Biology* **2005,** 25, (1), 162-171.
123. Stewart, D.; Killeen, E.; Naquin, R.; Alam, S.; Alam, J., Degradation of transcription factor Nrf2 via the ubiquitin-proteasome pathway and stabilization by cadmium. *Journal of Biological Chemistry* **2003,** 278, (4), 2396-2402.
124. de Vries, H. E.; Witte, M.; Hondius, D.; Rozemuller, A. J. M.; Drukarch, B.; Hoozemans, J.; van Horssen, J., Nrf2-induced antioxidant protection: A promising target to counteract ROS-mediated damage in neurodegenerative disease? *Free Radical Biology and Medicine* **2008,** 45, (10), 1375-1383.
125. Ooe, H.; Maita, C.; Maita, H.; Iguchi-Ariga, S. M. M.; Ariga, H., Specific cleavage of DJ-1 under an oxidative condition. *Neuroscience Letters* **2006,** 406, (3), 165-168.
126. Hulleman, J. D.; Mirzaei, H.; Guigard, E.; Taylor, K. L.; Ray, S. S.; Kay, C. M.; Regnier, F. E.; Rochet, J. C., Destabilization of DJ-1 by familial substitution and oxidative modifications: Implications for Parkinson's disease. *Biochemistry* **2007,** 46, (19), 5776-5789.
127. Li, C.; Liu, Z.; Tian, J.; Li, G.; Jiang, W.; Zhang, G.; Chen, F.; Lin, P.; Ye, Z., Protective roles of Asperosaponin VI, a triterpene saponin isolated from Dipsacus asper Wall on acute myocardial infarction in rats. *European Journal of Pharmacology* 627, (1-3), 235-241.
128. Gao, F. F.; Jia, Q. Y.; Guo, F. X.; Zhang, Y. M.; Huang, Z. Q.; Zhou, Y. Q.; Chen, Y. C.; Shi, G. G., Egr-1, a central and unifying role in cardioprotection from ischemia-reperfusion injury? *Cellular Physiology and Biochemistry* **2009,** 24, (5-6), 519-526.
129. Liao, Z.; Yin, D.; Wang, W.; Zeng, G.; Liu, D.; Chen, H.; Huang, Q.; He, M., Cardioprotective effect of sasanquasaponin preconditioning via bradykinin-NO pathway in isolated rat heart. *Phytotherapy Research* **2009,** 23, (8), 1146-1153.
130. Godman, C. A.; Chheda, K. P.; Hightower, L. E.; Perdrizet, G.; Shin, D. G.; Giardina, C., Hyperbaric oxygen induces a cytoprotective and angiogenic response in human microvascular endothelial cells. *Cell Stress and Chaperones* **2009**, 1-12.
131. Yoon, H. Y.; Kang, N. I.; Lee, H. K.; Jang, K. Y.; Park, J. W.; Park, B. H., Sulforaphane protects kidneys against ischemia-reperfusion injury through induction

of the Nrf2-dependent phase 2 enzyme. *Biochemical Pharmacology* **2008,** 75, (11), 2214-2223.
132. Jin, Z. G.; Melaragno, M. G.; Liao, D. F.; Yan, C.; Haendeler, J.; Suh, Y. A.; Lambeth, J. D.; Berk, B. C., Cyclophilin A is a secreted growth factor induced by oxidative stress. *Circulation Research* **2000,** 87, (9), 789-796.
133. Seko, Y.; Fujimura, T.; Taka, H.; Mineki, R.; Murayama, K.; Nagai, R., Hypoxia followed by reoxygenation induces secretion of cyclophilin A from cultured rat cardiac myocytes. *Biochemical and Biophysical Research Communications* **2004,** 317, (1), 162-168.
134. Steinmann, B.; Bruckner, P.; Superti-Furga, A., Cyclosporin A slows collagen triple-helix formation in vivo: Indirect evidence for a physiologic role of peptidyl-prolyl cis-trans-isomerase. *Journal of Biological Chemistry* **1991,** 266, (2), 1299-1303.
135. Kyu, J. C.; Yu, J. P.; Min, J. L.; Jin, H. K.; Ha, J.; Choe, W.; Sung, S. K., Overexpressed cyclophilin A in cancer cells renders resistance to hypoxia- and cisplatin-induced cell death. *Cancer Research* **2007,** 67, (8), 3654-3662.
136. Trinkle-Mulcahy, L.; Boulon, S.; Lam, Y. W.; Urcia, R.; Boisvert, F. M.; Vandermoere, F.; Morrice, N. A.; Swift, S.; Rothbauer, U.; Leonhardt, H.; Lamond, A., Identifying specific protein interaction partners using quantitative mass spectrometry and bead proteomes. *Journal of Cell Biology* **2008,** 183, (2), 223-239.
137. Lin, Y. F.; Tsai, W. P.; Liu, H. G.; Liang, P. H., Intracellular β-tubulin/chaperonin containing TCP1-β complex serves as a novel chemotherapeutic target against drug-resistant tumors. *Cancer Research* **2009,** 69, (17), 6879-6888.
138. Nijman, S. M. B.; Luna-Vargas, M. P. A.; Velds, A.; Brummelkamp, T. R.; Dirac, A. M. G.; Sixma, T. K.; Bernards, R., A genomic and functional inventory of deubiquitinating enzymes. *Cell* **2005,** 123, (5), 773-786.
139. Zhang, D.; Zaugg, K.; Mak, T. W.; Elledge, S. J., A Role for the Deubiquitinating Enzyme USP28 in Control of the DNA-Damage Response. *Cell* **2006,** 126, (3), 529-542.
140. Moazed, D.; Johnson, A. D., A deubiquitinating enzyme interacts with SIR4 and regulates silencing in S. cerevisiae. *Cell* **1996,** 86, (4), 667-677.
141. Li, M.; Chen, D.; Shiloh, A.; Luo, J.; Nikolaev, A. Y.; Qin, J.; Gu, W., Deubiquitination of p53 by HAUSP is an important pathway for p53 stabilization. *Nature* **2002,** 416, (6881), 648-653.
142. Peschiaroli, A.; Skaar, J. R.; Pagano, M.; Melino, G., The ubiquitin-specific protease USP47 is a novel B-TRCP interactor regulating cell survival. *Oncogene* **2010,** 29, (9), 1384-1393.
143. Feldman, D. E.; Chauhan, V.; Koong, A. C., The unfolded protein response: A novel component of the hypoxic stress response in tumors. *Molecular Cancer Research* **2005,** 3, (11), 597-605.
144. Tu, B. P.; Weissman, J. S., Oxidative protein folding in eukaryotes: Mechanisms and consequences. *Journal of Cell Biology* **2004,** 164, (3), 341-346.
145. Tu, B. P.; Weissman, J. S., The FAD- and O2-dependent reaction cycle of Ero1-mediated oxidative protein folding in the endoplasmic reticulum. *Molecular Cell* **2002,** 10, (5), 983-994.
146. Sun, G. D.; Kobayashi, T.; Abe, M.; Tada, N.; Adachi, H.; Shiota, A.; Totsuka, Y.; Hino, O., The endoplasmic reticulum stress-inducible protein Niban regulates eIF2α and S6K1/4E-BP1 phosphorylation. *Biochemical and Biophysical Research Communications* **2007,** 360, (1), 181-187.
147. Wouters, B. G.; Koritzinsky, M., Hypoxia signalling through mTOR and the unfolded protein response in cancer. *Nature Reviews Cancer* **2008,** 8, (11), 851-864.

148. Cannon, C. P.; Gibson, C. M.; Lambrew, C. T.; Shoultz, D. A.; Levy, D.; French, W. J.; Gore, J. M.; Weaver, W. D.; Rogers, W. J.; Tiefenbrunn, A. J., Relationship of symptom-onset-to-balloon time and door-to-balloon time with mortality in patients undergoing angioplasty for acute myocardial infarction. *JAMA* **2000,** 283, (22), 2941-7.
149. D'Amico, M.; Di Filippo, C.; La, M.; Solito, E.; McLean, P. G.; Flower, R. J.; Oliani, S. M.; Perretti, M., Lipocortin 1 reduces myocardial ischemia-reperfusion injury by affecting local leulkocyte. *FASEB Journal* **2000,** 14, (13), 1867-1869.
150. Frangogiannis, N. G., The immune system and cardiac repair. *Pharmacological Research* **2008,** 58, (2), 88-111.
151. Frangogiannis, N. G.; Michael, L. H.; Entman, M. L., Myofibroblasts in reperfused myocardial infarcts express the embryonic form of smooth muscle myosin heavy chain (SMemb). *Cardiovascular Research* **2000,** 48, (1), 89-100.
152. Corbett, S. A.; Schwarzbauer, J. E., Fibronectin-fibrin cross-linking: A regulator of cell behavior. *Trends in Cardiovascular Medicine* **1998,** 8, (8), 357-362.
153. Vanhoutte, D.; Schellings, M.; Pinto, Y.; Heymans, S., Relevance of matrix metalloproteinases and their inhibitors after myocardial infarction: A temporal and spatial window. *Cardiovascular Research* **2006,** 69, (3), 604-613.
154. Dobaczewski, M.; Bujak, M.; Zymek, P.; Ren, G.; Entman, M. L.; Frangogiannis, N. G., Extracellular matrix remodeling in canine and mouse myocardial infarcts. *Cell and Tissue Research* **2006,** 324, (3), 475-488.
155. Huebener, P.; Abou-Khamis, T.; Zymek, P.; Bujak, M.; Ying, X.; Chatila, K.; Haudek, S.; Thakker, G.; Frangogiannis, N. G., CD44 is critically involved in infarct healing by regulating the inflammatory and fibrotic response. *Journal of Immunology* **2008,** 180, (4), 2625-2633.
156. Welch, M. P.; Odland, G. F.; Clark, R. A. F., Temporal relationships of F-actin bundle formation, collagen and fibronectin matrix assembly, and fibronectin receptor expression to wound contraction. *Journal of Cell Biology* **1990,** 110, (1), 133-145.
157. Sottile, J.; Hocking, D. C., Fibronectin polymerization regulates the composition and stability of extracellular matrix fibrils and cell-matrix adhesions. *Molecular Biology of the Cell* **2002,** 13, (10), 3546-3559.
158. Frangogiannis, N. G.; Ren, G.; Dewald, O.; Zymek, P.; Haudek, S.; Koerting, A.; Winkelmann, K.; Michael, L. H.; Lawler, J.; Entman, M. L., Critical role of endogenous thrombospondin-1 in preventing expansion of healing myocardial infarcts. *Circulation* **2005,** 111, (22), 2935-2942.
159. Willems, I. E. M. G.; Arends, J. W.; Daemen, M. J. A. P., Tenascin and fibronectin expression in healing human myocardial scars. *Journal of Pathology* **1996,** 179, (3), 321-325.
160. Imanaka-Yoshida, K.; Hiroe, M.; Nishikawa, T.; Ishiyama, S.; Shimojo, T.; Ohta, Y.; Sakakura, T.; Yoshida, T., Tenascin-C modulates adhesion of cardiomyocytes to extracellular matrix during tissue remodeling after myocardial infarction. *Laboratory Investigation* **2001,** 81, (7), 1015-1024.
161. Hashimoto, S. I.; Suzuki, T.; Dong, H. Y.; Yamazaki, N.; Matsushima, K., Serial analysis of gene expression in human monocytes and macrophages. *Blood* **1999,** 94, (3), 837-844.
162. Trueblood, N. A.; Xie, Z.; Communal, C.; Sam, F.; Ngoy, S.; Liaw, L.; Jenkins, A. W.; Wang, J.; Sawyer, D. B.; Bing, O. H. L.; Apstein, C. S.; Colucci, W. S.; Singh, K., Exaggerated left ventricular dilation and reduced collagen deposition after myocardial infarction in mice lacking osteopontin. *Circulation Research* **2001,** 88, (10), 1080-1087.

163. Krishnamurthy, P.; Peterson, J. T.; Subramanian, V.; Singh, M.; Singh, K., Inhibition of matrix metalloproteinases improves left ventricular function in mice lacking osteopontin after myocardial infarction. *Molecular and Cellular Biochemistry* **2009,** 322, (1-2), 53-62.
164. Schellings, M. W. M.; Vanhoutte, D.; Swinnen, M.; Cleutjens, J. P.; Debets, J.; Van Leeuwen, R. E. W.; D'Hooge, J.; Van Werf, F. D.; Carmeliet, P.; Pinto, Y. M.; Sage, E. H.; Heymans, S., Absence of SPARC results in increased cardiac rupture and dysfunction after acute myocardial infarction. *Journal of Experimental Medicine* **2009,** 206, (1), 113-123.
165. Kudo, Y.; Ogawa, I.; Kitajima, S.; Kitagawa, M.; Kawai, H.; Gaffney, P. M.; Miyauchi, M.; Takata, T., Periostin promotes invasion and anchorage-independent growth in the metastatic process of head and neck cancer. *Cancer Research* **2006,** 66, (14), 6928-6935.
166. Wagner, R. A.; Tabibiazar, R.; Powers, J.; Bernstein, D.; Quertermous, T., Genome-wide expression profiling of a cardiac pressure overload model identifies major metabolic and signaling pathway responses. *Journal of Molecular and Cellular Cardiology* **2004,** 37, (6), 1159-1170.
167. Blaxall, B. C.; Spang, R.; Rockman, H. A.; Koch, W. J., Differential myocardial gene expression in the development and rescue of murine heart failure. *Physiological Genomics* **2004,** 15, 105-114.
168. Shimazaki, M.; Nakamura, K.; Kii, I.; Kashima, T.; Amizuka, N.; Li, M.; Saito, M.; Fukuda, K.; Nishiyama, T.; Kitajima, S.; Saga, Y.; Fukayama, M.; Sata, M.; Kudo, A., Periostin is essential for cardiac healing after acute myocardial infarction. *Journal of Experimental Medicine* **2008,** 205, (2), 295-303.
169. Oka, T.; Xu, J.; Kaiser, R. A.; Melendez, J.; Hambleton, M.; Sargent, M. A.; Lorts, A.; Brunskill, E. W.; Dorn Ii, G. W.; Conway, S. J.; Aronow, B. J.; Robbins, J.; Molkentin, J. D., Genetic manipulation of periostin expression reveals a role in cardiac hypertrophy and ventricular remodeling. *Circulation Research* **2007,** 101, (3), 313-321.
170. Lerman, R. H.; Apstein, C. S.; Kagan, H. M., Myocardial healing and repair after experimental infarction in the rabbit. *Circulation Research* **1983,** 53, (3), 378-388.
171. Dobaczewski, M.; Gonzalez-Quesada, C.; Frangogiannis, N. G., The extracellular matrix as a modulator of the inflammatory and reparative response following myocardial infarction. *Journal of Molecular and Cellular Cardiology* **2010,** 48, (3), 504-511.
172. Lunde, K.; Solheim, S.; Aakhus, S.; Arnesen, H.; Abdelnoor, M.; Egeland, T.; Endresen, K.; Ilebekk, A.; Mangschau, A.; Fjeld, J. G.; Smith, H. J.; Taraldsrud, E.; Grøgaard, H. K.; Bjørnerheim, R.; Brekke, M.; Müller, C.; Hopp, E.; Ragnarsson, A.; Brinchmann, J. E.; Forfang, K., Intracoronary injection of mononuclear bone marrow cells in acute myocardial infarction. *New England Journal of Medicine* **2006,** 355, (12), 1199-1209.
173. Assmus, B.; Honold, J.; Schächinger, V.; Britten, M. B.; Fischer-Rasokat, U.; Lehmann, R.; Teupe, C.; Pistorius, K.; Martin, H.; Abolmaali, N. D.; Tonn, T.; Dimmeler, S.; Zeiher, A. M., Transcoronary transplantation of progenitor cells after myocardial infarction. *New England Journal of Medicine* **2006,** 355, (12), 1222-1232.
174. Chen, S. L.; Fang, W. W.; Ye, F.; Liu, Y. H.; Qian, J.; Shan, S. J.; Zhang, J. J.; Chunhua, R. Z.; Liao, L. M.; Lin, S.; Sun, J. P., Effect on left ventricular function of intracoronary transplantation of autologous bone marrow mesenchymal stem cell in patients with acute myocardial infarction. *American Journal of Cardiology* **2004,** 94, (1), 92-95.

175. Hagège, A. A.; Marolleau, J. P.; Vilquin, J. T.; Alhéritière, A.; Peyrard, S.; Duboc, D.; Abergel, E.; Messas, E.; Mousseaux, E.; Schwartz, K.; Desnos, M.; Menasché, P., Skeletal myoblast transplantation in ischemic heart failure: Long-term follow-up of the first phase I cohort of patients. *Circulation* **2006,** 114, (SUPPL. 1), I108-I113.
176. Gnecchi, M.; Zhang, Z.; Ni, A.; Dzau, V. J., Paracrine mechanisms in adult stem cell signaling and therapy. *Circulation Research* **2008,** 103, (11), 1204-1219.
177. Sze, S. K.; de Kleijn, D. P. V.; Lai, R. C.; Tan, E. K. W.; Zhao, H.; Yeo, K. S.; Low, T. Y.; Lian, Q.; Lee, C. N.; Mitchell, W.; El Oakley, R. M.; Lim, S. K., Elucidating the secretion proteome of human embryonic stem cell-derived mesenchymal stem cells. *Molecular and Cellular Proteomics* **2007,** 6, (10), 1680-1689.
178. Ping, P., Getting to the heart of proteomics. *New England Journal of Medicine* **2009,** 360, (5), 532-534.
179. Ménard, C.; Pupier, S.; Mornet, D.; Kitzmann, M.; Nargeot, J.; Lory, P., Modulation of L-type calcium channel expression during retinoic acid- induced differentiation of H9C2 cardiac cells. *Journal of Biological Chemistry* **1999,** 274, (41), 29063-29070.
180. Hescheler, J.; Meyer, R.; Plant, S.; Krautwurst, D.; Rosenthal, W.; Schultz, G., Morphological, biochemical, and electrophysiological characterization of a clonal cell (H9c2) line from rat heart. *Circulation Research* **1991,** 69, (6), 1476-1486.
181. Florens, L.; Carozza, M. J.; Swanson, S. K.; Fournier, M.; Coleman, M. K.; Workman, J. L.; Washburn, M. P., Analyzing chromatin remodeling complexes using shotgun proteomics and normalized spectral abundance factors. *Methods* **2006,** 40, (4), 303-311.
182. Zhang, J.; Liem, D. A.; Mueller, M.; Wang, Y.; Zong, C.; Deng, N.; Vondriska, T. M.; Korge, P.; Drews, O.; Maclellan, W. R.; Honda, H.; Weiss, J. N.; Apweiler, R.; Ping, P., Altered proteome biology of cardiac mitochondria under stress conditions. *Journal of proteome research* **2008,** 7, (6), 2204-2214.
183. Pevzner, P. A.; Mulyukov, Z.; Dancik, V.; Tang, C. L., Efficiency of database search for identification of mutated and modified proteins via mass spectrometry. *Genome Research* **2001,** 11, (2), 290-299.
184. Karagiannis, G. S.; Pavlou, M. P.; Diamandis, E. P., Cancer secretomics reveal pathophysiological pathways in cancer molecular oncology. *Molecular Oncology* **2010**.
185. Bendtsen, J. D.; Nielsen, H.; Von Heijne, G.; Brunak, S., Improved prediction of signal peptides: SignalP 3.0. *Journal of Molecular Biology* **2004,** 340, (4), 783-795.
186. Bendtsen, J. D.; Jensen, L. J.; Blom, N.; Von Heijne, G.; Brunak, S., Feature-based prediction of non-classical and leaderless protein secretion. *Protein Engineering, Design and Selection* **2004,** 17, (4), 349-356.
187. Mathivanan, S.; Simpson, R. J., ExoCarta: A compendium of exosomal proteins and RNA. *Proteomics* **2009,** 9, (21), 4997-5000.
188. Mayer, G., Capillary rarefaction, hypoxia, VEGF and angiogenesis in chronic renal disease. *Nephrology Dialysis Transplantation* **2011,** 26, (4), 1132-1137.
189. Breen, E.; Tang, K.; Olfert, M.; Knapp, A.; Wagner, P., Skeletal muscle capillarity during hypoxia: VEGF and its activation. *High Altitude Medicine and Biology* **2008,** 9, (2), 158-166.
190. Koh, J. M.; Lee, Y. S.; Kim, Y. S.; Park, S. H.; Hun Lee, S.; Kim, H. H.; Lee, M. S.; Lee, K. U.; Kim, G. S., Heat shock protein 60 causes osteoclastic bone resorption via toll-like receptor-2 in estrogen deficiency. *Bone* **2009,** 45, (4), 650-660.
191. Dahl, A.; Eriksson, P. S.; Persson, A. I.; Karlsson, G.; Davidsson, P.; Ekman, R.; Westman-Brinkmalm, A., Proteome analysis of conditioned medium from cultured

adult hippocampal progenitors. *Rapid Communications in Mass Spectrometry* **2003,** 17, (19), 2195-2202.
192. Konrad, L.; Albrecht, M.; Renneberg, H.; Ulrix, W.; Hoeben, E.; Verhoeven, G.; Aumüller, G., Mesenchymal entactin-1 (nidogen-1) is required for adhesion of peritubular cells of the rat testis in vitro. *European Journal of Cell Biology* **2000,** 79, (2), 112-120.
193. Santillo, M.; Secondo, A.; Serù, R.; Damiano, S.; Garbi, C.; Taverna, E.; Rosa, P.; Giovedì, S.; Benfenati, F.; Mondola, P., Evidence of calcium- and SNARE-dependent release of CuZn superoxide dismutase from rat pituitary GH3 cells and synaptosomes in response to depolarization. *Journal of Neurochemistry* **2007,** 102, (3), 679-685.
194. Wang, P.; Du, H.; Zhang, R. Y.; Guan, Y. F.; Xu, T. Y.; Xu, Q. Y.; Su, D. F.; Miao, C. Y., Circulating and local visfatin/Nampt/PBEF levels in spontaneously hypertensive rats, stroke-prone spontaneously hypertensive rats and Wistar-Kyoto rats. *Journal of Physiological Sciences* **2010,** 60, (5), 317-324.
195. Zybailov, B.; Mosley, A. L.; Sardiu, M. E.; Coleman, M. K.; Florens, L.; Washburn, M. P., Statistical analysis of membrane proteome expression changes in Saccharomyces cerevisiae. *Journal of proteome research* **2006,** 5, (9), 2339-2347.
196. Ishihama, Y.; Oda, Y.; Tabata, T.; Sato, T.; Nagasu, T.; Rappsilber, J.; Mann, M., Exponentially modified protein abundance index (emPAI) for estimation of absolute protein amount in proteomics by the number of sequenced peptides per protein. *Molecular and Cellular Proteomics* **2005,** 4, (9), 1265-1272.
197. Brown, K. E.; Broadhurst, K. A.; Mathahs, M. M.; Brunt, E. M.; Schmidt, W. N., Expression of HSP47, a collagen-specific chaperone, in normal and diseased human liver. *Laboratory Investigation* **2005,** 85, (6), 789-797.
198. Hattori, T.; Von Der Mark, K.; Kawaki, H.; Yutani, Y.; Kubota, S.; Nakanishi, T.; Eberspaecher, H.; De Crombrugghe, B.; Takigawa, M., Downregulation of rheumatoid arthritis-related antigen RA-A47 (HSP47/colligin-2) in chondrocytic cell lines induces apoptosis and cell-surface expression of RA-A47 in association with CD9. *Journal of Cellular Physiology* **2005,** 202, (1), 191-204.
199. Kaiser, W. J.; Holbrook, L. M.; Tucker, K. L.; Stanley, R. G.; Gibbins, J. M., A functional proteomic method for the enrichment of peripheral membrane proteins reveals the collagen binding protein Hsp47 is exposed on the surface of activated human platelets. *Journal of proteome research* **2009,** 8, (6), 2903-2914.
200. Yokota, S. I.; Kubota, H.; Matsuoka, Y.; Naitoh, M.; Hirata, D.; Minota, S.; Takahashi, H.; Fujii, N.; Nagata, K., Prevalence of HSP47 antigen and autoantibodies to HSP47 in the sera of patients with mixed connective tissue disease. *Biochemical and Biophysical Research Communications* **2003,** 303, (2), 413-418.
201. Hofbauer, K. H.; Gess, B.; Lohaus, C.; Meyer, H. E.; Katschinski, D.; Kurtz, A., Oxygen tension regulates the expression of a group of procollagen hydroxylases. *European Journal of Biochemistry* **2003,** 270, (22), 4515-4522.
202. Mongiat, M.; Fu, J.; Oldershaw, R.; Greenhalgh, R.; Gown, A. M.; Iozzo, R. V., Perlecan protein core interacts with extracellular matrix protein 1 (ECM1), a glycoprotein involved in bone formation and angiogenesis. *Journal of Biological Chemistry* **2003,** 278, (19), 17491-17499.
203. Mongiat, M.; Sweeney, S. M.; San Antonio, J. D.; Fu, J.; Iozzo, R. V., Endorepellin, a novel inhibitor of angiogenesis derived from the C terminus of perlecan. *Journal of Biological Chemistry* **2003,** 278, (6), 4238-4249.
204. Han, Z.; Lin, G. J.; Chi, F. L.; Wang, S. Y.; Huang, J. M.; Liu, H. J.; Zhang, L. R., The relationship between the extracellular matrix and the angiogenesis and metastasis of laryngeal carcinoma. *ORL* **2008,** 70, (6), 352-358.

205. Tanaka, T.; Duke-Cohan, J. S.; Kameoka, J.; Yaron, A.; Lee, I.; Schlossman, S. F.; Morimoto, C., Enhancement of antigen-induced T-cell proliferation by soluble CD26/dipeptidyl peptidase IV. *Proceedings of the National Academy of Sciences of the United States of America* **1994,** 91, (8), 3082-3086.
206. Duke-Cohan, J. S.; Gu, J.; McLaughlin, D. F.; Xu, Y.; Freeman, G. J.; Schlossman, S. F., Attractin (DPPT-L), a member of the CUB family of cell adhesion and guidance proteins, is secreted by activated human T lymphocytes and modulates immune cell interactions. *Proceedings of the National Academy of Sciences of the United States of America* **1998,** 95, (19), 11336-11341.
207. Duke-Cohan, J. S.; Morimoto, C.; Rocker, J. A.; Schlossman, S. F., Serum high molecular weight dipeptidyl peptidase IV (CD26) is similar to a novel antigen DPPT-L released from activated T cells. *Journal of Immunology* **1996,** 156, (5), 1714-1721.
208. Corsi, A.; Xu, T.; Chen, X. D.; Boyde, A.; Liang, J.; Mankani, M.; Sommer, B.; Iozzo, R. V.; Eichstetter, I.; Robey, P. G.; Bianco, P.; Young, M. F., Phenotypic effects of biglycan deficiency are linked to collagen fibril abnormalities, are synergized by decorin deficiency, and mimic Ehlers-Danlos-like changes in bone and other connective tissues. *Journal of Bone and Mineral Research* **2002,** 17, (7), 1180-1189.
209. Westermann, D.; Mersmann, J.; Melchior, A.; Freudenberger, T.; Petrik, C.; Schaefer, L.; Lüllmann-Rauch, R.; Lettau, O.; Jacoby, C.; Schrader, J.; Brand-Herrman, S. M.; Young, M. F.; Schultheiss, H. P.; Levkau, B.; Baba, H. A.; Unger, T.; Zacharowski, K.; Tschöpe, C.; Fischer, J. W., Biglycan is required for adaptive remodeling after myocardial infarction. *Circulation* **2008,** 117, (10), 1269-1276.
210. Csont, T.; Görbe, A.; Bereczki, E.; Szunyog, A.; Aypar, E.; Tóth, M. E.; Varga, Z. V.; Csonka, C.; Fülöp, F.; Sántha, M.; Ferdinandy, P., Biglycan protects cardiomyocytes against hypoxia/reoxygenation injury: Role of nitric oxide. *Journal of Molecular and Cellular Cardiology* **2010,** 48, (4), 649-652.
211. Wiesel, M. L.; Borg, J. Y.; Grunebaum, L.; Vasse, M.; Levesque, H.; Bierme, R.; Sie, P., Influence of protein S deficiency on the risk of arterial thrombosis. *INFLUENCE DU DEFICIT CONSTITUTIONNEL EN PROTEINE S SUR LE RISQUE THROMBOTIQUE ARTERIEL* **1991,** 20, (22), 1023-1027.
212. Allaart, C. F.; Aronson, D. C.; Ruys, T.; Rosendaal, F. R.; Van Bockel, J. H.; Bertina, R. M.; Briet, E., Hereditary protein S deficiency in young adults with arterial occlusive disease. *Thrombosis and Haemostasis* **1990,** 64, (2), 206-210.
213. Zanata, S. M.; Lopes, M. H.; Mercadante, A. F.; Hajj, G. N. M.; Chiarini, L. B.; Nomizo, R.; Freitas, A. R. O.; Cabral, A. L. B.; Lee, K. S.; Juliano, M. A.; De Oliveira, E.; Jachieri, S. G.; Burlingame, A.; Huang, L.; Linden, R.; Brentani, R. R.; Martins, V. R., Stress-inducible protein 1 is a cell surface ligand for cellular prion that triggers neuroprotection. *EMBO Journal* **2002,** 21, (13), 3307-3316.
214. Valadi, H.; Ekström, K.; Bossios, A.; Sjöstrand, M.; Lee, J. J.; Lötvall, J. O., Exosome-mediated transfer of mRNAs and microRNAs is a novel mechanism of genetic exchange between cells. *Nature Cell Biology* **2007,** 9, (6), 654-659.
215. Liu, Z.; Patel, K.; Schmidt, H.; Andrews, W.; Pini, A.; Sundaresan, V., Extracellular Ig domains 1 and 2 of Robo are important for ligand (Slit) binding. *Molecular and Cellular Neuroscience* **2004,** 26, (2), 232-240.
216. Sundaresan, V.; Chung, G.; Heppell-Parton, A.; Xiong, J.; Grundy, C.; Roberts, I.; James, L.; Cahn, A.; Bench, A.; Douglas, J.; Minna, J.; Sekido, Y.; Lerman, M.; Latif, F.; Bergh, J.; Li, H.; Lowe, N.; Ogilvie, D.; Rabbitts, P., Homozygous deletions at 3p12 in breast and lung cancer. *Oncogene* **1998,** 17, (13), 1723-1729.

217. Sundaresan, V.; Roberts, I.; Bateman, A.; Bankier, A.; Sheppard, M.; Hobbs, C.; Xiong, J.; Minna, J.; Latif, F.; Lerman, M.; Rabbitts, P., The DUTT1 gene, a novel NCAM family member is expressed in developing murine neural tissues and has an unusually broad pattern of expression. *Molecular and Cellular Neurosciences* **1998,** 11, (1-2), 29-35.
218. Stansfield, W. E.; Andersen, N. M.; Tang, R. H.; Selzman, C. H., Periostin Is a Novel Factor in Cardiac Remodeling After Experimental and Clinical Unloading of the Failing Heart. *Annals of Thoracic Surgery* **2009,** 88, (6), 1916-1921.
219. Distler, J. H. W.; Jüngel, A.; Pileckyte, M.; Zwerina, J.; Michel, B. A.; Gay, R. E.; Kowal-Bielecka, O.; Matucci-Cerinic, M.; Schett, G.; Marti, H. H.; Gay, S.; Distler, O., Hypoxia-induced increase in the production of extracellular matrix proteins in systemic sclerosis. *Arthritis and Rheumatism* **2007,** 56, (12), 4203-4215.
220. Osada-Oka, M.; Ikeda, T.; Akiba, S.; Sato, T., Hypoxia stimulates the autocrine regulation of migration of vascular smooth muscle cells via HIF-1α-dependent expression of thrombospondin-1. *Journal of Cellular Biochemistry* **2008,** 104, (5), 1918-1926.
221. Chen, D.; Asahara, T.; Krasinski, K.; Witzenbichler, B.; Yang, J.; Magner, M.; Kearney, M.; Frazier, W. A.; Isner, J. M.; Andrés, V., Antibody blockade of thrombospondin accelerates reendothelialization and reduces neointima formation in balloon-injured rat carotid artery. *Circulation* **1999,** 100, (8), 849-854.
222. Tanoue, T.; Takeichi, M., Mammalian Fat1 cadherin regulates actin dynamics and cell-cell contact. *Journal of Cell Biology* **2004,** 165, (4), 517-528.
223. Moeller, M. J.; Soofi, A.; Braun, G. S.; Li, X.; Watzl, G.; Kriz, W.; Holzman, L. B., Protocadherin FAT1 binds Ena/VASP proteins and is necessary for actin dynamics and cell polarization. *EMBO Journal* **2004,** 23, (19), 3769-3779.
224. Kumagai, T.; Nangaku, M.; Kojima, I.; Nagai, R.; Ingelfinger, J. R.; Miyata, T.; Fujita, T.; Inagi, R., Glyoxalase I overexpression ameliorates renal ischemia-reperfusion injury in rats. *American Journal of Physiology - Renal Physiology* **2009,** 296, (4), F912-F921.
225. Oh-Hashi, K.; Imai, K.; Koga, H.; Hirata, Y.; Kiuchi, K., Knockdown of transmembrane protein 132A by RNA interference facilitates serum starvation-induced cell death in Neuro2a cells. *Molecular and Cellular Biochemistry* **2010,** 342, (1-2), 117-123.
226. Vorotnikova, E.; Triesb, M.; Braunhut, S., Retinoids and TIMP1 Prevent Radiation-Induced Apoptosis of Capillary Endothelial Cells. *Radiation Research* **2004,** 161, (2), 174-184.
227. Park, J. E.; Tan, H. S.; Datta, A.; Lai, R. C.; Zhang, H.; Meng, W.; Lim, S. K.; Sze, S. K., Hypoxic tumor cell modulates its microenvironment to enhance angiogenic and metastatic potential by secretion of proteins and exosomes. *Molecular and Cellular Proteomics* **2010,** 9, (6), 1085-1099.
228. Zannad, F.; Rossignol, P.; Iraqi, W., Extracellular matrix fibrotic markers in heart failure. *Heart Failure Reviews* **2010,** 15, (4), 319-329.
229. Sardiu, M. E.; Washburn, M. P., Enriching quantitative proteomics with SI N. *Nature Biotechnology* **2010,** 28, (1), 40-42.
230. Beck, M.; Malmström, J. A.; Lange, V.; Schmidt, A.; Deutsch, E. W.; Aebersold, R., Visual proteomics of the human pathogen Leptospira interrogans. *Nature Methods* **2009,** 6, (11), 817-823.
231. Ryu, S.; Gallis, B.; Young, A. G.; Shaffer, S. A.; Radulovic, D.; Goodlett, D. R., Comparison of a label-free quantitative proteomic method based on peptide ion current area to the isotope coded affinity tag method. *Cancer Informatics* **2008,** 6, 243-255.